ISSN 2986 - 0776

# Journal of Applied Mathematics in Science and Technology

Volume No. 13
Issue No. 2
May- August 2025

ENRICHED PUBLICATIONS

ENRICHED PUBLICATIONS PVT.LTD

JE - 18,Gupta Colony, Khirki Extn,
Malviya Nagar, New Delhi - 110017.
E- Mail: info@enrichedpublication.com
Phone :- +91-8877340707

ISSN 2986 - 0776

# Journal of Applied Mathematics in Science and Technology

**Aims and Scope**

The Journal of Applied Mathematics in Science and Technology is published quarterly by Enriched publications. Journal of Applied Mathematics in Science and Technology is peer reviewed journal and monitored by a team of reputed editorial board members. This journal consists of research articles, reviews, and case studies on Science Technology. This journal mainly focuses on the latest and most common subjects of its domain.

ISSN 2986 - 0776

# Journal of Applied Mathematics in Science and Technology

ISSN 2986 - 0776

# Journal of Applied Mathematics in Science and Technology

(Volume No. 13, Issue No. 2, May- August 2025)

## Contents

ISSN 2986 - 0776

# Computational analysis of multi-layered Navier–Stokes system by Atangana–Baleanu derivative

**Awatif Muflih Alqahtania and Akanksha Shukla b**
aDepartment of Mathematics, Shaqra University, Riyadh, Saudi Arabia;
bDepartment of Mathematics,
Amity School of Applied Science, Amity University Rajasthan, Jaipur, India

## A B S T R A C T

*In our present paper, we have employed the Atangana–Baleanu derivative in the multi-layered Navier–Stokes condition to analysethe nature of the flow. Actually, the stream, the impacts and mod ifications caused by the operator and the mathematical techniqueapproach are the main subjects of our attention. In this exploratorywork, the Laplace transform strategy and the Atangana–Baleanufractional operator were combined. Due to the Atangana–Baleanu operator's convergence in many engineering and technologicalissues, it is employed. We have also carefully evaluated the presence and uniqueness of the outcome. To visualize the variationsin the flow, we have presented the graphs of the stream's velocitycomponents in each direction during the study*

***ARTICLE HISTORY***
*Received 11 April 2023 Accepted 29 November 2023*

***KEYWORDS***
*Navier–Stokes equation; Atangana–Baleanuderivative; Laplace transform;existence and oneness*

***MATHEMATICS SUBJECT***
*CLASSIFICATIONS Primary 92B05; 92C60; Secondary 26A33*

## 1. Background

The Navier–Stokes (NS) condition, a well-known controlling state of viscus fluid stream improvement, was discovered in 1822. This condition, which is a combination of the second law, strength conditions, and congruity conditions, is conceivably known as Newton'ssecond law of fluid growth. When illustrating the real research of different consistent andplanning qualities, NS circumstances are helpful. This circumstance sets apart a few realobjects near the airplane's wings, such as the blood flow, wind current, and fluid flow inpipes. The Navier–Stokes condition establishes the link among strain, the operational outerpowers of the liquid, and the fluid flow reaction. Quantitative data on shock waves, disturbances, and solitons have been successfully obtained using the Navier–Stokes condition[1–6] and conventional liquid elements. Navier–Stokes conditions are regarded as important mathematical tools for a more thorough understanding of variety of real challenges in a number of crucial characteristics, such as their thermodynamics, aviation sciences,geophysics, the petroleum industry, plasma physical research, etc. [7–12]. Halfway inspection, which was described in advance in letters between Leibniz and L'Hospital in 1695,is a general improvement of the study of whole number solicitation to whimsical solicitation. Fractional analysis is constantly positioned to work on current mathematical models due to its unique potential to identify peculiar action and memory effects [13–26], which are the key components of tangled peculiarities. By working together, professionals likeCaputo, Riemann, Liouville, Ross and Miller, Podlubny, and others were able to resolve themathematical basis for fragmented solicitation auxiliaries. Incomplete Postmodern mathconjecture was connected to real-world applications and included theories about chaos,electrodynamics, signal processing, thermodynamics, financial perspectives, and severalother fields [27–34].

In elementary mathematics, we frequently represented a variety of genuine qualities in a little sophisticated way, such as the distinction from conventional examination. The continuous plan depends on the fragmented soliciting subordinates depicted by Caputo quicklythe typical alteration. We acquired the game plan of the fractional solicitation NS condition about the time that the projected estimation was finished. Therefore,under various fragmented solicitations of the NS circumstances, we might acquire variouscourses of action. With the use of numerous fractional solicitation subordinates, we canseparate the distinct NS conditions' components thanks to continuing systems. To locatea solution that fits a certain problem strategy, we can pick the best possible fragmentedsolicitation. The current article makes the assumption that an in-compressible liquid progression of density ρ has a period fragmentary Navier–Stokes condition and kinematicaccuracy $\upsilon = \beta\rho$ . It appears as:

$$\begin{cases} D_\eta{}^\beta F + (F.\nabla)\, F = \rho\nabla^2 F - \frac{1}{\rho}\nabla g, \\ \nabla.F = 0, \\ F = 0, \text{ on } \Omega \times (0,\, T)\,. \end{cases}$$

Here, $F = (\mu, \nu, w)$, $q$, *and* $\eta$ denote liquid vector, tension and time, separately. $(\Lambda, \omega, \zeta)$ represents the spatial parts in $\Omega$. The aforementioned situations might also be described as:

$$D_\eta{}^\gamma\,(\beta) + \beta\frac{\partial\beta}{\partial\Lambda} + \psi\frac{\partial\beta}{\partial\omega} + \Theta\frac{\partial\beta}{\partial\zeta} = \rho\left[\frac{\partial^2\beta}{\partial\Lambda^2} + \frac{\partial^2\beta}{\partial\omega^2} + \frac{\partial^2\beta}{\partial\zeta^2}\right] - \frac{1}{\rho}\frac{\partial g}{\partial\Lambda},$$

$$D_\eta{}^\gamma\,(\psi) + \beta\frac{\partial\psi}{\partial\Lambda} + \psi\frac{\partial\psi}{\partial\omega} + \Theta\frac{\partial\psi}{\partial\zeta} = \rho\left[\frac{\partial^2\psi}{\partial\Lambda^2} + \frac{\partial^2\psi}{\partial\omega^2} + \frac{\partial^2\psi}{\partial\zeta^2}\right] - \frac{1}{\rho}\frac{\partial g}{\partial\omega},$$

$$D_\eta{}^\gamma\,(\Theta) + \beta\frac{\partial\Theta}{\partial\Lambda} + \psi\frac{\partial\Theta}{\partial\omega} + \Theta\frac{\partial\Theta}{\partial\zeta} = \rho\left[\frac{\partial^2\Theta}{\partial\Lambda^2} + \frac{\partial^2\Theta}{\partial\omega^2} + \frac{\partial^2\Theta}{\partial\zeta^2}\right] - \frac{1}{\rho}\frac{\partial g}{\partial\zeta},$$

with following initial conditions (i.e. at $t = 0$)

$$\begin{cases} \beta\,(\Lambda, \omega, \zeta, 0) = -0.5\Lambda + \omega + \zeta, \\ \psi\,(\Lambda, \omega, \zeta, 0) = \Lambda - 0.5\omega + \zeta, \\ \Theta\,(\Lambda, \omega, \zeta, 0) = \Lambda + \omega - 0.5\zeta\,. \end{cases}$$

In this section, some basic expert duties are covered. For a moment, suppose that Herrmann and Hilfer's fractional partial differential conditions, like time-fractional NS conditions, are not completely predetermined by applications in a variety of scientific a  planning fields. Recently, El-Shahed and Salem conducted a sporadic presentation of NS circumstances in 2005. For summing out-of-date NS conditions, makers employed Laplacechange, constrained Hankel change, and finite Fourier Sine change. By combining HPMand LTA, Kumar et al. deductively addressed a nonlinear partial model of the NS condition. By using the homotopy evaluation technique, Ganji et al., in addition to Ragab et al.,has resolved non-straight time fragmented Navier–Stokes system. ADM was developed byOdibat, Momani, and Birajdar to provide numerical estimates of the time-fractional NScondition. While Chaurasia and Kumar had inclined to a comparative condition by combining limited Hankel change and Laplace change, Kumar et al. obtained a canny plan of thetime-partial NS condition utilizing a combination of ADM and Laplace change. To handle nonlinear and instantaneous ODEs and PDEs, M. Rawashdeh and S. Maitama introducedNDM in 2014. The partial order Whitham–Broer–Kaup conditions, fractional order heatand wave conditions, fractional actual models, fractional order PDEs with relative deferment, and the fractional order dissemination conditions are just a few of the real-worldissues that were concentrated using NDM.

The sensible strategy of fractional soliciting NS circumstances is emphasized on the ongoing creation. Since a long time ago, examiners have been interested in the arrangement of typical NS conditions. Actually, the main area of agreement between researchersand mathematicians is the intelligent designs of the fragmented request NS condition. Thiswas the active endeavour to develop or promote the ongoing systems for the strategiesof NS soliciting that was not complete. A noteworthy portion of them have developedinnovative methods to deal with Navier–Stokes of fragmentary order. In this way, streamresearch efforts make a sensible addition to the Navier–Stokes partial order conditions'logical framework.

In more recent works, Chu et al. used the variation iteration transform approach along with Caputo derivative and Laplace transform to solve the problem. Singh and Kumarused the fractional reduced differential transform technique to get the approximate solution of the system, whereas Kavvas and Ercan used a completely different strategy to findthe solution of the Navier–Stokes system. They made use of the momentum equationsystem.

In this paper, we performed logical operations, particularly the Laplace transformation approach, but we also assessed them and presented an argument in favour of the application of the recommended calculations. In this work, we first apply existence and onenesstheorem to show the existence and oneness of result. Using the Laplace transform, wewill continue to solve the problem iteratively. In order to find an approximate solutionof Navier–Stokes system, this work employs a unique technique and strategy. Our focus isin fact primarily on the stream, the effects and adjustments brought about by the

operator, and a novel mathematical approach.

The current article is divided into six areas; area 1 deals with the introduction andbackground of the problem, and Section 2 has prerequisites related to the topic. Area 3comprises the existence of the solution, whereas segments 4 and 5 deal with the onenessof framework and the solution of system with Laplace transform, respectively. The paperis concluded in part 6. We have acknowledged the researchers and scientists whose studywas crucial in our findings. References are attached at the end.

## 2. Definition and preliminaries

### 2.1. Atangana–Baleanu fractional derivative

Let h ∈ H(0, 1) and 0 <ω< 1, the Atangana–Baleanu Fractional derivative in Caputosense is defined as [35]:

$$T_\omega(h)(x) = \frac{B(\omega)}{1-\omega}\int_0^x E_\omega\left[-\frac{\omega}{1-\omega}(x-s)^\omega\right]h'(s)\,\mathrm{d}s. \qquad (1)$$

### 2.2. Atangana–Baleanu integral operator

The Atangana–Baleanu integral operator of function 'f' and of order α is explained as [35]:

$${}^{AB}_{a}I_0^\alpha f(t) = \frac{1-\alpha}{B(\alpha)}f(t) + \frac{\alpha}{B(\alpha)\Gamma\alpha}\int_a^t f(y)(t-y)^{\alpha-1}\,\mathrm{d}y. \qquad (2)$$

### 2.3. Atangana–Baleanu integral operator (in caputo sense)

The Atangana–Baleanu integral operator (in Caputo sense) of function 'f' and of order α is explained as [35]:

$${}^{ABC}_{a}I_t^\alpha f(t) = \frac{1-\alpha}{B(\alpha)}f(t) + \frac{\alpha}{B(\alpha)\Gamma\alpha}\int_0^t f(y)(t-y)^{\alpha-1}\,\mathrm{d}y. \qquad (3)$$

### 2.4. Laplace change of Atangana–Baleanu derivative

The Laplace change of the Atangana–Baleanu derivative of order τ is explained below:

$$L\{{}^{ABC}D^\tau f(t)\} = \frac{M(\tau)}{1-\tau}.\frac{p^\tau L\{f(t)\} - p^{\tau-1}f(0)}{p^\tau + \frac{\tau}{1-\tau}}, \qquad (4)$$

for more details, refer [35–45].

## 3. Existence of solution

Multi-dimensional Navier–Stokes condition is given as below

$$
\begin{aligned}
D_t^{\iota}(\beta)+\beta\frac{\partial\beta}{\partial\Lambda}+\psi\frac{\partial\beta}{\partial\omega}+\Theta\frac{\partial\beta}{\partial\zeta}&=\rho\left[\frac{\partial^2\beta}{\partial\Lambda^2}+\frac{\partial^2\beta}{\partial\omega^2}+\frac{\partial^2\beta}{\partial\zeta^2}\right],\\
D_t^{\iota}(\psi)+\beta\frac{\partial\psi}{\partial\Lambda}+\psi\frac{\partial\psi}{\partial\omega}+\Theta\frac{\partial\psi}{\partial\zeta}&=\rho\left[\frac{\partial^2\psi}{\partial\Lambda^2}+\frac{\partial^2\psi}{\partial\omega^2}+\frac{\partial^2\psi}{\partial\zeta^2}\right],\\
D_t^{\iota}(\Theta)+\beta\frac{\partial\Theta}{\partial\Lambda}+\psi\frac{\partial\Theta}{\partial\omega}+\Theta\frac{\partial\Theta}{\partial\zeta}&=\rho\left[\frac{\partial^2\Theta}{\partial\Lambda^2}+\frac{\partial^2\Theta}{\partial\omega^2}+\frac{\partial^2\Theta}{\partial\zeta^2}\right].
\end{aligned}
\tag{5}
$$

or

$$
\begin{aligned}
D_t^{\iota}(\beta)&=\rho\left[\frac{\partial^2\beta}{\partial\Lambda^2}+\frac{\partial^2\beta}{\partial\omega^2}+\frac{\partial^2\beta}{\partial\zeta^2}\right]-\left[\beta\frac{\partial\beta}{\partial\Lambda}+\psi\frac{\partial\beta}{\partial\omega}+\Theta\frac{\partial\beta}{\partial\zeta}\right],\\
D_t^{\iota}(\psi)&=\rho\left[\frac{\partial^2\psi}{\partial\Lambda^2}+\frac{\partial^2\psi}{\partial\omega^2}+\frac{\partial^2\psi}{\partial\zeta^2}\right]-\left[\beta\frac{\partial\psi}{\partial\Lambda}+\psi\frac{\partial\psi}{\partial\omega}+\Theta\frac{\partial\psi}{\partial\zeta}\right],\\
D_t^{\iota}(\Theta)&=\rho\left[\frac{\partial^2\Theta}{\partial\Lambda^2}+\frac{\partial^2\Theta}{\partial\omega^2}+\frac{\partial^2\Theta}{\partial\zeta^2}\right]-\left[\beta\frac{\partial\Theta}{\partial\Lambda}+\psi\frac{\partial\Theta}{\partial\omega}+\Theta\frac{\partial\Theta}{\partial\zeta}\right].
\end{aligned}
\tag{6}
$$

Now changing the derivatives to Atangana–Baleanu fractional derivative in the Caputo sense, we have [46–55]:

$$
\begin{aligned}
{}^{ABC}D_t^{\iota}(\beta)&=\rho\left[\frac{\partial^2\beta}{\partial\Lambda^2}+\frac{\partial^2\beta}{\partial\omega^2}+\frac{\partial^2\beta}{\partial\zeta^2}\right]-\left[\beta\frac{\partial\beta}{\partial\Lambda}+\psi\frac{\partial\beta}{\partial\omega}+\Theta\frac{\partial\beta}{\partial\zeta}\right],\\
{}^{ABC}D_t^{\iota}(\psi)&=\rho\left[\frac{\partial^2\psi}{\partial\Lambda^2}+\frac{\partial^2\psi}{\partial\omega^2}+\frac{\partial^2\psi}{\partial\zeta^2}\right]-\left[\beta\frac{\partial\psi}{\partial\Lambda}+\psi\frac{\partial\psi}{\partial\omega}+\Theta\frac{\partial\psi}{\partial\zeta}\right],\\
{}^{ABC}D_t^{\iota}(\Theta)&=\rho\left[\frac{\partial^2\Theta}{\partial\Lambda^2}+\frac{\partial^2\Theta}{\partial\omega^2}+\frac{\partial^2\Theta}{\partial\zeta^2}\right]-\left[\beta\frac{\partial\Theta}{\partial\Lambda}+\psi\frac{\partial\Theta}{\partial\omega}+\Theta\frac{\partial\Theta}{\partial\zeta}\right].
\end{aligned}
\tag{7}
$$

Now, suppose the function $f(\Lambda,\omega,\zeta,t,\beta,\beta'_{\Lambda},\beta'_{\omega},\beta'_{\zeta},\beta''_{\Lambda},\beta''_{\omega},\beta''_{\zeta})$ satisfies Lipschitz condition,

$$
\begin{aligned}
&\Big\|f\left(\Lambda,\omega,\zeta,t,\beta,\beta'_{\Lambda},\beta'_{\omega},\beta'_{\zeta},\beta''_{\Lambda},\beta''_{\omega},\beta''_{\zeta}\right)\\
&\quad-f\left(\Lambda,\omega,\zeta,t,\beta_1,\beta'_{1\Lambda},\beta'_{1\omega},\beta'_{1\zeta},\beta''_{1\Lambda},\beta''_{1\omega},\beta''_{1\zeta}\right)\Big\|\\
&\le M\left|\beta-\beta_1\right|+K_1\left|\beta'_{\Lambda}-\beta'_{1\Lambda}\right|+K_2\left|\beta'_{\omega}-\beta'_{1\omega}\right|+K_3\left|\beta'_{\zeta}-\beta'_{1\zeta}\right|\\
&\quad+L_1\left|\beta''_{\Lambda}-\beta''_{1\Lambda}\right|+L_2\left|\beta''_{\omega}-\beta''_{1\omega}\right|+L_3\left|\beta''_{\zeta}-\beta''_{1\zeta}\right|,
\end{aligned}
$$

again, assume that

$$\left\|\beta'_{\Lambda}-\beta'_{1\Lambda}\right\| \leq \delta_1 \left\|\beta-\beta_1\right\|, \left\|\beta'_{\omega}-\beta'_{1\omega}\right\| \leq \delta_2 \left\|\beta-\beta_1\right\|,$$
$$\left\|\beta'_{\zeta}-\beta'_{1\zeta}\right\| \leq \delta_3 \left\|\beta-\beta_1\right\|, \left\|\beta''_{\Lambda}-\beta''_{1\Lambda}\right\| \leq \delta_4 \left\|\beta-\beta_1\right\|,$$
$$\left\|\beta''_{\omega}-\beta''_{1\omega}\right\| \leq \delta_5 \left\|\beta-\beta_1\right\|, \left\|\beta''_{\zeta}-\beta''_{1\zeta}\right\| \leq \delta_6 \left\|\beta-\beta_1\right\|,$$

where $\delta_1, \delta_2, \delta_3, \delta_4, \delta_5$ *and* $\delta_6 \in R^+$ such that $M + K_1\delta_1 + K_2\delta_2 + K_3\delta_3 + L_1\delta_4 + L_2\delta_5 + L_3\delta_6 \leq 1$, then result of system occurs if $t_{\max}$ is s.t.

$$\frac{1-\iota}{B(\iota)} + \frac{t_{\max}^{\iota}}{B(\iota)\Gamma\iota} < 1.$$

**Theorem 3.1:** *Show that the results of the given system* (5) *exist iff*

***Proof:*** Applying the basic assumption of fractional mathematics, we obtain:

$$\beta(\Lambda,\omega,\zeta,t) - \beta(\Lambda,\omega,\zeta,0) = \frac{1-\iota}{B(\iota)} f\left(\Lambda,\omega,\zeta,t,\beta,\beta'_{\Lambda},\beta'_{\omega},\beta'_{\zeta},\beta''_{\Lambda},\beta''_{\omega},\beta''_{\zeta}\right)$$
$$+ \frac{\iota}{B(\iota)\Gamma\iota}\int_0^t (t-y)^{\iota-1} f\left(\Lambda,\omega,\zeta,t,\beta,\beta'_{\Lambda},\beta'_{\omega},\beta'_{\zeta},\beta''_{\Lambda},\beta''_{\omega},\beta''_{\zeta}\right) dy, \tag{8}$$

or

$$\beta(\Lambda,\omega,\zeta,t) = \beta_0 + \frac{1-\iota}{B(\iota)} f\left(\Lambda,\omega,\zeta,t,\beta,\beta'_{\Lambda},\beta'_{\omega},\beta'_{\zeta},\beta''_{\Lambda},\beta''_{\omega},\beta''_{\zeta}\right)$$
$$+ \frac{\iota}{B(\iota)\Gamma\iota}\int_0^t (t-y)^{\iota-1} f\left(\Lambda,\omega,\zeta,t,\beta,\beta'_{\Lambda},\beta'_{\omega},\beta'_{\zeta},\beta''_{\Lambda},\beta''_{\omega},\beta''_{\zeta}\right) dy. \tag{9}$$

Now,

$$\beta_n(\Lambda,\omega,\zeta,t) = \beta_0 + \frac{1-\iota}{B(\iota)} f\left(\Lambda,\omega,\zeta,t,\beta_{n-1},\beta'_{\Lambda,n-1},\right.$$
$$\left.\beta'_{\omega,n-1},\beta'_{\zeta,n-1},\beta''_{\Lambda,n-1},\beta''_{\omega,n-1},\beta''_{\zeta,n-1}\right) + \frac{\iota}{B(\iota)\Gamma\iota}$$
$$\times \int_0^t (t-y)^{\iota-1} f\left(\Lambda,\omega,\zeta,t,\beta_{n-1},\beta'_{\Lambda,n-1},\right.$$
$$\left.\beta'_{\omega,n-1},\beta'_{\zeta,n-1},\beta''_{\Lambda,n-1},\beta''_{\omega,n-1},\beta''_{\zeta,n-1}\right) dy, \tag{10}$$

suppose $\gamma_n = \beta_n - \beta_{n-1}$

So,

$$\gamma_n = \frac{1-\iota}{B(\iota)}\Big[f\left(\Lambda,\omega,\zeta,t,\beta_{n-1},\beta'_{\Lambda,n-1},\beta'_{\omega,n-1},\beta'_{\zeta,n-1},\beta''_{\Lambda,n-1},\beta''_{\omega,n-1},\beta''_{\zeta,n-1}\right)$$
$$-f\left(\Lambda,\omega,\zeta,t,\beta_{n-2},\beta'_{\Lambda,n-2},\beta'_{\omega,n-2},\beta'_{\zeta,n-2},\beta''_{\Lambda,n-2},\beta''_{\omega,n-2},\beta''_{\zeta,n-2}\right)\Big]$$
$$+\frac{\iota}{B(\iota)\Gamma\iota}\int_0^t (t-y)^{\iota-1}\big[f\left(\Lambda,\omega,\zeta,t,\beta_{n-1},\beta'_{\Lambda,n-1},\right.$$
$$\left.\beta'_{\omega,n-1},\beta'_{\zeta,n-1},\beta''_{\Lambda,n-1},\beta''_{\omega,n-1},\beta''_{\zeta,n-1}\right)$$
$$-f\left(\Lambda,\omega,\zeta,t,\beta_{n-2},\beta'_{\Lambda,n-2},\beta'_{\omega,n-2},\beta'_{\zeta,n-2},\beta''_{\Lambda,n-2},\beta''_{\omega,n-2},\beta''_{\zeta,n-2}\right)\big]\,\mathrm{d}y. \tag{11}$$

We see that,

Hence taking norm both sides, we have

$$\|\gamma_n\| = \|\beta_n - \beta_{n-1}\|,$$
$$\leq \frac{1-\iota}{B(\iota)}\Big\|f\left(\Lambda,\omega,\zeta,t,\beta_{n-1},\beta'_{\Lambda,n-1},\beta'_{\omega,n-1},\beta'_{\zeta,n-1},\beta''_{\Lambda,n-1},\beta''_{\omega,n-1},\beta''_{\zeta,n-1}\right)$$
$$-f\left(\Lambda,\omega,\zeta,t,\beta_{n-2},\beta'_{\Lambda,n-2},\beta'_{\omega,n-2},\beta'_{\zeta,n-2},\beta''_{\Lambda,n-2},\beta''_{\omega,n-2},\beta''_{\zeta,n-2}\right)\Big\|$$
$$+\frac{\iota}{B(\iota)\Gamma\iota}\Big\|\int_0^t (t-y)^{\iota-1}\big[f\left(\Lambda,\omega,\zeta,t,\beta_{n-1},\beta'_{\Lambda,n-1},\right.$$
$$\left.\beta'_{\omega,n-1},\beta'_{\zeta,n-1},\beta''_{\Lambda,n-1},\beta''_{\omega,n-1},\beta''_{\zeta,n-1}\right)$$
$$-f\left(\Lambda,\omega,\zeta,t,\beta_{n-2},\beta'_{\Lambda,n-2},\beta'_{\omega,n-2},\beta'_{\zeta,n-2},\beta''_{\Lambda,n-2},\beta''_{\omega,n-2},\beta''_{\zeta,n-2}\right)\big]\,\mathrm{d}y\Big\|, \tag{12}$$

or

$$\|\gamma_n\| \leq \frac{1-\iota}{B(\iota)}\big[M\|\beta_{n-1}-\beta_{n-2}\| + K_1\|\beta'_{\Lambda,n-1}-\beta'_{\Lambda,n-2}\|$$
$$+K_2\|\beta'_{\omega,n-1}-\beta'_{\omega,n-2}\| + K_3\|\beta'_{\zeta,n-1}-\beta'_{\zeta,n-2}\| + L_1\|\beta''_{\Lambda,n-1}-\beta''_{\Lambda,n-2}\|$$
$$+L_2\|\beta''_{\omega,n-1}-\beta''_{\omega,n-2}\| + L_3\|\beta''_{\zeta,n-1}-\beta''_{\zeta,n-2}\|\big]$$
$$+\frac{\iota}{B(\iota)\Gamma\iota}\big[M\|\beta_{n-1}-\beta_{n-2}\| + K_1\|\beta'_{\Lambda,n-1}-\beta'_{\Lambda,n-2}\| + K_2\|\beta'_{\omega,n-1}-\beta'_{\omega,n-2}\|$$
$$+K_3\|\beta'_{\zeta,n-1}-\beta'_{\zeta,n-2}\| + L_1\|\beta''_{\Lambda,n-1}-\beta''_{\Lambda,n-2}\| + L_2\|\beta''_{\omega,n-1}-\beta''_{\omega,n-2}\|$$
$$+L_3\|\beta''_{\zeta,n-1}-\beta''_{\zeta,n-2}\|\big]\int_0^t (t-y)^{\iota-1}\,\mathrm{d}y. \tag{13}$$

It gives,

$$\leq \Big[M \left\|\beta_{n-1} - \beta_{n-2}\right\| + K_1 \left\|\beta'_{\Lambda,n-1} - \beta'_{\Lambda,n-2}\right\| + K_2 \left\|\beta'_{\omega,n-1} - \beta'_{\omega,n-2}\right\|$$
$$+ K_3 \left\|\beta'_{\zeta,n-1} - \beta'_{\zeta,n-2}\right\| + L_1 \left\|\beta''_{\Lambda,n-1} - \beta''_{\Lambda,n-2}\right\| + L_2 \left\|\beta''_{\omega,n-1} - \beta''_{\omega,n-2}\right\|$$
$$+ L_3 \left\|\beta''_{\zeta,n-1} - \beta''_{\zeta,n-2}\right\|\Big]\left[\frac{1-\iota}{B(\iota)} + \frac{\iota}{B(\iota)\Gamma\iota}\int_0^t (t-y)^{\iota-1}\,\mathrm{d}y\right]. \tag{14}$$

Let $\|\gamma'_{n-1}\| \leq \delta_1\|\gamma_{n-1}\|$ and $\|\gamma''_{n-1}\| \leq \delta_2\|\gamma_{n-1}\|$, hence

$$\|\gamma_n\| \leq [M \left\|\gamma_{n-1}\right\| + K_1\delta_1 \left\|\gamma_{n-1}\right\| + K_2\delta_2 \left\|\gamma_{n-1}\right\| + K_3\delta_3 \left\|\gamma_{n-1}\right\|$$
$$+ L_1\delta_4 \left\|\gamma_{n-1} + L_2\delta_5 \left\|\gamma_{n-1}\right\| + L_3\delta_6 \left\|\gamma_{n-1}\right\|\right\|]$$
$$\times \left[\frac{1-\iota}{B(\iota)} + \frac{\iota}{B(\iota)\Gamma\iota}\int_0^t (t-y)^{\iota-1}\,\mathrm{d}y\right], \tag{15}$$

$$\|\gamma_n\| \leq \|\gamma_{n-1}\| \left[M + K_1\delta_1 + K_2\delta_2 + K_3\delta_3 + L_1\delta_4 + L_2\delta_5 + L_3\delta_6\right]$$
$$\times \left[\frac{1-\iota}{B(\iota)} + \frac{\iota}{B(\iota)\Gamma\iota}\int_0^t (t-y)^{\iota-1}\,\mathrm{d}y\right], \tag{16}$$

$$\|\gamma_n\| \leq \|\gamma_0\| \left[M + K_1\delta_1 + K_2\delta_2 + K_3\delta_3 + L_1\delta_4 + L_2\delta_5 + L_3\delta_6\right]^n$$
$$\times \left[\frac{1-\iota}{B(\iota)} + \frac{\iota}{B(\iota)\Gamma\iota}\int_0^t (t-y)^{\iota-1}\,\mathrm{d}y\right]^n. \tag{17}$$

Now, let $M + K_1\delta_1 + K_2\delta_2 + K_3\delta_3 + L_1\delta_4 + L_2\delta_5 + L_3\delta_6 = \delta_7 < 1$ hence, we have

$$\|\gamma_n\| \leq \|\gamma_0\| \,\delta_7^n\left[\frac{1-\iota}{B(\iota)} + \frac{t_{\max}^{\iota}}{B(\iota)\Gamma\iota}\right]^n. \tag{18}$$

Therefore, system has a solution if $t_{\max}$. is s.t.

$$\left(\frac{1-\iota}{B(\iota)} + \frac{t_{\max}^{\iota}}{B(\iota)\Gamma\iota}\right)\delta_7 < 1, \tag{19}$$

or,

$$\left(\frac{1-\iota}{B(\iota)} + \frac{t_{\max}^{\iota}}{B(\iota)\Gamma\iota}\right) < 1. \tag{20}$$

Hence, it shows that a solution of system exists. ■

## 4. Oneness of solution

We shall demonstrate the originality of the system's solution in this section. Assume there are two solutions to the system's initial equation (21), β and β1. Suppos

$$\beta\left(\Lambda,\omega,\zeta,t\right)-\beta_1\left(\Lambda,\omega,\zeta,0\right)=\frac{1-\iota}{B(\iota)}\left[f\left(t,\beta\right)-f\left(t,\beta_1\right)\right] + \frac{\iota}{B(\iota)\Gamma\iota}\int_0^t \left(t-y\right)^{\iota-1}\left[f\left(s,\beta\right)-f\left(s,\beta_1\right]\right)\,\mathrm{d}s. \quad (21)$$

Using the norm on both sides, we now obtain

$$\left\|\beta\left(\Lambda,\omega,\zeta,t\right)-\beta_1\left(\Lambda,\omega,\zeta,0\right)\right\|\le\frac{1-\iota}{B(\iota)}\left\|f\left(t,\beta\right)-f\left(t,\beta_1\right)\right\| + \frac{\iota}{B(\iota)\Gamma\iota}\int_0^t \left\|\left(t-y\right)^{\iota-1}\left[f\left(s,\beta\right)-f\left(s,\beta_1\right)\right]\right\|\,\mathrm{d}s. \quad (22)$$

Given that we are aware that G is a Lipschitz operator if G(f) − G(g)| ≤ σf − g|, where f and g are components of the range set and σ is the lowest number which fulfil the constraints. We thus obtain β =β1 by applying Lipschitz constraint and bearing inmind that outcome is constrained. Applying the Lipschitz condition and keeping in mindthat the result is limited in the same way, so we get ψ = ψ1 and = 1

## 5. Solution of model by Laplace transform with Atangana–Baleanu derivative

The given system of equations is

$$\left.\begin{aligned}
{}^{ABC}D^{\iota}(\beta)&=\rho\left[\frac{\partial^2\beta}{\partial\Lambda^2}+\frac{\partial^2\beta}{\partial\omega^2}+\frac{\partial^2\beta}{\partial\zeta^2}\right]-\left[\beta\frac{\partial\beta}{\partial\Lambda}+\psi\frac{\partial\beta}{\partial\omega}+\Theta\frac{\partial\beta}{\partial\zeta}\right]\\
{}^{ABC}D^{\iota}(\psi)&=\rho\left[\frac{\partial^2\psi}{\partial\Lambda^2}+\frac{\partial^2\psi}{\partial\omega^2}+\frac{\partial^2\psi}{\partial\zeta^2}\right]-\left[\beta\frac{\partial\psi}{\partial\Lambda}+\psi\frac{\partial\psi}{\partial\omega}+\Theta\frac{\partial\psi}{\partial\zeta}\right]\\
{}^{ABC}D^{\iota}(\Theta)&=\rho\left[\frac{\partial^2\Theta}{\partial\Lambda^2}+\frac{\partial^2\Theta}{\partial\omega^2}+\frac{\partial^2\Theta}{\partial\zeta^2}\right]-\left[\beta\frac{\partial\Theta}{\partial\Lambda}+\psi\frac{\partial\Theta}{\partial\omega}+\Theta\frac{\partial\Theta}{\partial\zeta}\right]
\end{aligned}\right\}\quad (23)$$

Since we know that $L\{{}^{ABC}D^{\tau}f(t)\}=\frac{M(\tau)}{1-\tau}.\frac{p^{\tau}L\{f(t)\}-p^{\tau-1}f(0)}{p^{\tau}+\frac{\tau}{1-\tau}}$.

Take Laplace transform both sides in the first equation of the system,

$$L\left\{{}^{ABC}D^{\iota}(\beta)\right\} = L\left\{\rho\left[\frac{\partial^2\beta}{\partial\Lambda^2}+\frac{\partial^2\beta}{\partial\omega^2}+\frac{\partial^2\beta}{\partial\zeta^2}\right]-\left[\beta\frac{\partial\beta}{\partial\Lambda}+\psi\frac{\partial\beta}{\partial\omega}+\Theta\frac{\partial\beta}{\partial\zeta}\right]\right\},$$

or,

$$\frac{M(\iota)}{1-\iota}.\frac{p^{\iota}L\{\beta(t)\}-p^{\iota-1}\beta(0)}{p^{\iota}+\frac{\iota}{1-\iota}}$$
$$= L\left\{\rho\left[\frac{\partial^2\beta}{\partial\Lambda^2}+\frac{\partial^2\beta}{\partial\omega^2}+\frac{\partial^2\beta}{\partial\zeta^2}\right]-\left[\beta\frac{\partial\beta}{\partial\Lambda}+\psi\frac{\partial\beta}{\partial\omega}+\Theta\frac{\partial\beta}{\partial\zeta}\right]\right\},$$

or,

$$\frac{p^{\iota}L\{\beta(t)\}-p^{\iota-1}\beta(0)}{p^{\iota}+\frac{\iota}{1-\iota}}$$
$$= \frac{(1-\iota)}{M(\iota)}.L\left\{\rho\left[\frac{\partial^2\beta}{\partial\Lambda^2}+\frac{\partial^2\beta}{\partial\omega^2}+\frac{\partial^2\beta}{\partial\zeta^2}\right]-\left[\beta\frac{\partial\beta}{\partial\Lambda}+\psi\frac{\partial\beta}{\partial\omega}+\Theta\frac{\partial\beta}{\partial\zeta}\right]\right\},$$

or,

$$p^{\iota}L\{\beta(t)\}-p^{\iota-1}\beta(0)$$

$$= \left(p^{\iota}+\frac{\iota}{1-\iota}\right)\frac{(1-\iota)}{M(\iota)}.L\left\{\rho\left[\frac{\partial^2\beta}{\partial\Lambda^2}+\frac{\partial^2\beta}{\partial\omega^2}+\frac{\partial^2\beta}{\partial\zeta^2}\right]-\left[\beta\frac{\partial\beta}{\partial\Lambda}+\psi\frac{\partial\beta}{\partial\omega}+\Theta\frac{\partial\beta}{\partial\zeta}\right]\right\},$$

or,

$$p^{\iota}L\{\beta(t)\}-p^{\iota-1}\beta(0)$$
$$= \frac{\left(p^{\iota}+\iota-\iota p^{\iota}\right)}{M(\iota)}.L\left\{\rho\left[\frac{\partial^2\beta}{\partial\Lambda^2}+\frac{\partial^2\beta}{\partial\omega^2}+\frac{\partial^2\beta}{\partial\zeta^2}\right]-\left[\beta\frac{\partial\beta}{\partial\Lambda}+\psi\frac{\partial\beta}{\partial\omega}+\Theta\frac{\partial\beta}{\partial\zeta}\right]\right\},$$

or,

$$p^{\iota}L\{\beta(t)\} = p^{\iota-1}\beta(0)+\frac{\left(p^{\iota}+\iota-\iota p^{\iota}\right)}{M(\iota)}$$
$$\cdot L\left\{\rho\left[\frac{\partial^2\beta}{\partial\Lambda^2}+\frac{\partial^2\beta}{\partial\omega^2}+\frac{\partial^2\beta}{\partial\zeta^2}\right]-\left[\beta\frac{\partial\beta}{\partial\Lambda}+\psi\frac{\partial\beta}{\partial\omega}+\Theta\frac{\partial\beta}{\partial\zeta}\right]\right\},$$

or,

$$L\{\beta(t)\} = \frac{\beta(0)}{p} + \frac{\left(1-\iota+\iota p^{-\iota}\right)}{M(\iota)} \cdot L\left\{\rho\left[\frac{\partial^2\beta}{\partial\Lambda^2}+\frac{\partial^2\beta}{\partial\omega^2}+\frac{\partial^2\beta}{\partial\zeta^2}\right]-\left[\beta\frac{\partial\beta}{\partial\Lambda}+\psi\frac{\partial\beta}{\partial\omega}+\Theta\frac{\partial\beta}{\partial\zeta}\right]\right\},$$

or,

$$\beta(t) = \beta(0) + L^{-1} \times \left[\frac{\left(1-\iota+\iota p^{-\iota}\right)}{M(\iota)}.L\left\{\rho\left(\frac{\partial^2\beta}{\partial\Lambda^2}+\frac{\partial^2\beta}{\partial\omega^2}+\frac{\partial^2\beta}{\partial\zeta^2}\right)-\left(\beta\frac{\partial\beta}{\partial\Lambda}+\psi\frac{\partial\beta}{\partial\omega}+\Theta\frac{\partial\beta}{\partial\zeta}\right)\right\}\right].$$

In the same way, we get

$$\beta_{n+1}(t) = \beta(0) + L^{-1}\left[\frac{\left(1-\iota+\iota p^{-\iota}\right)}{M(\iota)}.L\left\{\rho\left(\frac{\partial^2\beta_n}{\partial\Lambda^2}+\frac{\partial^2\beta_n}{\partial\omega^2}+\frac{\partial^2\beta_n}{\partial\zeta^2}\right)-\left(\beta_n\frac{\partial\beta_n}{\partial\Lambda}+\psi_n\frac{\partial\beta_n}{\partial\omega}+\Theta_n\frac{\partial\beta_n}{\partial\zeta}\right)\right\}\right].$$

Now put n = 1, we have

$$\beta_1(t) = \beta(0) + L^{-1}\left[\frac{\left(1-\iota+\iota p^{-\iota}\right)}{M(\iota)}.L\left\{\rho\left(\frac{\partial^2\beta_0}{\partial\Lambda^2}+\frac{\partial^2\beta_0}{\partial\omega^2}+\frac{\partial^2\beta_0}{\partial\zeta^2}\right)-\left(\beta_0\frac{\partial\beta_0}{\partial\Lambda}+\psi_0\frac{\partial\beta_0}{\partial\omega}+\Theta_0\frac{\partial\beta_0}{\partial\zeta}\right)\right\}\right].$$

Putting all the necessary values and after simplification, we have

$$\beta_1(t) = -0.5\Lambda + \omega + \zeta - 1.125\Lambda\,(2-\iota)\left(1-\iota+\frac{\iota t^{\iota}}{\iota!}\right).$$

By the same procedure, we get

$$\psi_1(t) = \Lambda - 0.5\omega + \zeta - 1.125\omega\,(2-\iota)\left(1-\iota+\frac{\iota t^{\iota}}{\iota!}\right),$$

and

$$\Theta_1(t) = \Lambda + \omega - 0.5\zeta - 1.125Z\,(2-\iota)\left(1-\iota+\frac{\iota t^{\iota}}{\iota!}\right).$$

Now putting $n=2$ and after simplification, we have

$$\begin{aligned}\beta_2(t) = &-0.5\Lambda + \omega + \zeta - 0.375\Lambda\,(2-\iota)\left(1-\iota+\frac{\iota t^{\iota}}{\iota!}\right) + 0.75\omega\,(2-\iota)\left(1-\iota+\frac{\iota t^{\iota}}{\iota!}\right)\\ &-0.375\Lambda\,(2-\iota)\left(1-\iota+\frac{\iota t^{\iota}}{\iota!}\right) - 0.5625\Lambda(2-\iota)^2\left(1-\iota+\frac{\iota t^{\iota}}{\iota!}\right)^2\\ &+1.125\omega(2-\iota)^2\left(1-\iota+\frac{\iota t^{\iota}}{\iota!}\right)^2 + 0.28125\zeta(2-\iota)^2\left(1-\iota+\frac{\iota t^{\iota}}{\iota!}\right)^2\\ &-0.6328\Lambda(2-\iota)^3\left(1-\iota+\frac{\iota t^{\iota}}{\iota!}\right)^3,\end{aligned}$$

and

$$\begin{aligned}\psi_2(t) = &\Lambda - 0.5\omega + \zeta - 1.125\omega\,(2-\iota)\left(1-\iota+\frac{\iota t^{\iota}}{\iota!}\right) + 1.125\Lambda(2-\iota)^2\left(1-\iota+\frac{\iota t^{\iota}}{\iota!}\right)^2\\ &-0.5625\omega(2-\iota)^2\left(1-\iota+\frac{\iota t^{\iota}}{\iota!}\right)^2 + 1.125\zeta(2-\iota)^2\left(1-\iota+\frac{\iota t^{\iota}}{\iota!}\right)^2\\ &-0.6328\Lambda(2-\iota)^3\left(1-\iota+\frac{\iota t^{\iota}}{\iota!}\right)^3,\end{aligned}$$

and

$$\begin{aligned}\Theta_2(t) = &\Lambda + \omega - 0.5\zeta - 1.125\zeta\,(2-\iota)\left(1-\iota+\frac{\iota t^{\iota}}{\iota!}\right) + 1.125\Lambda(2-\iota)^2\left(1-\iota+\frac{\iota t^{\iota}}{\iota!}\right)^2\\ &+1.125\omega(2-\iota)^2\left(1-\iota+\frac{\iota t^{\iota}}{\iota!}\right)^2 - 0.5625\zeta(2-\iota)^2\left(1-\iota+\frac{\iota t^{\iota}}{\iota!}\right)^2\\ &-0.6328\Lambda(2-\iota)^3\left(1-\iota+\frac{\iota t^{\iota}}{\iota!}\right)^3.\end{aligned}$$

Solution of the system is obtained by $\beta = \beta_0 + \beta_1 + \beta_2 + \cdots$, $\psi = \psi_0 + \psi_1 + \psi_2 + \cdots$ and $\Theta = \Theta_0 + \Theta_1 + \Theta_2 + \cdots$ So, putting the values of iterations, we have

$$\begin{aligned}\beta = &-1.5\Lambda + 3\omega + 3\zeta - 1.5\Lambda\,(2-\iota)\left(1-\iota+\frac{\iota t^{\iota}}{\iota!}\right) + 0.75\omega\,(2-\iota)\left(1-\iota+\frac{\iota t^{\iota}}{\iota!}\right)\\ &-0.375\zeta\,(2-\iota)\left(1-\iota+\frac{\iota t^{\iota}}{\iota!}\right) - 0.5625\Lambda(2-\iota)^2\left(1-\iota+\frac{\iota t^{\iota}}{\iota!}\right)^2\\ &+1.125\omega(2-\iota)^2\left(1-\iota+\frac{\iota t^{\iota}}{\iota!}\right)^2 + 0.28125\zeta(2-\iota)^2\left(1-\iota+\frac{\iota t^{\iota}}{\iota!}\right)^2\\ &-0.6328\Lambda(2-\iota)^3\left(1-\iota+\frac{\iota t^{\iota}}{\iota!}\right)^3 + \cdots, \qquad (24)\end{aligned}$$

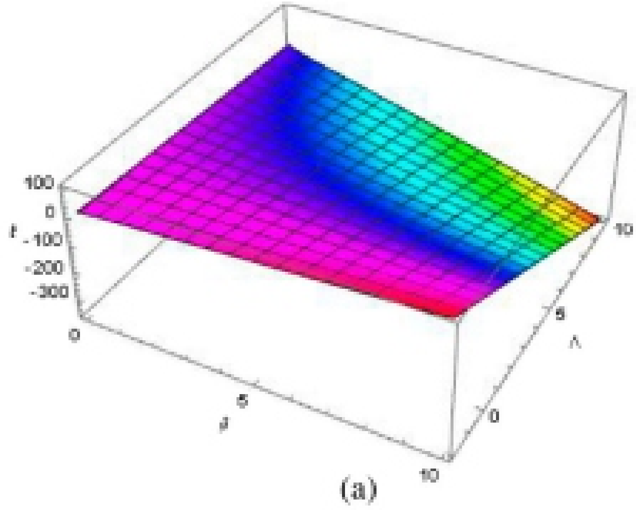


(a)

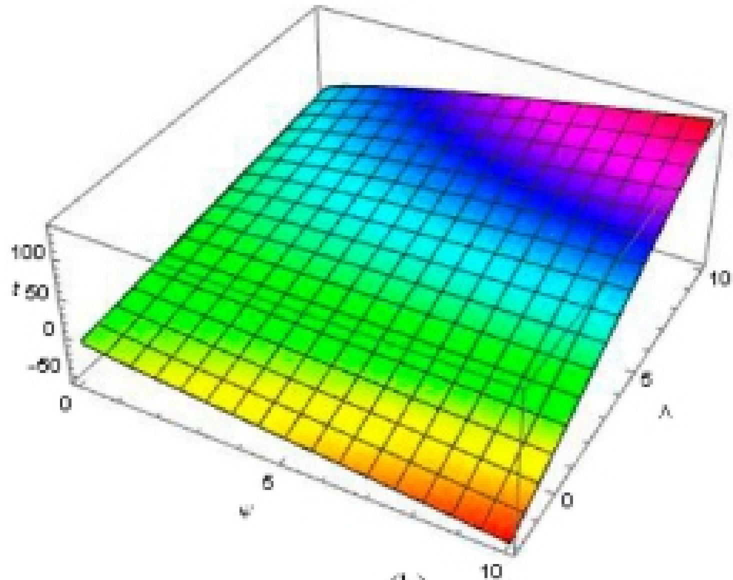


(b)

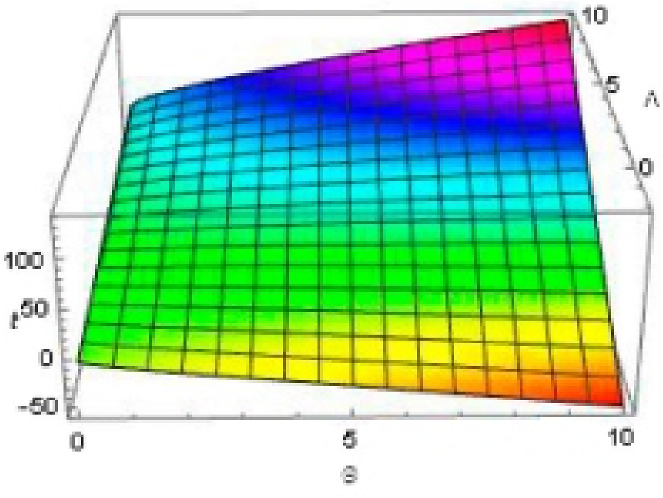


(c)

**Figure 1.** Graphical representation of results for $\iota = 0.5$. (a) Representation of $\beta$ for $\iota = 0.5$, (b) representation of $\psi$ for $\iota = 0.5$, and (c) representation of $\Theta$ for $\iota = 0.5$.

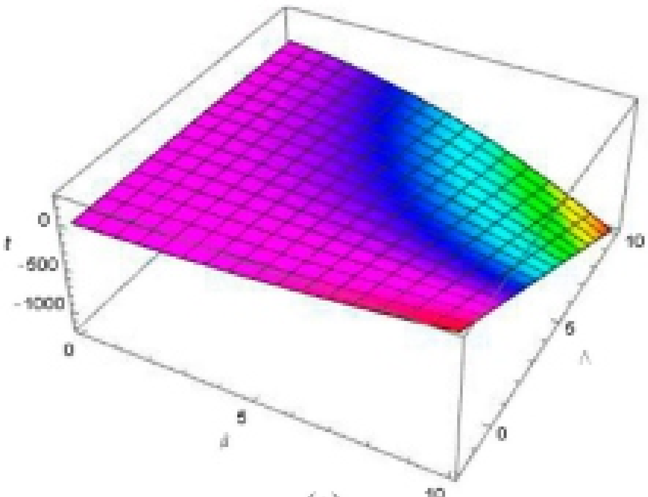

(a)

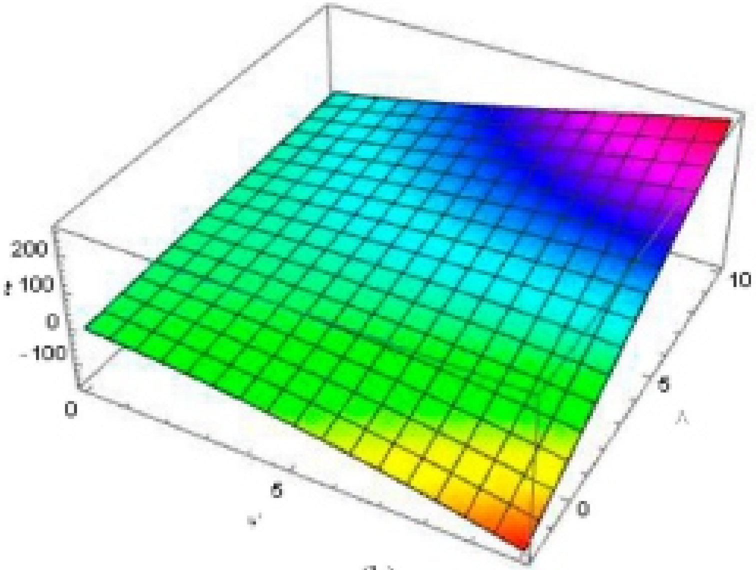

(b)

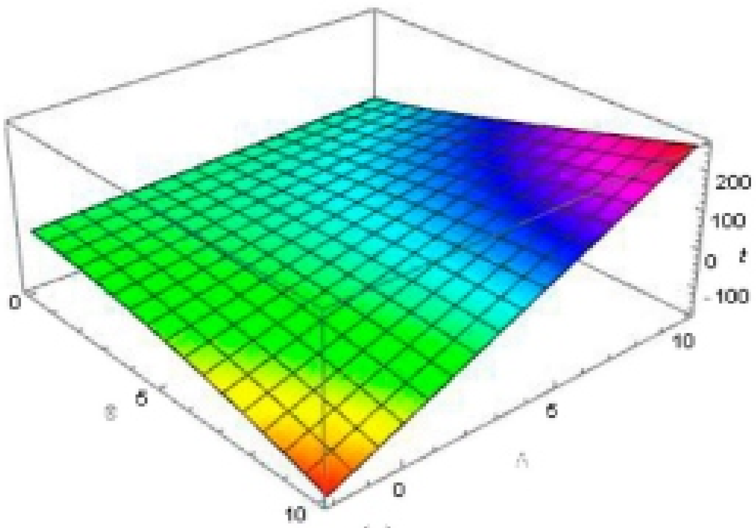

(c)

**Figure 2.** Graphical representation of results for $\iota = 0.7$. (a) Representation of $\beta$ for $\iota = 0.7$, (b) representation of $\psi$ for $\iota = 0.7$, and (c) representation of $\Theta$ for $\iota = 0.7$.

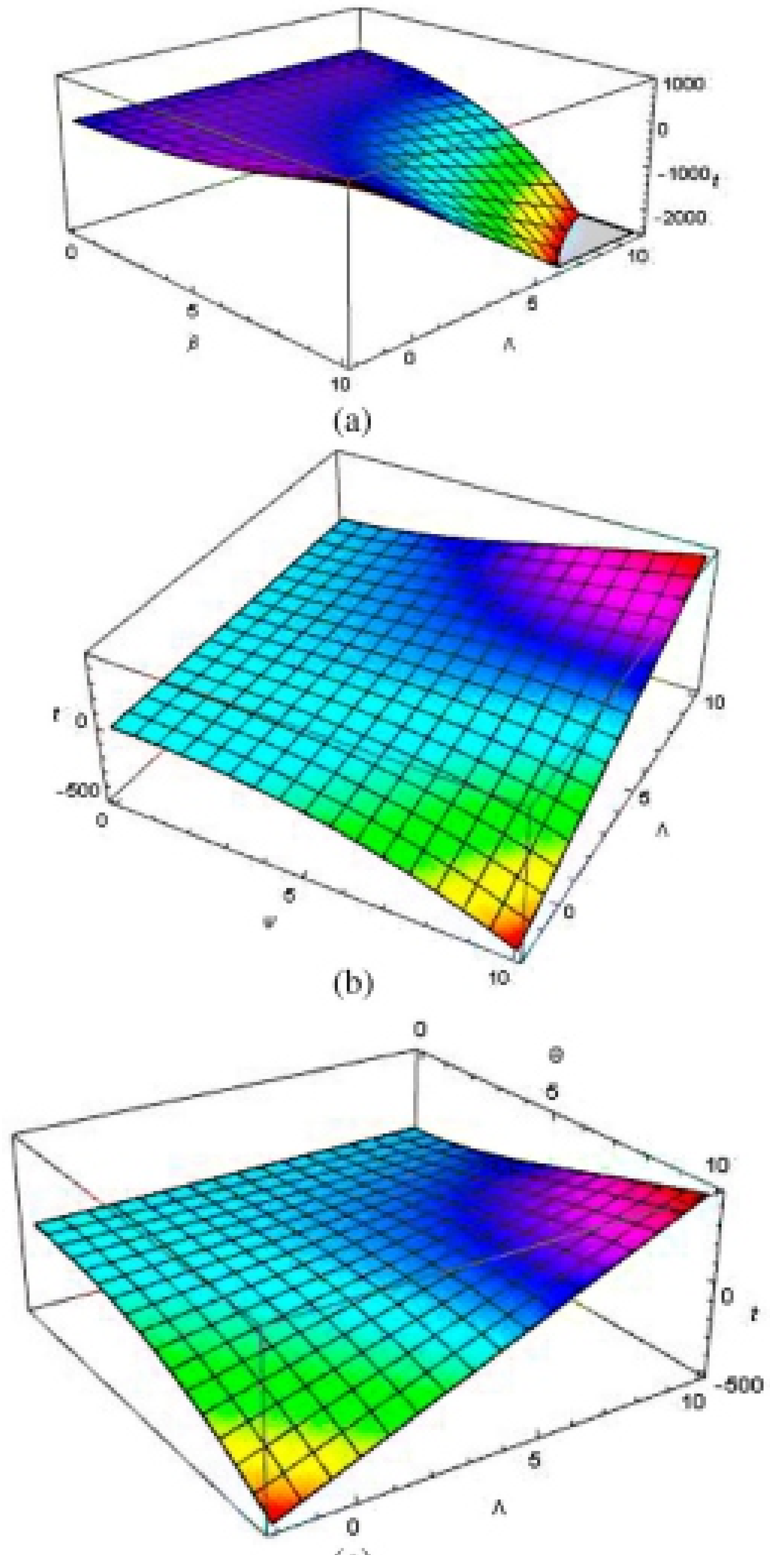


**Figure 3.** Graphical representation of results for $\iota = 0.9$. (a) Representation of $\beta$ for $\iota = 0.9$, (b) representation of $\psi$ for $\iota = 0.9$, and (c) representation of $\Theta$ for $\iota = 0.9$.

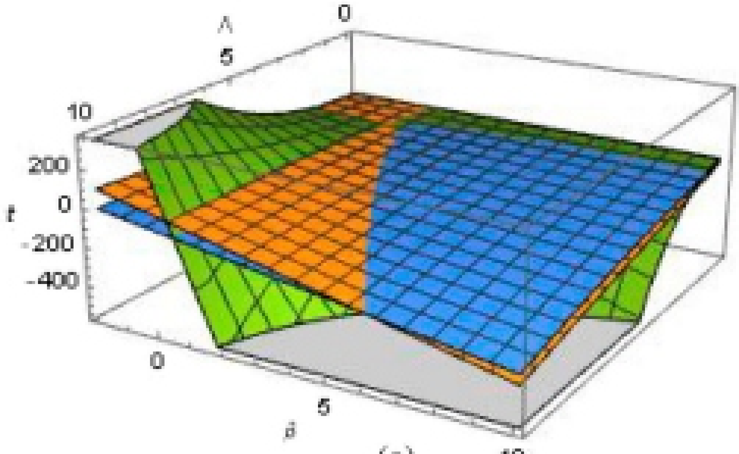


(a)

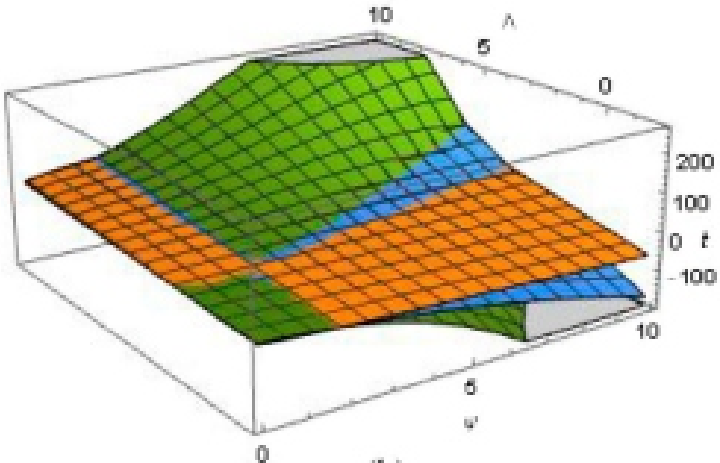


(b)

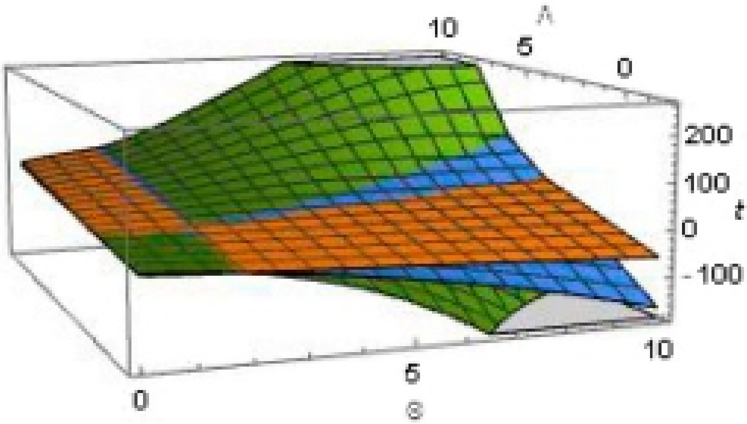


(c)

**Figure 4.** Comparison of results for $\iota = 0.5, 0.7$ and $0.9$. (a) Comparison of $\beta$ for $\iota = 0.5, 0.7$ and $0.9$, (b) comparison of $\psi$ for $\iota = 0.5, 0.7$ and $0.9$, and (c) comparison of $\Theta$ for $\iota = 0.5, 0.7$ and $0.9$.

and

$$\psi = 3\Lambda - 1.5\omega + 3\zeta - 2.25\omega(2-\iota)\left(1-\iota+\frac{\iota t^{\iota}}{\iota!}\right) + 1.125\Lambda(2-\iota)^2\left(1-\iota+\frac{\iota t^{\iota}}{\iota!}\right)^2$$
$$- 0.5625\omega(2-\iota)^2\left(1-\iota+\frac{\iota t^{\iota}}{\iota!}\right)^2 + 1.125\zeta(2-\iota)^2\left(1-\iota+\frac{\iota t^{\iota}}{\iota!}\right)^2$$
$$- 0.6328\omega(2-\iota)^3\left(1-\iota+\frac{\iota t^{\iota}}{\iota!}\right)^3 + \cdots, \tag{25}$$

and

$$\Theta = 3\Lambda + 3\omega - 1.5\zeta - 2.25\zeta(2-\iota)\left(1-\iota+\frac{\iota t^{\iota}}{\iota!}\right) + 1.125\Lambda(2-\iota)^2\left(1-\iota+\frac{\iota t^{\iota}}{\iota!}\right)^2$$
$$- 0.5625\zeta(2-\iota)^2\left(1-\iota+\frac{\iota t^{\iota}}{\iota!}\right)^2 + 1.125\omega(2-\iota)^2\left(1-\iota+\frac{\iota t^{\iota}}{\iota!}\right)^2$$
$$- 0.6328\zeta(2-\iota)^3\left(1-\iota+\frac{\iota t^{\iota}}{\iota!}\right)^3 + \cdots \tag{26}$$

which are the required solutions of the given system. Figures 1–3 are the graphical representations of the solutions for $\iota = 0.5, 0.7$ and $0.9$ (assuming $\omega = 1$ and $\zeta = 1$).

## 6. Conclusion

This study used the Atangana–Baleanu derivative to explore the multi-dimensional Navier–Stokes issue. We were able to resolve the issue and get their graphical representations with the use of the Laplace transform. Furthermore, we have demonstrated thevalidity of the methodology used and found that this innovative approach converges andis applicable to a range of fractional calculus problems. For ι = 0.5, 0.7 and ι = 0.9, graphsdepict the changes in the x-direction (β component), the y-direction (ψ component), andthe z-direction ( component). Apart from this, we have also shown the changes in β,φ and  for various values of ι (in Figure 4). We may employ a number of techniques toexamine the rate of change of flow. Even some graphical information may be found to aidin understanding the results and predicting the direction of future studies

## Acknowledgments

Awatif Muflih Alqahtani oversaw the investigation, analysed the findings, and organised the necessary research materials. The paper was written by Akanksha Shukla, who also completed all the

mathematical computations and data summaries for the graphs. The document was read, modified, and polished by both the authors.

**Disclosure statement**

No potential conflict of interest was reported by the author(s).

**Data availability statement**

The article has cited where statistics are available.

**ORCID**

Akanksha Shukla http://orcid.org/0000-0003-3193-516X

***References***

*[1] Temam R. Navier-Stokes equations: theory and numerical analysis. Vol. 343. American Math ematical Soc.; 2001.*

*[2] Debbi L. Well-posedness of the multidimensional fractional stochastic Navier–Stokes equations on the torus and on bounded domains. J Math Fluid Mech. 2016;18(1):25–69. doi:10.1007/s00021-015-0234-5*

*[3] Qu F, Sun D, Bai J. A new genuinely two-dimensional Riemann solver for multidimensional Euler and Navier–Stokes equations. Comput Phys Commun. 2019;243:1–11. doi:10.1016/j.cpc.2019.05.011*

*[4] Jin X, Cai S, Li H, et al. NSFnets (Navier-Stokes flow nets): physics-informed neural networks for the incompressible Navier-Stokes equations. J Comput Phys. 2021;426:109951. doi:10.1016/j.jcp.2020.109951*

*[5] Boscheri W, Dimarco G, Tavelli M. An efficient second order all mach finite volume solver for the compressible Navier–Stokes equations. Comput Methods Appl Mech Eng. 2021;374:113602. doi: 10.1016/j.cma.2020.113602*

*[6] Cheskidov A, Luo X. Sharp nonuniqueness for the Navier-Stokes equations. arXiv preprint arXiv:2009.06596; 2020.*

*[7] Ren J, Wang G, Ma B. Multidimensional extension and application of entropy-consistent scheme for Navier-Stokes equations on unstructured grids. In: 23rd AIAA Computational Fluid Dynamics Conference; 2017. p. 4403.*

*[8] Kilbas AA, Srivastava HM, Trujillo JJ. Theory and applications of fractional differential equations. Vol. 204. Elsevier; 2006.*

*[9] Mahmood S, Shah R, Khan H, et al. Laplace adomian decomposition method for multi dimensional time fractional model of Navier-Stokes equation. Symmetry. 2019;11(2):149. doi: 10.3390/sym11020149*

*[10] Humpherys J, Lyng G, Zumbrun K. Multidimensional stability of large-amplitude Navier–Stokes shocks. Arch Ration Mech Anal. 2017;226:923–973. doi: 10.1007/s00205-017-1147-7*

*[11] Mukhtar S, Shah R, Noor S. The numerical investigation of a fractional-order multidimensional model of Navier–Stokes equation via novel techniques. Symmetry. 2022;14(6):1102. doi: 10.3390/sym14061102*

*[12] Shah R, Khan H, Baleanu D, et al. The analytical investigation of time-fractional multidimensional Navier–Stokes equation. Alex Eng J. 2020;59(5):2941–2956. doi: 10.1016/j.aej.2020.03.029*

*[13] Baleanu D, Jajarmi A, Mohammadi H, et al. A new study on the mathematical modelling of human liver with Caputo–Fabrizio fractional derivative. Chaos Solitons Fractals.2020;134:109705. doi: 10.1016/j.chaos.2020.109705*

*[14] Jajarmi A, Baleanu D, Sajjadi SS, et al. Analysis and some applications of a regularized ψ–Hilferfractional derivative. J Comput Appl Math. 2022;415:114476. doi: 10.1016/j.cam.2022.114476*

*[15] Defterli O, Baleanu D, Jajarmi A, et al. Fractional treatment: an accelerated mass-spring system.Rom Rep Phys. 2022;74:122.*

*[16] Khan A, Khan ZA, Abdeljawad T, et al. Analytical analysis of fractional-order sequentialhybrid system with numerical application. Adv Contin Discrete Model. 2022;2022(1):1–19.doi: 10.1186/s13662-021-03638-9*

*[17] Khan A, Abdeljawad T, Khan H. a numerical scheme for the generalized derivative based on Lagrange interpolation polynomial. Fractals. 2022;30(05):2240180. doi:10.1142/S0218348X22401806*

*[18] Hussain S, Madi EN, Khan H, et al. A numerical and analytical study of a stochastic epidemicSIR model in the light of white noise. Adv Math Phys. 2022.*

*[19] Khan H, Alam K, Gulzar H, et al. A case study of fractal-fractional tuberculosis model in China: existence and stability theories along with numerical simulations. Math Comput Simul. 2022;198:455–473. doi: 10.1016/j.matcom.2022.03.009*

*[20] Shah A, Ali Khan R, Khan H. A fractional-order hybrid system of differential equations: existence theory and numerical solutions. Math Methods Appl Sci. 2022;45(7):4024–4034. doi: 10.1002/mma.v45.7*

*[21] Khan H, Ahmad F, Tunç O, et al. On fractal-fractional covid-19 mathematical model. Chaos*

[22] Xu C, Liu Z, Pang Y, et al. Stochastic analysis of a COVID-19 model with effects of vaccination and different transition rates: real data approach. Chaos Solitons Fractals. 2023;170:113395.doi: 10.1016/j.chaos.2023.113395

[23] Xu C, Farman M, Hasan A, et al. Lyapunov stability and wave analysis of covid-19 omicron variant of real data with fractional operator. Alex Eng J. 2022;61(12):11787–11802. doi:10.1016/j.aej.2022.05.025

[24] Yao SW, Farman M, Akgul A, et al. Simulations and analysis of Covid-19 as a fractional modelwith different kernels. Fractals. 2023;13:2340051.

[25] Amin M, Farman M, Akgül A, et al. Effect of vaccination to control COVID-19 with fractalfractional operator. Alex Eng J. 2022;61(5):3551–3557. doi: 10.1016/j.aej.2021.09.006

[26] Farman M, Amin M, Akgül A, et al. Fractal–fractional operator for COVID-19 (Omicron) variant outbreak with analysis and modeling. Results Phys. 2022;39:105630. doi:10.1016/j.rinp.2022.105630

[27] Malagi NS, Veeresha P, Prasanna GD, et al. Novel approach for nonlinear time-fractionalSharma-Tasso-Olever equation using Elzaki transform. Int J Optim Control Theor 2023;13(1):46–58. doi: 10.11121/ijocta.2023.1265

[28] Uçar S. Analysis of a basic SEIRA model with Atangana-Baleanu derivative; 2020.

[29] Uçar E, Özdemir N. New fractional cancer mathematical model via IL-10 cytokine and antiPD-L1 inhibitor. Fractal Fract. 2023;7(2):151. doi: 10.3390/fractalfract7020151

[30] Uçar E, Uçar S, Evirgen F, et al. A fractional SAIDR model in the frame of Atangana–Baleanuderivative. Fractal Fract. 2021;5(2):32. doi: 10.3390/fractalfract5020032

[31] Kashyap AJ, Bhattacharjee D, Sarmah HK. A fractional model in exploring the role of fear inmass mortality of pelicans in the Salton sea. Int J Optim Control Theor Appl. 2021;11(3):28–51.doi: 10.11121/ijocta.2021.1123

[32] Özdemir N, Uçar E. Investigating of an immune system-cancer mathematical model withMittag-Leffler kernel; 2020.

[33] Evirgen F, Esmehan UÇAR, Sümeyra UÇAR, et al. Modelling influenza a disease dynamicsunder Caputo-Fabrizio fractional derivative with distinct contact rates. Math Model NumerSimul Appl. 2023;3(1):58–72.

[34] Evirgen F, Ucar E, ÖZDEMIR N, et al. The impact of nonsingular memory on the mathematicalmodel of Hepatitis C virus. Fractals. 2023;1:2340065.

[35] Dubey RS, Mishra MN, Goswami P. Effect of Covid-19 in India-A prediction throughmathematical modeling using Atangana Baleanu fractional derivative. J Interdiscip Math.2022;25(8):2431–2444. doi: 10.1080/09720502.2021.1978682

[36] Kumbinarasaiah S. A novel approach for multi dimensional fractional coupled Navier–Stokesequation. SeMA J. 2022;80(2):261–282.

[37] Kumar S, Ghosh S, Samet B, et al. An analysis for heat equations arises in diffusion process using new Yang-Abdel-Aty-Cattani fractional operator. Math Methods Appl Sci. 2020;43(9):6062–6080. doi: 10.1002/mma.v43.9

[38] Villedieu N, Quintino T, Ricchiuto M, et al. Third order residual distribution schemes for the Navier–Stokes equations. J Comput Phys. 2011;230(11):4301–4315. doi: 10.1016/j.jcp.2010.12. 026

[39] Atangana A, Akgül A. Can transfer function and Bode diagram be obtained from Sumudu transform. Alex Eng J. 2020;59(4):1971–1984. doi: 10.1016/j.aej.2019.12.028

[40] Khedr WS. Classical fundamental unique solution for the incompressible Navier-Stokes equation in RN. J Appl Math Phys. 2017;5(4):939–952. doi: 10.4236/jamp.2017.54083

[41] Prakash A, Kumar M, Baleanu D. A new iterative technique for a fractional model of nonlinear Zakharov–Kuznetsov equations via Sumudu transform. Appl Math Comput. 2018;334:30–40.

[42] Abgrall R, De Santis D. Linear and non-linear high order accurate residual distribution schemes for the discretization of the steady compressible Navier–Stokes equations. J Comput Phys. 2015;283:329–359. doi: 10.1016/j.jcp.2014.11.031

[43] Gómez-Aguilar JF. Chaos in a nonlinear Bloch system with Atangana–Baleanu fractional derivatives. Numer Methods Partial Differ Equ. 2018;34(5):1716–1738. doi: 10.1002/num. v34.5

[44] Yang XJ, Abdel-Aty M, Cattani C. A new general fractional-order derivataive with Rabotnov fractional-exponential kernel applied to model the anomalous heat transfer. Therm Sci. 2019;23(3 Part A):1677–1681. doi: 10.2298/TSCI180320239Y

[45] Jain R, Arekar K, Shanker Dubey R. Study of Bergman's minimal blood glucose-insulin model by Adomian decomposition method. J Inf Optim Sci. 2017;38(1):133–149.

[46] Li S. Time advancement of the Navier-Stokes equations: p-adaptive exponential methods. J Flow Control Meas Visual. 2020;8(2):63–76. doi: 10.4236/jfcmv.2020.82004

[47] Malyk IV, Gorbatenko M, Chaudhary A, et al. Numerical solution of nonlinear fractional diffusion equation in framework of the Yang–Abdel–Cattani derivative operator. Fractal Fract. 2021;5(3):64. doi: 10.3390/fractalfract5030064

[48] Shrahili M, Dubey RS, Shafay A. Inclusion of fading memory to Banister model of changes in physical condition. Discrete Contin Dyn Syst S. 2020;13(3):881–888. doi: 10.3934/dcdss.2020051

[49] Chu YM, Ali Shah N, Agarwal P, et al. Analysis of fractional multi-dimensional Navier–Stokes equation. Adv Differ Equ. 2021;2021(1):1–18. doi: 10.1186/s13662-020-03162-2

[50] Singh BK, Kumar P. FRDTM for numerical simulation of multi-dimensional, timefractional model of Navier–Stokes equation. Ain Shams Eng J. 2018;9(4):827–834. doi: 10.1016/j.asej.2016.04.009

[51] Kavvas ML, Ercan A. Generalizations of incompressible and compressible Navier–Stokes equations to fractional time and multi-fractional space. Sci Rep. 2022;12(1):1–16. doi: 10.1038/s41598-022-20911-3

ISSN 2986 - 0776

# Data assimilation in 2D hyperbolic/parabolic systems using a stabilized explicit finite difference scheme run backward in time

**Alfred S. Carasso**
Applied and Computational Mathematics Division, National Institute of Standards and Technology, Gaithersburg, MD, USA

**A B S T R A C T**

*An artificial example of a coupled system of three nonlinear partial differential equations generalizing 2D thermoelastic vibrations, is used to demonstrate the effectiveness, as well as the limitations, of a non iterative direct procedure in data assimilation.A stabilized explicit finite difference scheme, run backward intime, is used to find initial values, [u(., 0), v(., 0), w(., 0)], that canevolve into a useful approximation to a hypothetical target result[u  (., Tmax), v  (., Tmax), w  (Tmax)], at some realistic Tmax > 0. Highlynon smooth target data are considered, that may not correspond toactual solutions at time Tmax. Stabilization is achieved by applying acompensating smoothing operator at each time step. Such smoothing leads to a distortion away from the true solution, but that distortion is small enough to allow for useful results. Data assimilation isillustrated using 512 × 512 pixel images. Such images are associatedwith highly irregular non smooth intensity data that severely challenge ill-posed reconstruction procedures. Computational experiments show that efficient FFT-synthesized smoothing operators,based on (−)q with real q > 3, can be successfully applied, even innonlinear problems in non-rectangular domains. However, an example of failure illustrates the limitations of the method in problemswhere Tmax, and/or the nonlinearity, are not sufficiently small.*

***ARTICLE HISTORY*** *Received 24 May 2023 Accepted 7 November 2023*

***KEYWORDS*** *Time reversed hyperbolic/parabolic systems; non smooth data assimilation; stabilized explicit backward marching scheme; nonlinear problems; numerical experiments*

***MATHEMATICS SUBJECT*** *CLASSIFICATIONS 35M31; 35R25; 65M12; 65M30*

## 1. Introduction

In dissipative evolution equations, data assimilation refers to the ill-posed problem of finding initial values at time t = 0, that can evolve into useful approximations to givenhypothetical or desired target data, at a suitable time Tmax > 0. There is significant geophysical research activity in this area, using computationally intensive iterative methods,including neural networks coupled with machine learning, [1–15]. However, non iterativedirect procedures, based on stabilized explicit finite difference schemes marched backwardin time, while lagging the nonlinearities at the previous time step, may be a useful alternative in several data assimilation problems. This is demonstrated in [16,17] for the caseof 2D nonlinear advection diffusion equations. The present paper further illustrates the capabilities of such explicit schemes, by considering more challenging test problems, involving hyperbolic/parabolic systems, and consisting ofthree coupled 2D nonlinear evolution equations in three unknown functions.Backward marching stabilized explicit schemes have been successfully used in severalill-posed backward recovery problems, [18–25]. A compensating smoothing operator isapplied at every time step to prevent the computational instability that would otherwiseoccur, [26, p.59]. While such smoothing leads to a distortion away from the true solution,in many problems of interest, the accumulated error is small, and does not prevent usefulresults.In the backward recovery problems discussed in [18–25], initial values at t = 0 aresought from relatively smooth noisy data at time Tmax > 0, data that are known to approximate an actual solution to within a known small δ > 0, in an appropriate Lp norm. Inthe successful numerical experiments discussed in [18–25], the data at t = 0 are typically chosen to be grey-scale images, defined by highly non smooth intensity data that arenot easily synthesized mathematically. An example of such an image is shown in Figure 1below.

However, the data assimilation problem is fundamentally different from the above backward recovery problem. In the data assimilation case, the target data at time Tmax > 0 maynot be smooth, may not correspond to an actual solution, and may differ from an actualsolution by an unknown large δ > 0 in that same Lp norm. Moreover, it may not be possible to find useful initial values at t = 0. Unexpectedly, as shown in [16,17], and as will beshown below, stabilized explicit schemes may sometimes be useful in the data assimilationproblem, by using more aggressive smoothing at each time step.

In the present paper, the backward recovery problem in the coupled system discussedin [22] is of particular interest. In [22, Figures 2 and 3], the complex forward evolution ofthe three independent non negative initial images at t = 0, is made evident. In the solution at time Tmax = $7.5 \times 10^{-3}$, each image displays the influence of the other two images

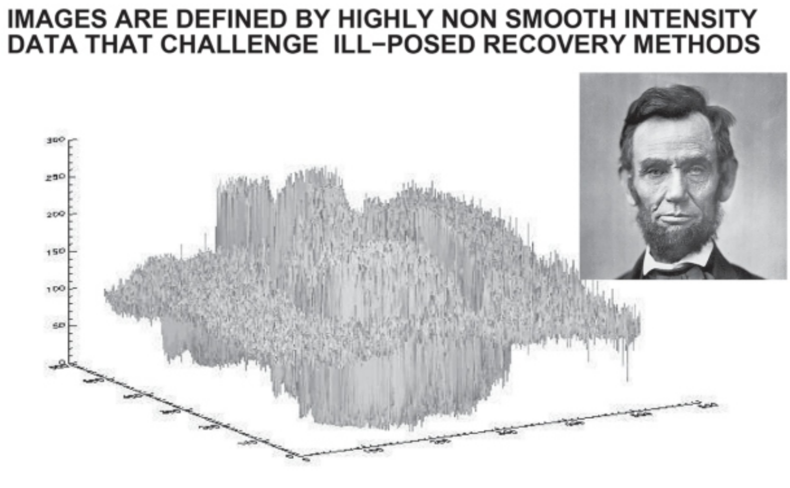


**Figure 1.** Plot of intensity values $u(x, y)$ versus $(x, y)$ in 512 × 512 pixel Abraham Lincoln image. Intensity values range from 0 to 255, and result in highly non smooth surface. Such images provide excellent test examples for ill-posed reconstruction methods.

as well as negative values. Nevertheless, as shown in the last row in Figure 2, successful recovery of the initial data was found possible from the data at Tmax.

As will now be shown, the stabilized explicit scheme developed in [22] can be useful evenin more challenging data assimilation problems. With positive constants α, β, and with L alinear or nonlinear second order elliptic differential operator in two space variables (x, y),defined on bounded domain in R2 with a smooth boundary ∂, the following systemwill be studied

$$
\begin{aligned}
&u_t = -\beta Lu - \alpha Lv,\\
&v_t = Lw + \alpha Lu,\\
&w_t = -Lv, \qquad\qquad\qquad\qquad\qquad\qquad\qquad\qquad\qquad\qquad\qquad\qquad (1)\\
&u(x,y,0) = f(x,y), \quad v(x,y,0) = g(x,y), \quad w(x,y,0) = h(x,y),\\
&u(x,y,t) = v(x,y,t) = w(x,y,t) = 0, \quad (x,y,t) \in \partial\Omega \times [0, T_{\max}].
\end{aligned}
$$

value of Tmax > 0, the following data assimilation problem is discussed: find initial values [u(., 0), v(., 0),w(., 0)], that can evolve according to Equation (1), into a useful approximation to the desired data at time Tmax. Here, non smooth hypothetical data are consideredthat may not correspond to an actual solution of Equation (1) at time Tmax.

In the simplest linear case with L = −,w = z, v = zt, the above system correspondsto the thermoelastic plate problem ztt = −2z − αu, ut = βu + αzt, with hingedboundary conditions, u = z = z = 0 on ∂. This case has been studied by severalauthors [27–30], and the solution operator is known to be a holomorphic semigroup.In the developments below, the principal results from [22] that will be needed willbe listed without proof, using notation identical to that used in [22] for the reader'sconvenience. In Section 2, the linear selfadjoint problem is discussed. In Section 3, Theorems 3.1 and 3.2 establish error estimates for the forward and backward explicit schemes.These estimates imply limitations on the class of problems wherein the explicit schememay be useful, as shown in Equation (17) in Section 3.1. Section 4 discusses the useof smoothing operators based on the Laplacian, and leads to Theorems 4.1 and 4.2.Section 5 describes nonlinear data assimilation experiments. Finally, Section 6 offers someconcluding remarks.

While there are no new theoretical results in the present paper other than the error estimate in Equation (17), the unexpected success of stabilized explicit schemes in the more challenging data assimilation problems considered here and in [16,17], is of great interest.The numerical experiments discussed in Section 5 below, together with those in [16,17],invite valuable scientific debate and comparisons with what might be achieved on similar examples, using artificial intelligence methods based on neural networks coupled withmachine learning.

**2. Linear autonomous selfadjoint L in Equation (1)**

In Equation (1), let <, > and 2, respectively denote the scalar product and normon L2() and let L denote a linear, second order, time-independent, positive definite selfadjoint variable coefficient elliptic differential operator in , with homogeneous Dirichet boundary conditions on ∂. Let {φm}∞ m=1, be the complete set of orthonormal eigenfunctions for L on , and let {λm}∞ m=1, sat

$$0 < \lambda 1 \leq \lambda 2 \leq \cdots \leq \lambda m \leq \cdots \uparrow \infty, \qquad (2)$$

be the corresponding eigenvalues. The initial value problem Equation (1) becomes ill-posed when the time direction isreversed. Such time-reversed computations are contemplated by allowing for possible negative time steps t in the explicit difference scheme Equation (8) below. With λm as inEquation (2), the positive constants α, β and the operator L as in Equation (1), fix ω > 0and p>1. Given t, define ν, , Q, ζm,rm, as follows:

$$\nu = (3 + \alpha + \alpha 2 + 2\beta), \ = \nu(I + L), \ Q = \exp(-\omega|t|p),$$

$$m = \nu(1 + \lambda m) > 3, \ rm = \exp -\omega|t|(\zeta m)p, \ m \geq 1. \qquad (3)$$

In the present discussion, the family {λm, φm} in Equation (2), is assumed known or precomputed. However, as will be illustrated below, in many practical computations, a different smoothing operator, based on a substitute elliptic operator L† with known characteristicpairs, such as the negative Laplacian, can be used instead. Since p>1 has non integer values typically, both the operators p and Q in Equation (3), must be synthesized in termsof the characteristic pairs {λm, φm} of L. With ζm,rm as in Equation (3), define for every of the characteristic pairs {λm, φm} of L. With ζm,rm as in Equation (3), define for every h ∈ L2(),

$$ph = \infty m{=}1(\zeta m)p < h, \varphi m > \varphi m, \ Qh = \infty m{=}1rm < h, \varphi m > \varphi m. \qquad (4)$$

Let G, S, and P, be the following 3 × 3 matrices

$$G = \begin{bmatrix} -\beta L & -\alpha L & 0 \\ \alpha L & 0 & L \\ 0 & -L & 0 \end{bmatrix}, \quad S = \begin{bmatrix} Q & 0 & 0 \\ 0 & Q & 0 \\ 0 & 0 & Q \end{bmatrix}, \quad P = \begin{bmatrix} \Lambda^p & 0 & 0 \\ 0 & \Lambda^p & 0 \\ 0 & 0 & \Lambda^p \end{bmatrix}. \qquad (5)$$

Let W be the three component vector [u, v,w] T. We may rewrite Equation (1) as theequivalent first order system,

$$Wt = GW, 0 < t \le Tmax, W(\cdot, 0) = [f , g, h]T. \qquad (6)$$

An explicit time-marching finite difference scheme will be studied for Equation (6), in which only the time variable is discretized, while the space variables remain continuous.With a given positive integer N, let |t| = Tmax/N be the time step magnitude, and let Wndenote W(·, nt), n = 0, 1, ... N. If W(·, t) is the unique solution of Equation (6), then

$$Wn+1 = Wn + tGWn + \tau\ n, \qquad (7)$$

where the 'truncation error' τ n = 12 (t)2G2W(·, t˜), with n|t| < t˜ < (n + 1)|t|. WithG and S as in Equation (5), let R be the linear operator R = S + tSG. Using the smoothingoperator S, we consider approximating Wn with Un ≡ [un, vn,wn]T, where

$$Un+1 = SUn + tSGUn \equiv RUn, n = 0, 1, ...(N - 1), U0 = [f , g, h]T. \qquad (8)$$

With t > 0 and the data U0 at time t = 0, the forward marching scheme in Equation (8)

aims to solve a well-posed problem. However, with t < 0, together with appropriate data U0 at time Tmax, marching backward from Tmax in Equation (8) attempts to solve an illposed problem. It remains to be seen whether Un can be a useful approximation to Wn, by proper choices of ω, p, and |t|. Define the following norms for three component vectorssuch as W(·, t) and Un,

$$\begin{aligned} \| W(\cdot,t) \|_2 &= \left\{ \| u(\cdot,t) \|_2^2 + \| v(\cdot,t) \|_2^2 + \| w(\cdot,t) \|_2^2 \right\}^{1/2}, \\ \| U^n \|_2 &= \left\{ \| u^n \|_2^2 + \| v^n \|_2^2 + \| w^n \|_2^2 \right\}^{1/2}, \\ |||W|||_{2,\infty} &= \sup_{0 \le t \le T_{\max}} \{ \| W(\cdot,t) \|_2 \}. \end{aligned} \qquad (9)$$

Lemma 2.1 below is proved in [22].

**Lemma 2.1:** *With $p > 1$, and $\zeta_m, r_m$, as in Equation (3), fix a positive integer J, and choose $\omega \ge (\zeta_J)^{1-p}$. Then,*

$$r_m\,(1 + |\Delta t|\zeta_m) \le 1 + |\Delta t|\zeta_J, \quad m \ge 1. \qquad (10)$$

## 3. Error estimates and stabilization penalties

Explicit time differencing in systems of partial differential involving heat conduction, generally requires stringent Courant stability restrictions on the time step t. The stabilizing smoothing operator S in the explicit scheme in Equation (8) leads to unconditional stability, but at the cost of introducing a small error at each time step. If the accumulated errorat the final time Tmax is sufficiently small, the stabilized explicit scheme would offer considerable advantages in the computation of multidimensional problems on fine meshes.Theorems 3.1 and 3.2 below are proved in [22].

Theorem 3.1: With t > 0, let Wn be the unique solution of Equation (6) at t = nt. Let Un be the corresponding solution of the forward explicit scheme in Equation (8), andlet p, ζJ, ω, be as in Lemma 2.1. If Z(t) ≡ Un − Wn, denotes the error at t = nt, n =0, 1, 2, ... , N, we have

$$\begin{aligned} &Z(t)\ 2 \leq et\zeta J\ \ Z(0)\ 2 + \omega(et\zeta J - 1)/\zeta J|||PW|||2,\infty + (et\zeta J - 1)/\zeta J \\ &\omega t\ |||PGW|||2,\infty + (t/2)|||G2W|||2,\infty. \qquad (11) \end{aligned}$$

In the forward problem, as t ↓ 0, we are left with the error originating in the possibly erroneous initial data U0 = [f , g, h]T, together with the stabilization penalty represented bythe second term in Equation (11). These errors grow monotonically as t ↑ Tmax. Clearly, ifTmax is large, the accumulated distortion may become unacceptably large as t ↑ Tmax, andthe stabilized explicit scheme is not useful in that case.Marching backward from t = Tmax in the backward problem, solutions exist only fora restricted class of data satisfying certain smoothness constraints. Such data are seldomknown with sufficient accuracy. This is especially true of the hypothetical data W (·, Tmax)in the present data assimilation problem. It will be assumed that the given dataW (·, Tmax),differ from the necessary exact data W(·, Tmax), by an unknown amount δ in the $\mathcal{L}^2(\Omega)$
norm.

$$W\ \ (\cdot, Tmax) - W(\cdot, Tmax)\ 2 \leq \delta. \qquad (12)$$

This leads to the following result.

**Theorem 3.2:** With t < 0, let Wn be the unique solution of the forward well-posed problem in Equation (6) at s = Tmax − n|t|. Let Un be the solution of the backward explicit scheme in Equation (8), with initial data U(0) = W (·, Tmax), as in Equation (12). Letp, ζJ, ω, be as in Lemma 2.1. If Z(s) ≡ Un − Wn, denotes the error at s = Tmax − n|t|, n =0, 1, 2, ... , N, we have, with δ as in Equation (12),

$$Z(s)\ 2\leq \delta\ en|t|\zeta J + \omega(en|t|\zeta J - 1)/\zeta J|||PW|||2,\infty$$
$$+(en|t|\zeta J - 1)/\zeta J\ \omega|t|\ |||PGW|||2,\infty + (|t|/2)|||G2W|||2,\infty \quad . \qquad (13)$$

## 3.1. Application to data assimilation

In Theorems 3.1 and 3.2 above, define the constants K1 through K5 as follows, and consider the values shown in Table 1 below.

$$K1 = e\zeta JTmax\ ,\ K2 = \omega(e\zeta\ Tmax - 1)/\zeta J,\ K3 = |t|K2,\ K4 = K3/(2\omega),$$
$$K5 = K2|||PW|||2,\infty + K3|||PGW|||2,\infty + K4|||G2\ W|||2,\infty. \qquad (14)$$

As outlined in the Introduction, data assimilation applied to the system in Equation (1), is the problem of finding initial values [u(., 0), v(., 0),w(., 0)], at t = 0, that can evolveinto useful approximations to W (·, Tmax), the given hypothetical data at an appropriatetime Tmax > 0. If the true solution in Equation (1) does not have exceedingly valuesfor |||PW|||2,∞, |||PGW|||2,∞, or |||G2W|||2,∞, the parameter values chosen in Table 1,together with Theorem 3.2, indicate that marching backward to time t = 0 from the data W at Tmax, leads to an error Z(0), satisfying

$$Z(0)\ 2\leq \delta K1 + K5, \qquad (15)$$

with the constant K5 defined in Equation (14) presumed small. Next, from Theorem 3.1, marching forward to time Tmax using the inexact computed initial values U(·, 0), leads toan error Z(Tmax), satisfying

$$Z(Tmax)\ 2\leq K1(\delta K1 + K5) + K5. \qquad (16)$$

The error Z(Tmax) in Theorem 3.1 is the difference at time Tmax, between the unknown unique solution W(·, t) in Equation (6), and the computed numerical approximation to

**Table 1.** Values of $K_1$ through $K_4$ in Equation (14), with following parameter values: $T_{\max} = 6 \times 10^{-4}, |\Delta t| = 3 \times 10^{-7}, p = 3.5, \zeta_J = 3017, \omega = \zeta_J^{(1-p)} = 2 \times 10^{-9}$.

| $K_1 = e^{\zeta_J T_{\max}}$ | $K_2 = (\zeta_J)^{-p}(K_1 - 1)$ | $K_3 = \lvert\Delta t\rvert K_2$ | $K_4 = K_3/(2\omega)$ |
|---|---|---|---|
| $K_1 < 6.2$ | $K_2 < 3.5 \times 10^{-12}$ | $K_3 < 1.1 \times 10^{-18}$ | $K_4 < 2.8 \times 10^{-10}$ |

it, U(·, t), provided by the stabilized forward explicit scheme. However, W (·, Tmax) −W(·,(Tmax) 2≤ δ, if W (·, Tmax) is the given hypothetical data. Hence, using the triangleinequality, we find

$$W^*(\cdot, T_{max}) - U(\cdot, T_{max})\ 2 \leq \delta(1 + K2\ 1\ ) + K5(1 + K1). \qquad (17)$$

Therefore, data assimilation is successful only if the inexact computed initial values U(·, 0) at t = 0, lead to a sufficiently small right hand side in Equation (17). Clearly, the value ofζJTmax, together with the unknown value of δ, will play a vital role.

**4. Using the Laplacian for smoothing when L has variable coefficients**

As previously noted, the developments in Sections 2 and 3 presuppose knowledge of the characteristic pairs of the variable coefficient elliptic operator L, or the precomputation ofa sufficiently large number of such pairs. However, it is often possible to use a substitutesmoothing operator Q†, based on a different elliptic operator with known characteristicpairs.Let denote the Laplacian operator in , with homogeneous Dirichlet boundary conditions on ∂. With ν, L, , as in Equation (3), let = ν(I − ). For any real q>1 and > 0, define

$$Q = \exp\{-|t|\ q\}, \qquad (18)$$

Closed form expressions for the eigenfunctions of the Laplacian are known for specific domains that are important in applications, including rectangles, circles, and spheres [31].On such domains, it may be advantageous to construct smoothing operators Q basedon the Laplacian, in lieu of the smoothing operator Q in Equation (3). Such a programis feasible for those differential operators L for which the following result is valid: Givenany ω > 0, and p > 1, there exist > 0, and real q ≥ p, such that for all g ∈ L2() andsufficiently small |t|,

$$\exp\{-|t|\ q\}g\ 2 \leq \exp\{-\omega|t|p\}g\ 2, \Leftarrow\Rightarrow\ Qg\ 2 \leq Qg\ 2\ . \qquad (19)$$

The linear operator H = (exp{−|t| q})(exp{ω|t|p})is well-defined on the range of (exp{−ω|t|p}), which is dense in L2(). The inequality in Equation (19) would follow it can be shown that H can be extended to a bounded operator on all of L2(), with H 2≤ 1.

Equation (19) appears to be validated in numerous computational experiments. Resultsof a somewhat similar nature are known in the theory of Gaussian estimates for heatkernels. See e.g. [32–35], and the references therein. Let S and P be the following 3 × 3 matrices

$$S_\Delta = \begin{bmatrix} Q_\Delta & 0 & 0 \\ 0 & Q_\Delta & 0 \\ 0 & 0 & Q_\Delta \end{bmatrix}, \quad P_\Delta = \begin{bmatrix} \Gamma^q & 0 & 0 \\ 0 & \Gamma^q & 0 \\ 0 & 0 & \Gamma^q \end{bmatrix}.$$

The Laplacian stabilized explicit scheme corresponding to Equation (8) is given by

$$U^{n+1} = S_\Delta U^n + \Delta t S_\Delta G U^n \equiv R_\Delta U^n, \quad n = 0, 1, \dots (N-1), \quad U^0 = [f, g, h]^T, \quad (21)$$

**Remark 4.1:** Useful pairs (, q) in the Laplacian stabilized scheme in Equation (21) are generally found interactively after relatively few trials. In many data assimilationexperiments, typical values satisfy 2 < q < 4, 10−10 ≤ ≤ 10−6.

**Theorem 4.1:** Let p, ζJ, ω, be as in Lemma 2.1, and choose > 0 and q ≥ p, such that Equation (19) is satisfied. With t > 0, let Wn be the unique solution of Equation (6)at t = nt, and let Un be the corresponding solution of the forward explicit scheme inEquation (21). If Z(t) ≡ Un − Wn, denotes the error at t = nt, n = 0, 1, 2, ... , N, then

Z(t) 2 ≤ etζJ Z(0) 2 + (etζJ − 1)/ζJ|||PW|||2,∞
+ (etζJ − 1)/ζJ t |||PGW|||2,∞ + (t/2)|||G2W|||2,∞ . (22)

**Theorem 4.2:** Let p, ζJ, ω, be as in Lemma 2.1, and choose > 0 and q ≥ p, such that Equation (19) is satisfied. With t < 0, let Wn be the unique solution of the forward wellposed problem in Equation (6) at s = Tmax − n|t|. Let Un be the solution of the backwardexplicit scheme in Equation (21), with initial data U(0) = W (·, Tmax) as in Equation (12).If Z(s) ≡ Un − Wn, denotes the error at s = Tmax − n|t|, n = 0, 1, 2, ... , N, we have,with δ as in Equation (12),

Z(s) 2 ≤ δ en|t|ζJ +(en|t|ζJ − 1)/ζJ|||PW|||2,∞
+(en|t|ζJ − 1)/ζJ |t| |||PGW|||2,∞ + (|t|/2)|||G2W|||2,∞ .(23)

**Remark 4.2:** In rectangular regions, the Fast Fourier Transform is an efficient tool for synthesizing q for positive non-integer q, when = ν(I − ). In [22, Section 6.1], anapproach to the use of FFT Laplacian smoothing in non rectangular regions is discussed,and that approach is the one used in the numerical experiments described below.

## 5. Nonlinear computational experiments with FFT Laplacian smoothing

While the theoretical developments in Sections 2, 3, and 4, are restricted to linear, autonomous, selfadjoint elliptic operators L, the stabilized scheme in Equation (21) maybe applied to more general problems. Let  be the open elliptical region in the (x, y) plane,defined by

$$0 < x, y < 1, 2.75(x - 0.5) 2 + 1.75(y - 0.5) 2 \leq 1. \qquad (24)$$

Let L be the nonlinear differential operator defined as follows on functions z(x, y, t) on  × (0, Tmax):

$$Lz = -0.001s(z)\triangledown.\{q(x, y, t)\triangledown z\} - \gamma (zzx + zzy), (25)$$

where

$$s(z) = \exp\{0.0075 |z]\}, \gamma = 0.01,$$
$$q(x, y, t) = \exp(10t)1 + 2 \sin \pi x \sin \pi y \qquad \geq 1.(26)$$

With α = β = 3, and (x, y, t) ∈  × (0, Tmax), we now consider the system described in Equation (1). Such a system differs from that considered in Section 2, in that the operator L in Equation (25) is nonlinear, time-dependent, a theoretical developments in Sections 2, 3, and 4, do not apply to Equation (1) with L as in Equation (25). In particular, the hypothesis in Equation (19) is not applicable. Nevertheless, backward reconstruction of solutions to Equation (1) can still be attempted usingthe Laplacian stabilized explicit scheme in Equation (21). The above system is primarily of mathematical interest, and may not reflect any actual physical problem. It is designed totest the robustness of the stabilized explicit scheme in the presence of nonlinearities.

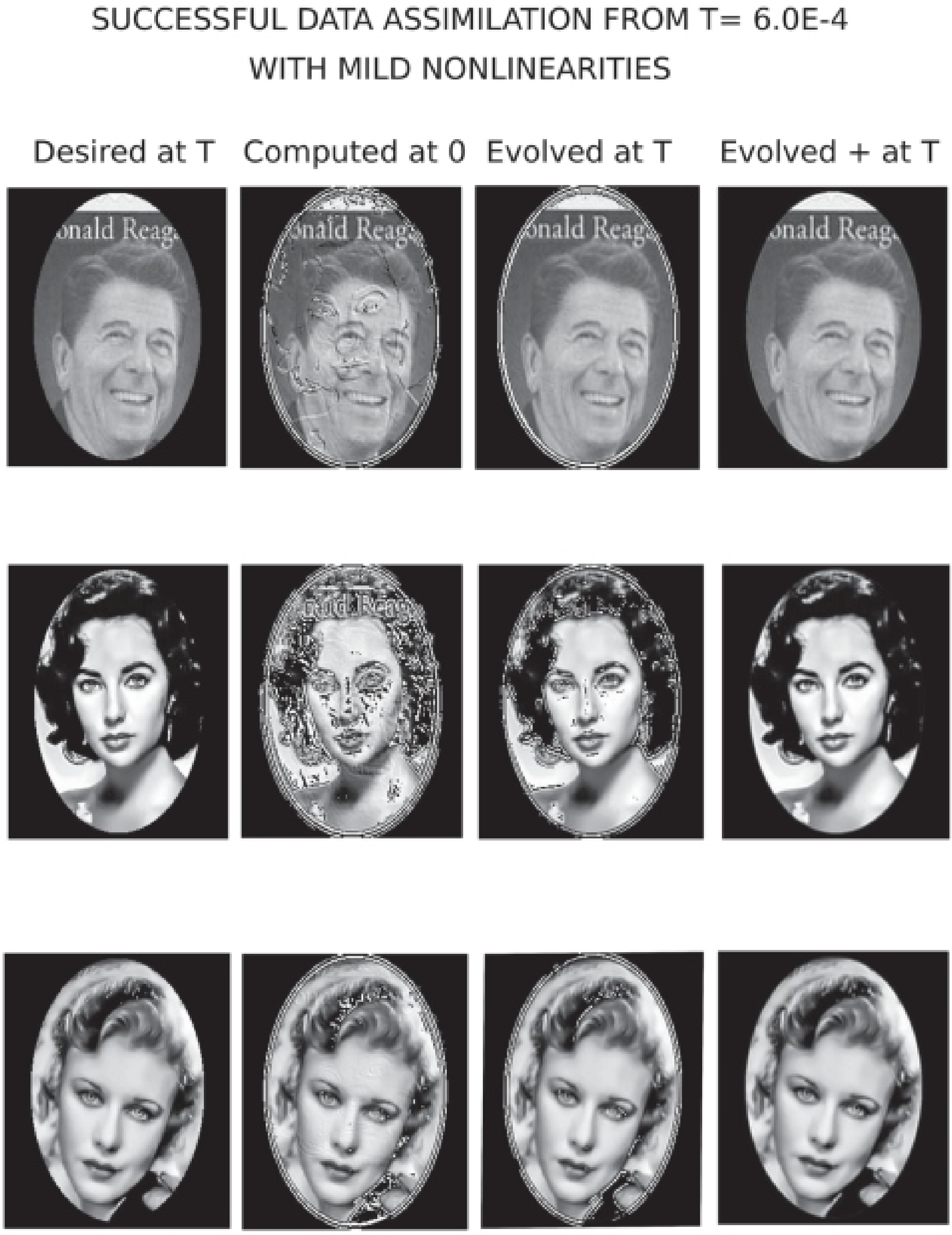


**Figure 2.** Leftmost column is the hypothetical data $W^*(\cdot, T_{\max})$. Second column from left is $U(\cdot, 0)$, the backward computation to $t = 0$, using the hypothetical data at $T_{\max}$. Third column from left is the forward evolution at time $T_{\max}$, of the computed initial data $U(\cdot, 0)$ at $t = 0$, shown in previous column. Last column is the result of applying the constraint $0 \leq z(x, y) \leq 255$ to the data in the previous column.

As outlined in the Introduction, data assimilation experiments will be conducted using highly non smooth hypothetical data, associated with 512 × 512 pixel gray scale imagesprescribed at a time Tmax. These data may not correspond to any actual solution of the system in Equation (1) at time Tmax. Nevertheless, the stabilized scheme in Equation (21) willbe used to find corresponding initial data at t = 0 that might evolve into useful approximations to the desired data at Tmax. This may not always be possible. The values for

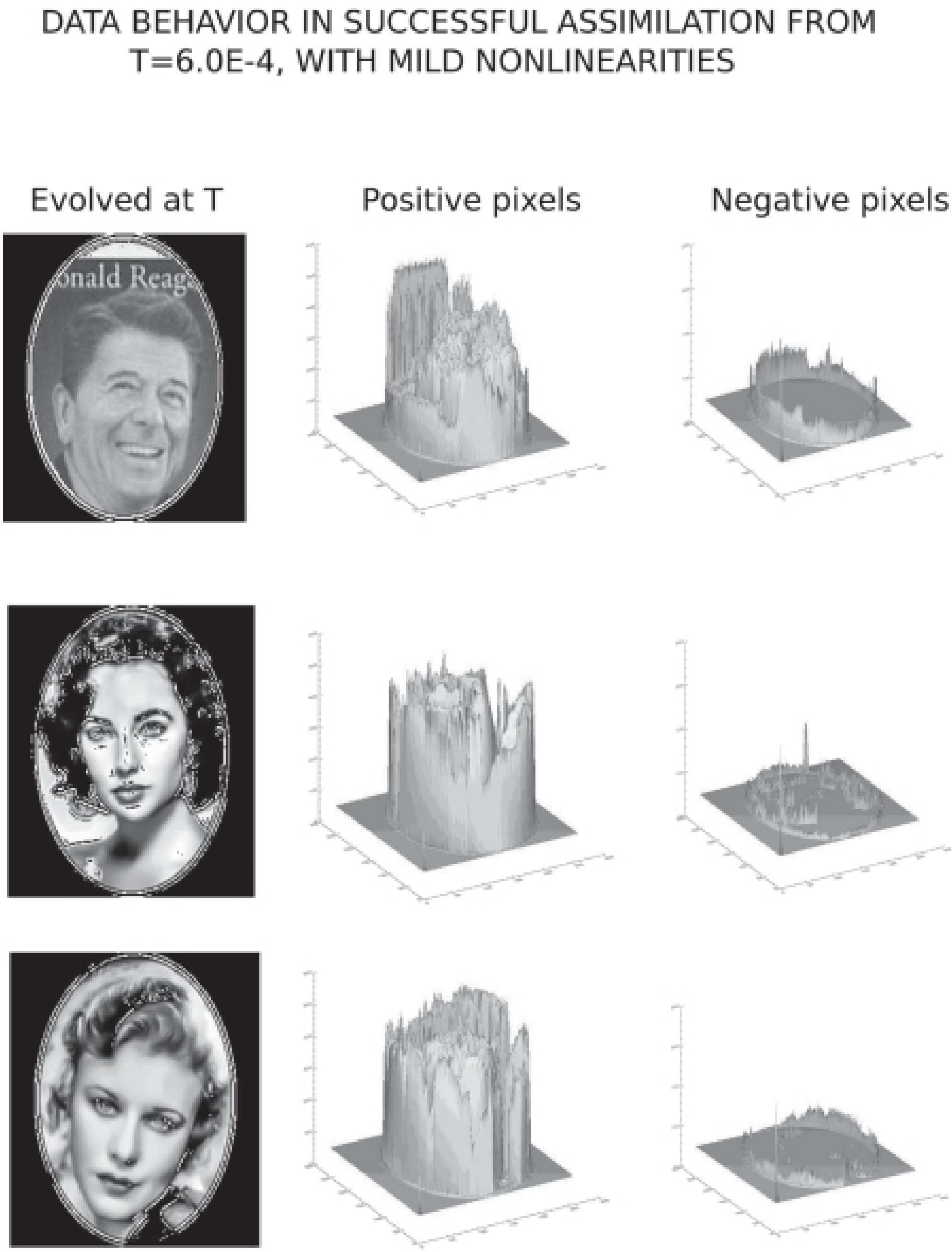


**Figure 3.** Magnitudes of positive and negative pixel values in 'Evolved' column in Figure 2. The relatively small negative values account for the successsful data assimilation, the small $\mathcal{L}^1$ relative errors in Table 2, as well as the behavior in the 'Evolved +' column in Figure 2.

**Table 2.** Successful data assimilation with mild nonlinearity.

| *Image* | *Desired at* $T_{max}$ | *Computed at 0* | *Evolved at* $T_{max}$ | $\mathcal{L}^1$ *Err* |
|---|---|---|---|---|
| *Reagan* | $0 \le u \le 255$ | $-153 \le u \le 360$ | $-29 \le u \le 316$ | 5% |
| *Taylor* | $0 \le v \le 255$ | $-122 \le v \le 395$ | $-37 \le v \le 285$ | 6% |
| *Rogers* | $0 \le w \le 255$ | $-33 \le w \le 286$ | $-25 \le w \le 283$ | 4% |

Note: Range of data values and $\mathcal{L}^1$ relative errors, from target at $T_{max} = 6.0 \times 10^{-4}$.

t, p, ω, ζJ, shown in Table 1, together with  = 6.0 × 10−12, q = 3.875, will be used in the experiments described below.The first experiment is summarized in Figures 2, 3, and Table 2. The columnin Figure 2 represents the hypothetical or desired data at Tmax = 6.0 × 10−4, consistingof the Ronald Reagan postage stamp image, u(x, y, Tmax), the Elizabeth Taylor image,v(x, y, Tmax), and the Ginger Rogers image, w(x, y, Tmax). Each of these three imageshas pixel values ranging from 0 to 255. Marching backward from these data producesthe second from the left column in Figure 2, corresponding to t = 0. The artifacts inthe images in that second column reflect the negative values that necessarily result att = 0, given the desired data at Tmax. This is documented in Table 2. Next, marchingforward to time Tmax, using these second column data, produces the resulting evolveddata in the third from the left column in Figure 2. The image artifacts in that third column have been noticeably reduced, and Table 2 confirms that the range of values inthe evolved data at Tmax, is a useful approximation to the desired range of values inthe leftmost column of Figure 2. Indeed, the L1 relative errors range from 4% to 6% inTable 2.

Figure 3 displays the intensity data associated with the evolved data at Tmax, shown in the third column of Figure 2. In the rightmost column of Figure 3, the magnitudes ofthe negative pixel values are shown, and compared with the significantly larger positivepixel values in the middle column of Figure 3. The results in Table 2 and Figure 3, suggestapplication of the following constraint to the evolved data at Tmax in the third column ofFigure 2, namely, replace any pixel value exceeding 255 by the value 255, and replace anynegative pixel value by the value zero. This results in the rightmost column 'Evolved +' inFigure 2, which is almost indistinguishable from the leftmost column in Figure 2. However, less successful results are obtained in this experiment when larger values of Tmax are used.

In the  next experiment, summarized in Figures 4, 5, and Table 3, a smaller value of Tmax is used, Tmax = 4.5 × 10−4, but a stronger nonlinearity is considered in the systemin Equation (1), with γ = 0.05 in Equation (26). Moreover, different hypothetical data areused in the leftmost column of Figure 4, with the USAF Resolution chart replacing theRonald Reagan stamp image, and an Alphanumeric image replacing the Ginger Rogersimage. Data assimilation is highly unsuccessful in this case, with severe artifacts in theimages in the second and third columns from the left in Figure 4, reflecting the very largenegative and positive pixel values shown in Table 3. Now, the L1 relative errors range from89% to 103% in Table 3. In Figure 5, the intensity data associated with the evolved data at Tmax, shows equally large positive and negative pixel values. Applying the constraint $0 \le z(x, y) \le 255$, is not meaningful in this case, and produces the barely recognizablerightmost column 'Evolved +' in Figure 4

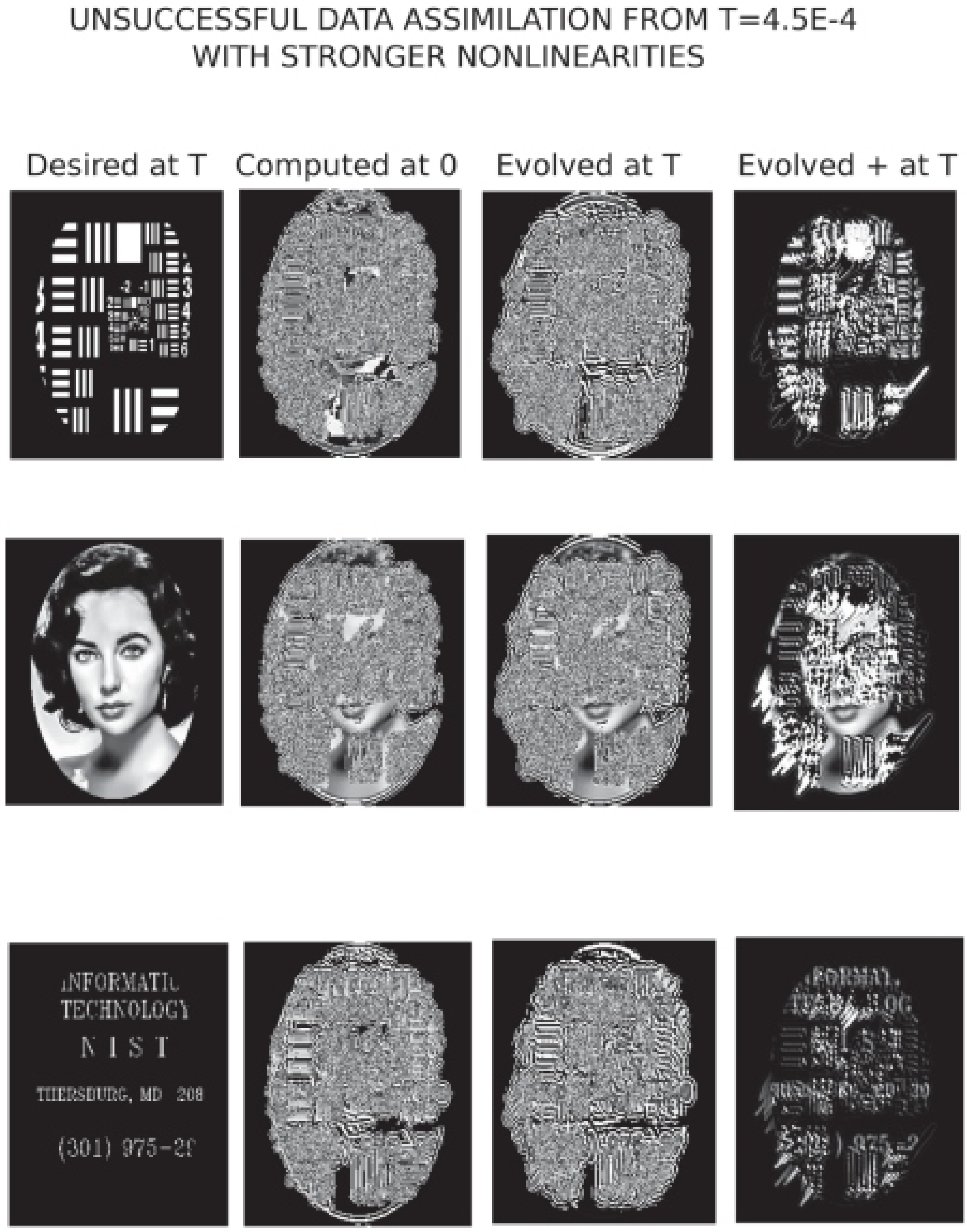


**Figure 4.** Leftmost column is the hypothetical data $W^*(\cdot, T_{\max})$. Second column from left is $U(\cdot, 0)$, the backward computation to $t = 0$, using the hypothetical data at $T_{\max}$. Third column from left is the forward evolution at time $T_{\max}$, of the computed initial data $U(\cdot, 0)$ at $t = 0$, shown in previous column. Last column is the result of applying the constraint $0 \le z(x, y) \le 255$ to the data in the previous column.

## 6. Concluding remarks

In [16,17], and the present paper, non iterative direct methods, based on stabilized explicit backward marching finite difference schemes, were applied to 2D data assimilation problems, involving highly non smooth target data that did not correspond to actual solutionsat time Tmax > 0. Successful and unsuccessful assimilation examples were presented. Ofsignificant interest is whether equally good or better results can be obtained, on these orsimilar examples, using iterative methods such as are discussed in [1–15]

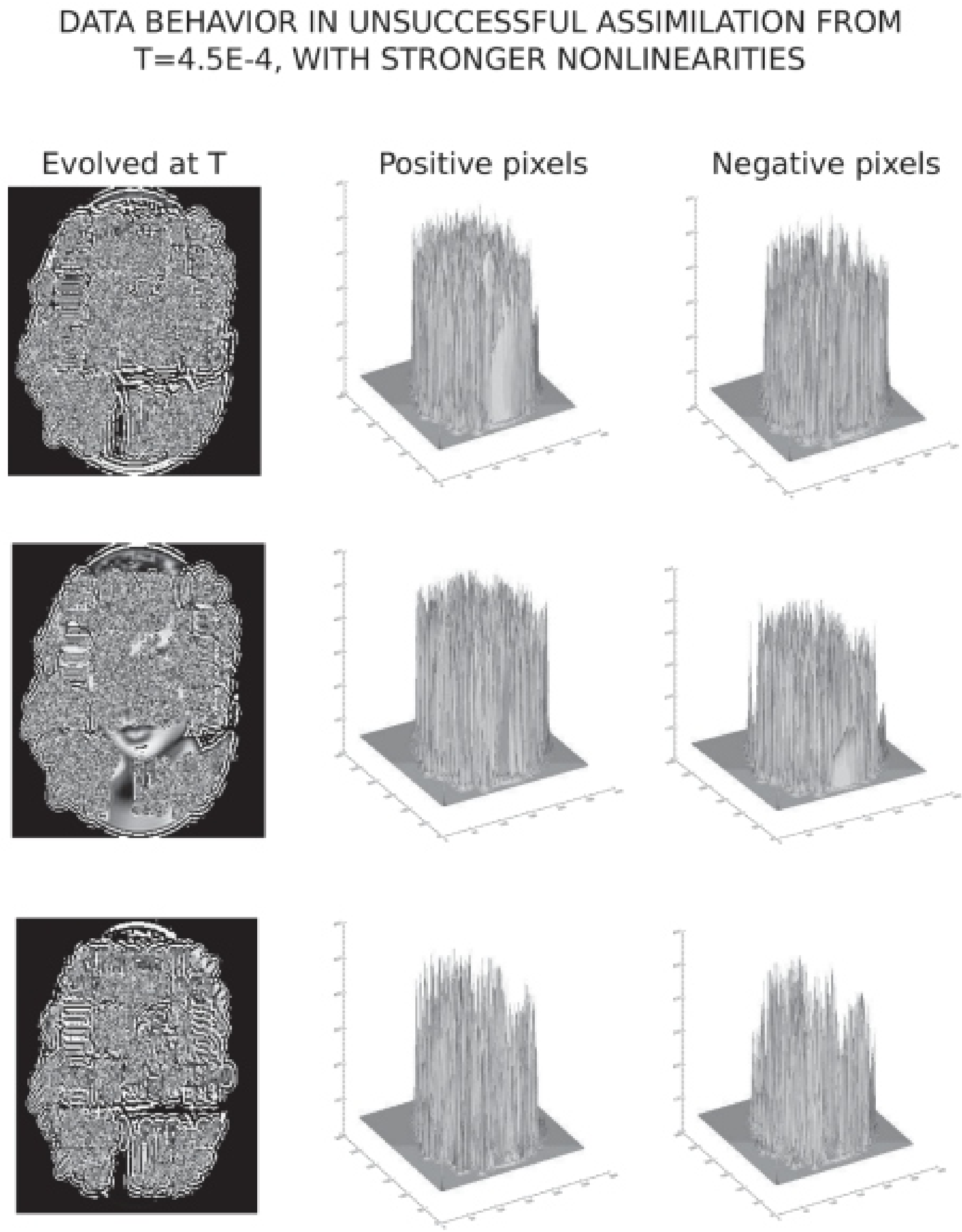


**Figure 5.** Magnitudes of positive and negative pixel values in 'Evolved' column in Figure 4. The equally large positive and negative values in this unsuccessful example are reflected in the large $\mathcal{L}^1$ relative errors in Table 3, and the behavior in the 'Evolved +' column in Figure 4.

**Table 3.** Unsuccessful data assimilation with stronger nonlinearity.

| *Image* | *Desired at $T_{max}$* | *Computed at 0* | *Evolved at $T_{max}$* | *$\mathcal{L}^1$ Err* |
|---|---|---|---|---|
| *USAF* | $0 \leq u \leq 255$ | $-6218 \leq u \leq 6594$ | $-9222 \leq u \leq 14508$ | 96% |
| *Taylor* | $0 \leq v \leq 255$ | $-5763 \leq v \leq 9109$ | $-9889 \leq v \leq 10963$ | 89% |
| *Alpha* | $0 \leq w \leq 255$ | $-2029 \leq w \leq 3250$ | $-4464 \leq w \leq 7429$ | 103% |

Note: Range of data values and $\mathcal{L}^1$ relative errors, from target at $T_{max} = 4.5 \times 10^{-4}$.

**Disclosure statement**

No potential conflict of interest was reported by the author(s).

***References***

*[1] He Q, Barajas-Solano D, Tartakovsky G, et al. Physics-informed neural networks for multiphysics data assimilation with application to subsurface transport. Adv Water Resour. 2020;141:103610. doi: 10.1016/j.advwatres.2020.103610*

*[2] Arcucci R, Zhu J, Hu S, et al. Deep data assimilation: integrating deep learning with data assimilation. Appl Sci. 2021;11:1114. doi: 10.3390/app11031114*

*[3] Antil H, Lohner R, Price R. Data assimilation with deep neural nets informed by nudging. preprint, Nov 2021. arXiv:abs/2111.11505.*

*[4] Chen C, Dou Y, Chen J, et al. A novel neural network training framework with data assimilation. J Supercomput. 2022;78:19020–19045. doi: 10.1007/s11227-04629-7*

*[5] Lundvall J, Kozlov V, Weinerfelt P. Iterative methods for data assimilation for Burgers' equation. J Inverse Ill-Posed Probl. 2006;14:505–535. doi: 10.1515/156939406778247589*

*[6] Auroux D, Blum J. A nudging-based data assimilation method for oceanographuc problems: the back and forth nudging (BFN) algorithm. Proc Geophys. 2008;15:305–319. doi: 10.5194/npg-15-305-2008*

*[7] Ou K, Jameson A. Unsteady adjoint method for the optimal control of advection and Burgers' equation using high order spectral difference method. In: 49th AIAA Aerospace Science Meeting; 2011 Jan 4–7; Orlando, Florida.*

*[8] Auroux D, Nodet M. The back and forth nudging algorithm for data assimilation problems: theoretical results on transport equations. ESAIM:COCV. 2012;18:318–342.*

*[9] Auroux D, Bansart P, Blum J. An evolution of the back and forth nudging for geophysical data assimilation: application to Burgers equation and comparison. Inverse Probl Sci Eng.*

*2013;21:399–419. doi: 10.1080/17415977.2012.712528*

*[10] Allahverdi N, Pozo A, Zuazua E. Numerical aspects of large-time optimal control of Burgers'equation. Esaim Math Model Numer Anal. 2016;50:1371–1401. doi: 10.1051/m2an/2015076*

*[11] Gosse L, Zuazua E. Filtered gradient algorithms for inverse design problems of onedimensional Burgers equation. In: Gosse L, Natalini R, editors. Innovative algorithms and analysis. Cham: Springer; 2017. p. 197–227. doi: 10.1007/978-3-319-49262-9*

*[12] de Campos Velho HF, Barbosa VCF, Cocke S. Special issue on inverse problems in geosciences. Inverse Probl Sci Eng. 2013;21:355–356. doi: 10.1080/17415977.2012.712532*

*[13] Gomez-Hernandez JJ, Xu T. Contaminant source identification in acquifers: a critical view.Math Geosci. 2022;54:437–458. doi: 10.1007/s11004-021-09976-4*

*[14] Xu T, Zhang W, Gomez-Hernandez JJ, et al. Non-point contaminant source identification in an acquifer using the ensemble smoother with multiple data assimilation. J Hydrol. 2022;606:127405. doi: 10.1016/j.jhydrol.2021.127405*

*[15] Vukicevic T, Steyskal M, Hecht M. Properties of advection algorithms in the context of variational data assimilation. MonWeather Rev. 2001;129:1221–1231. doi: 10.1175/1520-0493(2001) 129¡1221:POAAIT¿2.0.CO;2*

*[16] Carasso AS. Data assimilation in 2D viscous Burgers equation using a stabilized explicit finite difference scheme run backward in time. Inverse Probl Sci Eng. 2021;29:3475–3489. doi: 10.1080/17415977.2021.200947*

*[17] Carasso AS. Data assimilation in 2D nonlinear advection diffusion equations, using an explicit stabilized leapfrog scheme run backwrd in time. NIST Technical Note 2227, 2022 Jul 12.doi: 10.6028/NIST.TN2227*

*[18] Carasso AS. Compensating operators and stable backward in time marching in nonlinear parabolic equations. Int J Geomath. 2014;5:1–16. doi: 10.1007/s13137-014-0057-1*

*[19] Carasso AS. Stable explicit time-marching in well-posed or ill-posed nonlinear parabolic equations. Inverse Probl Sci Eng. 2016;24:1364–1384. doi: 10.1080/17415977.2015.1110150*

*[20] Carasso AS. Stable explicit marching scheme in ill-posed time-reversed viscous wave equations. Inverse Probl Sci Eng. 2016;24:1454–1474. doi: 10.1080/17415977.2015.1124429*

*[21] Carasso AS. Stabilized Richardson leapfrog scheme in explicit stepwise computation of forward or backward nonlinear parabolic equations. Inverse Probl Sci Eng. 2017;25:1–24. doi: 10.1080/17415977.2017.1281270*

*[22] Carasso AS. Stabilized backward in time explicit marching schemes in the numerical computation of ill-posed time-reversed hyperbolic/parabolic systems. Inverse Probl Sci Eng. 2018;1:1–32. doi: 10.1080/17415977.2018.1446952*

*[23] Carasso AS. Stable explicit stepwise marching scheme in ill- posed time-reversed 2D Burgers'equation. Inverse Probl Sci Eng. 2018;27(12):1–17. doi: 10.1080/17415977.2018.1523905*

*[24] Carasso AS. Computing ill-posed time-reversed 2D Navier-Stokes equations, using a stabilized explicit finite difference scheme marching backward in time. Inverse Probl Sci Eng. 2020;28:988–1010. doi: 10.1080/17415977.2019.1698564*

*[25] Carasso AS. Stabilized leapfrog scheme run backward in time, and the explicit O(t)2 stepwise computation of ill-posed time-reversed 2D Navier-Stokes equations. Inverse Probl Sci Eng. 2021; 29:3062–3085. doi: 10.1080/17415977.2021.1972997*

*[26] Richtmyer RD, Morton KW. Difference methods for initial value problems. 2nd ed., New York (NY): Wiley; 1967.*

*[27] Liu Z, Renardy M. A note on the equations of a thermoelastic plate. Appl Math Lett. 1995;8:1–6. doi: 10.1016/0893-9659(95)00020-Q*

*[28] Liu K, Liu Z. Exponential stability and analyticity of abstract linear thermoelastic systems. Z Angew Math Phys. 1997;48:885–904. doi: 10.1007/s000330050071*

*[29] Liu Z, Zheng S. Semigroups associated with dissipative systems. New York: Chapman and Hall/CRC; 1999.*

*[30] Lasiecka I, Triggiani R. Analyticity, and lack thereof, of thermoelastic semigroups. ESAIM Proc. 1998;4:199–222. doi: 10.1051/proc:1998029*

*[31] Morse PM, Feshbach H. Methods of theoretical physics. New York (NY): McGraw-Hill; 1953.*

*[32] Arendt W, Ter Elst AFM. Gaussian estimates for second order elliptic operators with boundary conditions. J Oper Theory. 1997;38:87–130.*

*[33] Aronson DG. Bounds for the fundamental solution of a parabolic equation. Bull Am Math Soc. 1967;73:890–896. doi: 10.1090/bull/1967-73-06*

*[34] Ouhabaz EM. Gaussian estimates and holomorphy of semigroups. Proc Am Math Soc. 1995;123:1465–1474. doi: 10.1090/proc/1995-123-05*

*[35] Ouhabaz EM. Gaussian upper bounds for heat kernels of second order elliptic operators with complex coefficients on arbitrary domains. J Oper Theory. 2004;51:335–360*

ISSN 2986 - 0776

# Newchirpsoliton solutions for the space-time fractional perturbed Gerdjikov–Ivanov equation with conformable derivative

**MohammedAlabedalhadia, Shrideh Al-Omarib, Mohammed Al-Smadic,d, Shaher Momanid,e and D.L. Sutharf**

aDepartment of Applied Science, Ajloun College, Al-Balqa Applied University, Ajloun, Jordan; bFaculty of Science, Al-Balqa Applied University, Amman, Jordan; cCollege of Commerce and Business, Lusail University, Lusail, Qatar; dNonlinear Dynamics Research Center (NDRC), Ajman University, Ajman, UAE; eDepartment of Mathematics, Faculty of Science, The University of Jordan, Amman, Jordan; fDepartment of Mathematics, Wollo University, Dessie, Ethiopia Amity School of Applied Science, Amity University Rajasthan, Jaipur, India

## A B S T R A C T

*The space–time perturbed fractional Gerdjikov–Ivanov equation is the main topic of this work, together with quintic nonlinearity and self-steepening, as it involves several intricate physical phenomena includingnonlinearity,self-steepeningandfractionalcalculus,where the fractional derivative is described by employing a conformable derivative.Inaddition,thegoverningequationistransformedintoan integer-order ordinary differential equation by using an appropriate fractionalcomplextransformation.Undercertainrestrictions,adirect algebraic method is employed to investigate the structures of chirp solitonsolutionsenfoldinghyperbolicfunctionalterms.Thedynamic behaviour and bifurcation of equilibria of the system are thoroughly examined; chirp soliton solutions under specified constraints are investigated and the evolving profiles of the obtained solutions are visualized. Moreover, this research offers valuable perspectives on thebehaviourofchirpsolitonsunderspecificconditions,whichhave practical applications in nonlinear physical systems and optical communication systems. The significant contribution of this work is the investigation and obtaining of novel chirp soliton solutions with hyperbolicfunctionaltermsunderparticularlimitationsusinganovel approach. It further extends the prior approaches by treating difficult fractional differential equations from a fresh angle, offering new tools, and closely examining soliton solutions*

***ARTICLEHISTORY*** *Received 20 April 2023 Accepted 4 December2023*

***KEYWORDS*** *Fractional calculus; self-steepening; fractional complex transformation; equilibria bifurcation; chirp soliton solutions*

***KEYWORDS*** *Mathematics Subject Classification: Primary 54C40, 14E20; Secondary 46E25, 20C20*

## 1. Introduction

Fractional differential equations have recently received significant attention from researchers due to their essential and influential role in various fields of science such as physics, engineering, control theory, signal processing, fractional dynamics, fluid mechanics,electromagneticandcontinuummechanics[1].Severalstructuresthatareused currently are investigated in mathematical models bymeansoffractionaldifferential equa tions (FDEs) [2,3]. Therefore, obtaining an exact or approximate solution to FDEs is of interest. Many exact and numerical methods have been developed and implemented to reachthisend. Inthesequenceof thesemethods,werecall theresidualpower series method [4], the reproducing kernel Hilbert space method [5], the differential transform method [6], the homotopy perturbation method [7], the homotopy analysis method [8], the extended trial equation method [9], the (G/G)-expansion method [10], the direct method [11], theRiccati-BernoulliSub-ODEtechnique[12], the modified Kudryashov method [13,14], the modified simple equation method [15], the generalized exponential rational function method[16], the auxiliary equation method [17], the (G/G2)-expansion method [18], the generalized Kudryashov scheme [19], Nucci's reduction method [20], Lie symmetry analysis [21], and many others, to mention but few. The theory of soliton is significant in contributing descriptions naturally for the nonlinear FDEs where it has important and miscellaneous usages in several aspects due to its interesting properties [22,23]. It has also attracted a lot of attention of scientists as it explores and investigates the exact solitary solutions for the nonlinear PDEs as it is functioning examination region in mathematical physics and diverse aspects of nonlinear sciences [24]. The soliton propagation dynamics have been investigated inversal fractional models as thenonlinear Schrödinger'sequation [25],theSasa–Satsumaequation[26],theBiswas–Milovicequation [27], the Lakshmanan–Porsezian–Daniel model [28] and the Schrödinger–Hirota equation [29].

The perturbed Gerdjikov–Ivanov (pGI) equation is a notable and significant nonlinear evolution equation in the optical fibre field. It has been studied in the last decade, which has been derived from the Schrödinger equation in quintic nonlinearity sense. Its solitons have importance intele communication industry of transmission of data with long-distance transoceanic and transcontinental. There are effective approaches that have been developedandutilized to construct optical soliton solutions for the integer-order and fractional pGI equation. In [30], Gerdjikov and Ivanov studied the nonlinear evolution equations. Optical solitons of the pGIequationhavebeenobtainedusingbalancedmodifiedextended tanh-function and the non-balanced Riccati-Bernoulli Sub-ODE methods in [31]. New soliton solutions of thepGImodelhavebeendevelopedin[32].In[33],theauthorsutilized the sine-Gordon equation method to establish optical solitons of space–time conformable fractional pGI equation. The dynamics of solitons in the pGI equation have been explored in [34] carried out formally by considering particular transformations and exerting newly well-established methods to obtain optical solitons of the model. The modified-unified method was used to obtain approximate analytic solutionsof the GIequationin[35]. Using the simplest equation method, the authors in [36]obtainednovel solitons

Using the simplest equation method, the authors in [36]obtainednovel solitonsolu tions for the pGI equation. In this paper, we consider the space–time perturbed fractional Gerdjikov–Ivanov equation in the form:

$$\begin{aligned} &iD_t^{\alpha}\varphi + a_1 D_x^{2\alpha}\varphi + a_2|\varphi|^2\varphi \\ &\quad = i(a_3\varphi^2 D_x^{\alpha}\varphi^* + b_1 D_x^{\alpha}\varphi + b_2 D_x^{\alpha}(|\varphi|^2\varphi) + c\varphi D_x^{\alpha}(|\varphi|^2)), 0 < \alpha \leq 1, \end{aligned} \tag{1}$$

where ϕ (x,t) is the complex conjugate of ϕ(x,t), ϕ(x,t) represents the complex-valued wave function of spatial and temporal independent variables x and t, respectively.The fractional term Dα tϕ denotes the temporal evolution, while the fractional term Dα x(|ϕ|2ϕ) is the dispersion of group velocity. The quintic nonlinearity term is |ϕ|2ϕ. The a1 anda2 arethecoefficientsofthedispersionofthegroupvelocityandthequinticnonlinearity term, respectively. Moreover, the parameters a3,b1,b2,andc denotes the nonlinear dispersion, inter-modal dispersion, self-steepening, and higher-order dispersion coefficients, respectively. The fractional derivative in (1) is described by means of conformable definition. Our investigation of Equation (1) is primarily driven by its potential to improve our knowledge of nonlinear wave dynamics and its practical significance in a variety of physical systems. Our decision is based on multiple important factors, namely, the modelling of optical pulses inside optical fibres is greatly aided by Equation (1), which has immediate consequences for maximizing signal transmission and reducing distortion in optical communication systems. Moreover, Equation (1), in the larger framework of nonlinear physics, is a part of a class of equations that provide insights into nonlinear dynamics by describing nonlinear wave behaviour in a variety of physical phenomena, from fluid dynamics to plasma physics. Our approach is novel since fractional calculus is incorporated into our equation. Our work advances the use of fractional calculus in explaining nonlinear wave dynamics in a variety of physical systems. Fractional calculus is becoming more and more popular due to its capacity to explain intricate memory-dependent processes. We also study chirp solitons, which have practical significance, particularly in optical communication applications where precise pulse shaping is needed. Preserving the shape and stability of optical pulses requires an understanding of chirp soliton generation and behaviour. The method used to construct these chirp solitons solutions is a direct algebraic method that depends on assuming the desired solutions have specific expressions involving hyperbolic functions.

This article establishes chirp soliton solutions for the space–time pFGI Equation (1) based on efficient ansatzes with aid of a fractional complex travelling-wave transformation that reduced the proposed Equation (1) into integer-order ordinary differential equation (ODE). To the best of knowledge, the chirp solitons for the governing model (1) are presented for the first time in the literature, which is considered as a new contribution and a strong motivation for this work. It also studies the equilibrium bifurcation of Equation (1) for the first time, which is considered as a major tool in investigating the existence of

Equation (1) for the first time, which is considered as a major tool in investigating the existence of the solutions sought to be derived. The paper organized as introduction as first section. Section 2 presents a brief review of the conformable derivative definition and its essential properties which are used in our analysis. In Section 3, we apply a fractional complex travelling-wave transformation to the proposed Equation (1) and translate it into integerorder ordinary differential equation. The dynamical planner system of the corresponding integer-order ordinary differential equation will be studied in the same section. In Section 4 we construct the chirp soliton solutions for the governing Equation (1). Finally, some discussion and conclusions about the obtained result will be found in Section 5 and 6.

## 2. Brief reviewinconformablefractional derivative

Thefractional derivative is an interesting research area for many centuries. Several types of fractional derivative definitions were presentedintheliterature such as Riemann–Liouville [37], Liouville-Caputo definition [38], Caputo–Fabriziodefinition[39],Atangana-Baleanu definition [40]andmanyothers[41]. Khalil et al., [42], introduced the simplest, most natural and efficient definition of the fractional derivative. Let $w(t) :[0,+\infty) \rightarrow R$ be a function. Then the conformable fractional derivative of order $\alpha$ of w is given as

$$D_t^{\alpha} w(t) = \lim_{\epsilon \to 0} \frac{w(t + \epsilon t^{1-\alpha}) - w(t)}{\epsilon}, \tag{2}$$

for all $t > 0, \alpha \in (0,1]$. The function w is $\alpha$-conformable differentiable at a point t when the limit in (2) exists. The conformable derivative obeys many renowned required properties that appears in the classical derivative like the product and quotient rules [43].

**Theorem 2.1: [43]** Let the functions $w1 = w1(t)$ and $w2 = w2(t)$ be $\alpha$-conformable differ entiable at any point $t > 0$, $\alpha \in (0,1]$. Then, we have

(i) $D_t^{\alpha}(aw_1 + bw_2) = aD_t^{\alpha} w_1 + bD_t^{\alpha} w_2, \forall a, b \in \mathbb{R}$.
(ii) $D_t^{\alpha}(t^n) = nt^{n-\alpha}, \forall n \in \mathbb{R}$.
(iii) $D_t^{\alpha}(a) = 0$, *where a is any constant.*
(iv) $D_t^{\alpha}(w_1 w_2) = w_1 D_t^{\alpha} w_2 + w_2 D_t^{\alpha} w_1$.
(v) $D_t^{\alpha}\left(\frac{w_1}{w_2}\right) = \frac{w_2 D_t^{\alpha} w_1 - w_1 D_t^{\alpha} w_2}{w_2^2}$.
(vi) *if* $w_1$ *is differentiable, then* $D_t^{\alpha}(w_1)(t) = t^{1-\alpha} \frac{dw_1}{dt}$.

Moreover, the conformable differential operator conforms to the crucial property, chain rule.

**Theorem 2.2: [43]** Suppose w1(t) be α-conformable differentiable function and w2(t) be differentiable well-defined in the range of w1(t). Then, we have

$$D_t^{\alpha}(w_1(t) o w_2(t)) = t^{1-\alpha}\frac{dw_2}{dt}\frac{d}{dt}(w_1(w_2(t))). \tag{3}$$

**3. Analysis ofgoverningequationandequilibriabifurcations**

To tackle the chirp soliton structure for the space–time pFGI Equation (1), we present the following fractional complex transformation

$$\varphi(x,t) = \Psi(\xi)e^{i\left(\phi(\xi)-\lambda\frac{t^{\alpha}}{\alpha}\right)}, \xi = \frac{x^{\alpha}}{\alpha} - v\frac{t^{\alpha}}{\alpha}, \tag{4}$$

where (ξ)represents the real-valued unknown amplitude function of the coordinate ξ, φ(ξ)givesthephasemodificationparameter,whileλandvarethefrequencyandthespeed of soliton, respectively. The corresponding chirp is presented as

$$\delta\omega(x,t) = -\frac{\partial}{\partial x}\left(\phi(\xi) - \lambda\frac{t^{\alpha}}{\alpha}\right) = -\phi'(\xi), \tag{5}$$

where the prime sign denotes the derivative with respect to the travelling coordinate ξ. The transformation (4) with the aid of the properties of the conformable derivative leads to ensure the following relations for the fractional differential terms in (1),

$$\begin{aligned}
D_t^{\alpha}\varphi &= -(v\Psi' + iv\Psi\phi' + i\lambda\Psi)e^{i\left(\phi(\xi)-\lambda\frac{t^{\alpha}}{\alpha}\right)},\\
D_x^{\alpha}\varphi &= (\Psi' + i\Psi\phi')e^{i\left(\phi(\xi)-\lambda\frac{t^{\alpha}}{\alpha}\right)},\\
D_x^{2\alpha}\varphi &= (2i\Psi'\phi' - \Psi(\phi')^2 + \Psi'' + i\Psi\phi'')e^{i\left(\phi(\xi)-\lambda\frac{t^{\alpha}}{\alpha}\right)},\\
D_x^{\alpha}\varphi^* &= (\Psi' - i\Psi\phi')e^{-i\left(\phi(\xi)-\lambda\frac{t^{\alpha}}{\alpha}\right)},\\
D_x^{\alpha}(|\varphi|^2\varphi) &= (3\Psi^2\Psi' + i\Psi^3\phi')e^{i\left(\phi(\xi)-\lambda\frac{t^{\alpha}}{\alpha}\right)},\\
D_x^{\alpha}(|\varphi|^2) &= 2\Psi\Psi'.
\end{aligned} \tag{6}$$

Substitute the relations in (6) in the governing Equation (1). Then simplify the result, respectively, to get complex expression of its imaginary and real parts,

$$-(v+b_1)\Psi' - (a_3+3b_2+2c)\Psi^2\Psi' + 2a_1\Psi'\phi' + a_1\Psi\phi'' = 0, \tag{7}$$
$$(v-a_3+b_1)\Psi\phi' + b_2\Psi^3\phi' - a_1\Psi(\phi')^2 + \lambda\Psi + a_2\Psi^3 + a_1\Psi'' = 0. \tag{8}$$

In order to solve these coupled equations, we choose the ansatz in the form

$$\phi'(\xi) = A\Psi^2(\xi) + B, \tag{9}$$

where the parameters A and B are determined by inserting the ansat (9) intotheimaginary part (7). After some simplifications and setting the coefficients of the independent terms, and 2 ,tobezerowefindthevalueofA and B as

$$A = \frac{a_3+3b_2+2c}{4a_1}, B = \frac{v+b_1}{2a_1}. \tag{10}$$

Using the values in (10) in (5), the resultant chirp can be written as.

$$\delta\omega(x,t) = -\left(\frac{a_3+3b_2+2c}{4a_1}\right)\Psi^2(\xi) - \frac{v+b_1}{2a_1}. \tag{11}$$

Consequently, the real part of (8) together with aid of (9) and (10) are addressed in the form

$$\begin{aligned} a_1\Psi'' &+ (\lambda - a_1B^2 + (v-a_3+b_1)B)\Psi \\ &+ (a_2 + b_2B - 2a_1AB + (v-a_3+b_1)A)\Psi^3 \\ &+ (b_2A - a_1A^2)\Psi^5 = 0. \end{aligned} \tag{12}$$

The integer-order ODE (12) can be rewritten as.

$$\Psi'' + R_1\Psi + R_2\Psi^3 + R_3\Psi^5 = 0, \tag{13}$$

where the parameters R1,R2 and R3 are given by

$$
\begin{aligned}
R_1 &= \frac{4a_1\lambda + (v+b_1)(v-2a_3+b_1)}{4a_1^2},\\
R_2 &= -\frac{-4a_1a_2 + a_3^2 - 2(v+b_1)b_2 + a_3(2c+3b_2)}{4a_1^2},\\
R_3 &= -\frac{(2c+a_3-b_2)(2c+a_3+3b_2)}{16a_1^2}
\end{aligned}
\tag{14}
$$

provided that a1= 0. In light of studying the dynamical plane and the bifurcation of the equilibria for the integer-order ODE (12), we assume d dξ = ˆ . Then the integer-order ODE(13) transformed into the following dynamical system.

$$
\frac{d\Psi}{d\xi} = \hat{\Psi}, \frac{d\hat{\Psi}}{d\xi} = -(R_1\Psi + R_2\Psi^3 + R_3\Psi^5). \tag{15}
$$

This dynamical planner system is equivalent to

$$
\hat{\Psi}d\hat{\Psi} + (R_1\Psi + R_2\Psi^3 + R_3\Psi^5)d\Psi = 0. \tag{16}
$$

Now, integrate both sides to get the Hamiltonian function

$$
\mathcal{H}(\Psi, \hat{\Psi}) = 6\hat{\Psi}^2 + 6R_1\Psi^2 + 3R_2\Psi^4 + 2R_3\Psi^6 = \hbar \in \mathbb{R}. \tag{17}
$$

Then, it easy to see that all critical points of the dynamical system (15) are in the form √E( i,0).Let = R2 2 −4R1R3, ± 1 =± −R2− 2R3 critical points can be listed in the following cases:

**Case I**. There are five critical points for the system (15): $E_1(0,0)$ and $E_{2,3,4,5}(\Psi_i^{\mp}, 0), i = 1, 2$, if one of the following conditions satisfies: $R_1 > 0, R_2 < 0$, and $0 < R_3 < \frac{R_2^2}{4R_1}$, or $R_1 \langle 0, R_2 \rangle\, 0$, and $\frac{R_2^2}{4R_1} < R_3 < 0$.

**Case II**. There are three critical points for the system (15): $E_1(0,0)$ and $E_{2,3}(\Psi_1^{\pm}, 0)$, if one of the following conditions satisfies: $R_1 > 0, R_2 \le 0$, and $R_3 < 0$, or $R_1 > 0, R_2 \le 0$, and $0 < R_3 < \frac{R_2^2}{4R_1}$, or $R_1 \langle 0, R_2 \rangle\, 0$, and $\frac{R_2^2}{4R_1} < R_3 < 0$.

**Case III**. There are three critical points for the system (15): $E_1(0,0)$ and $E_{2,3}(\Psi_2^{\pm},0)$, if one of the following conditions satisfies: $R_1 \leq 0, R_2 < 0$, and $R_3 > 0$, or $R_1 > 0, R_2 < 0$, and $0 < R_3 < \frac{R_2^2}{4R_1}$, or $R_1 < 0, R_2 \geq 0$, and $\frac{R_2^2}{4R_1} < R_3 < 0$.

**Case IV**. There is unique critical point for the system (15): $E(0,0)$, if none of the above conditions are cross.

The linearized system of the dynamical system (15) has the following coefficient matrix.

$$\mathcal{M}(\Psi,\hat{\Psi}) = \begin{bmatrix} 0 & 1 \\ -(R_1 + 3R_2\Psi^2 + 5R_3\Psi^4) & 0 \end{bmatrix}. \tag{18}$$

Clearly, the trace of the matrix $\mathcal{M}$ is zero, $Tr(\mathcal{M}(\Psi,\hat{\Psi})) = 0$.

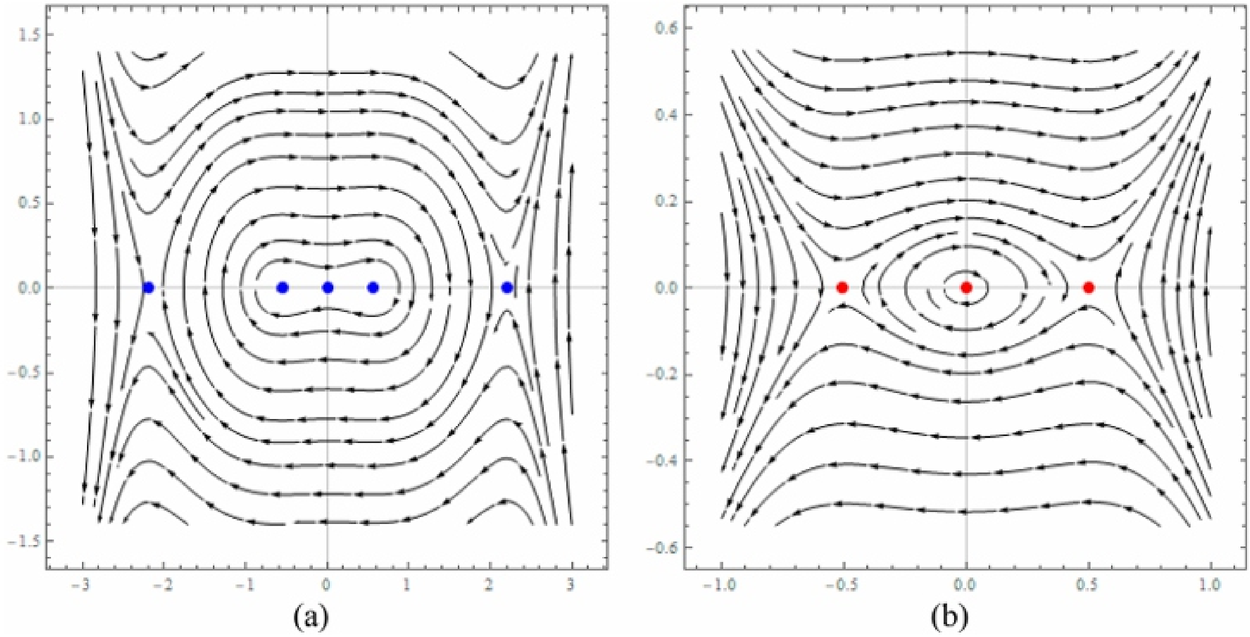

**Figure 1.** Stream plot of the phase portrait for the system (15) at: (a) $a_1 = 1, a_2 = 0.9, a_3 = 1, b_1 = 0.2, b_2 = 0.7, c = 0.00001, \lambda = 0.1$, and $v = 0.3$; (b) $a_1 = 1, a_2 = 0.01, a_3 = 1, b_1 = 0.1, b_2 = 0.4, c = 0.3, \lambda = 0.3$, and $v = 0.2$.

Let $\mathcal{D}(\Psi,\hat{\Psi}) = \det(\mathcal{M}(\Psi,\hat{\Psi}))$. Then we have the following values of $\mathcal{D}(\Psi,\hat{\Psi})$ at the critical points:

$$\mathcal{D}(E(0,0)) = R_1,\ \mathcal{D}(E(\Psi_1^{\pm},0)) = \frac{\Delta + R_2\sqrt{\Delta}}{R_3},\ \mathcal{D}(E(\Psi_2^{\pm},0)) = \frac{\Delta - R_2\sqrt{\Delta}}{R_3}. \tag{19}$$

Usingthetheoryofthedynamicalplannertheclassificationofthecriticalpointsfollows as: if D(E)<0,then the critical point is saddle. If D(E)>0, then the critical point is centre. Wedepictedthephaseportraitoftheobtainedcriticalpointsforthedynamicalsystem(15) at selected parameters in Figure 1.

Furthermore, the contour plot of the Hamiltonian function (17) is shown in Figure 2 at the same selected parameters in Figure 1, to ensure our obtained results.

Thebluecolourpoints inFigures1 and 2 represent the obtained critical points at the selected parameters, which are classified as: E1(0,0), D(E1) $\sim = -0.087 < 0$; saddle, E2,3($\pm$0.56, 0), D(E2,3) $\sim = 0.16 > 0$; centre, and E4,5($\pm$2.2,0), D(E4,5) $\sim = -2.56 < 0$; saddle critical point. While red points represent the gotten critical points at the mentioned parameters, their classification as: E1(0,0), D(E1) $\sim = 0.17 > 0$; centre, and E2,3($\pm$0.5,0), D(E2,3) $\sim = -0.37 < 0$; saddle, which is appeared clearly in the Figures. Mathematica 11 software is used in computing all arithmetic symbols and procedures.

**4. Chirpsoliton solutions for the space–timepFGIequation**

The proposed method begins by searching for solutions to Equation (13) in specific expressions that include hyperbolic functions. These expressions contain several specific parameters that must be determined by directly substituting these expressions into Equation (13) and deriving an overdetermined algebraic system in terms of the parameters to be found. Having solutions to this overdetermined algebraic system requires that

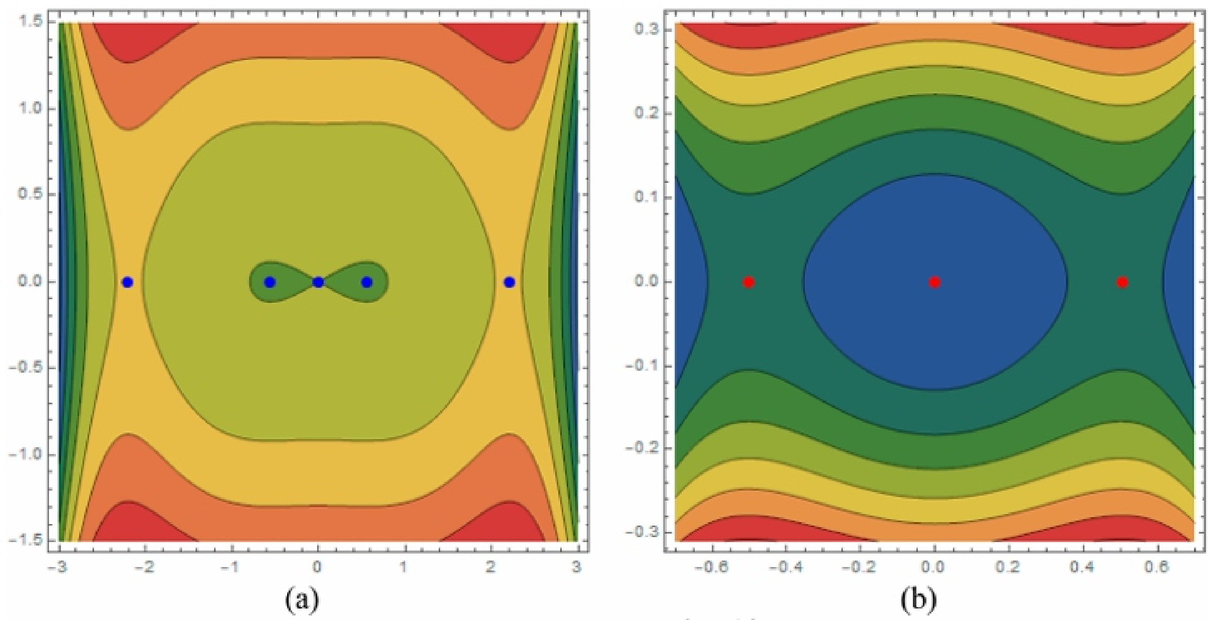


**Figure 2.** Contour plot of the Hamiltonian function $\mathcal{H}(\Psi, \hat{\Psi})$ at: (a) $a_1 = 1, a_2 = 0.9, a_3 = 1, b_1 = 0.2, b_2 = 0.7, c = 0.00001, \lambda = 0.1,$ and $v = 0.3$; (b) $a_1 = 1, a_2 = 0.01, a_3 = 1, b_1 = 0.1, b_2 = 0.4, c = 0.3, \lambda = 0.3,$ and $v = 0.2$.

some conditions be present on the parameters. In this section, we will extract three dif ferent solutions using three different expressions and set the necessary conditions for the existence of each of these important solutions.Then we will study the physical aspect of these solutions and study the extent to study the extent to which the fractional derivative affects its behaviour. This proposed method is distinguished from other methods in that it is easy to apply and has hig he fficiency next ractingsolutions in the form of expression scontaining hyperbolic functions. It also provides real conditions on the parameters for the existence of solutions. It is worth noting that this method was not used to find solutions to the governing model in this work.

### 4.1. Brightchirpsoliton

We consider a solution for the integer-order ODE (13) in the form

$$\Psi(\xi) = \frac{P_1}{P_2 + \cosh(\mu\xi)}, \tag{20}$$

where μ,P1 and P2 are constants to be determined. We substitute the formula (20) into the integer-order ODE (13), simplify the gotten result and group the coefficients of the independent terms in the numerator to get

$$\begin{aligned}
\text{fixed:}\quad & P_1P_2^4R_1 + P_1^3P_2^2R_2 + P_1^5R_3 - 2P_1P_2^2\mu^2, \\
\cosh(\mu\xi):\quad & 4P_1P_2^3R_1 + 2P_1^3P_2R_2 - 4P_1P_2\mu^2 - P_1P_2^3\mu^2, \\
\cosh^2(\mu\xi):\quad & 6P_1P_2^2R_1 + P_1^3R_2 - 2P_1\mu^2 - P_1P_2^2\mu^2, \\
\cosh^3(\mu\xi):\quad & 4P_1P_2R_1 + P_1P_2\mu^2, \\
\cosh^4(\mu\xi):\quad & P_1R_1 + P_1\mu^2.
\end{aligned} \tag{21}$$

Set the expressions in (21) to be zero, then solve the obtained non linearal gebraic system to obtain the following values

$$\begin{aligned}
\mu^{\pm} &= \pm\sqrt{-\frac{4a_1\lambda + (v+b_1)(v-2a_3+b_1)}{4a_1^2}}, \\
P_1^{\pm} &= \pm\sqrt{\frac{2(4a_1\lambda + (v+b_1)(v-2a_3+b_1))}{-4a_1a_2 + a_3^2 - 2(v+b_1)b_2 + a_3(2c+3b_2)}}, P_2 = 0.
\end{aligned} \tag{22}$$

The obtained values correspond to the essential constraints

$$\begin{aligned}
c = \frac{1}{2}(b_2 - a_3), \lambda \left\langle \frac{(v+b_1)(-v+2a_3-b_1)}{4a_1}, a_2 \right\rangle \\
\frac{a_3^2 - 2(v+b_1)b_2 + a_3(2c+3b_2)}{4a_1}, a_1 \neq 0.
\end{aligned} \tag{23}$$

By using (22) and (20) in (11), the corresponding chirp is given by.

$$\delta\omega(x,t) = -\left(\frac{a_3+3b_2+2c}{4a_1}\right) \left(\frac{\pm\sqrt{\frac{2(4a_1\lambda+(\nu+b_1)(\nu-2a_3+b_1))}{-4a_1a_2+a_3^2-2(\nu+b_1)b_2+a_3(2c+3b_2)}}}{\cosh\left(\pm\sqrt{-\frac{4a_1\lambda+(\nu+b_1)(\nu-2a_3+b_1)}{4a_1^2}}\left(\frac{x^\alpha}{\alpha}-\nu\frac{t^\alpha}{\alpha}\right)\right)}\right)^2 - \left(\frac{\nu+b_1}{2a_1}\right). \tag{24}$$

Also, the chirp factor $\phi(x,t)$ can be constructed by substituting the values in (22) and (20) in (9) and integrating the result with respect to $\xi$. Indeed it can be represented as

$$\phi_{1,2}(x,t) = \left(\frac{\nu+b_1}{2a_1}\right)\left(\frac{x^\alpha}{\alpha}-\nu\frac{t^\alpha}{\alpha}\right) + \frac{\left(\frac{a_3+3b_2+2c}{4a_1}\right)\left(\frac{2(4a_1\lambda+(\nu+b_1)(\nu-2a_3+b_1))}{-4a_1a_2+a_3^2-2(\nu+b_1)b_2+a_3(2c+3b_2)}\right)\tanh\left(\pm\sqrt{-\frac{4a_1\lambda+(\nu+b_1)(\nu-2a_3+b_1)}{4a_1^2}}\left(\frac{x^\alpha}{\alpha}-\nu\frac{t^\alpha}{\alpha}\right)\right)}{\pm\sqrt{-\frac{4a_1\lambda+(\nu+b_1)(\nu-2a_3+b_1)}{4a_1^2}}}. \tag{25}$$

Consequently, the bright chirp soliton solutions of the space–time pFGI equation can be established by inserting the values in (22) and (20) in the transformation (4). It falls to be:

$$\varphi_{1,2,3,4}(x,t) = \frac{\pm\sqrt{\frac{2(4a_1\lambda+(\nu+b_1)(\nu-2a_3+b_1))}{-4a_1a_2+a_3^2-2(\nu+b_1)b_2+a_3(2c+3b_2)}}}{\cosh\left(\pm\sqrt{-\frac{4a_1\lambda+(\nu+b_1)(\nu-2a_3+b_1)}{4a_1^2}}\left(\frac{x^\alpha}{\alpha}-\nu\frac{t^\alpha}{\alpha}\right)\right)} \times \mathrm{Exp}\left[i\left(\phi_{1,2}(x,t)-\lambda\frac{t^\alpha}{\alpha}\right)\right]. \tag{26}$$

The graphical representation of $|\varphi_1(x,t)|$ at $\mu^-$ and $P_1^-$ are shown in Figure 3, where the derivative is considered in the integer and the fractional sense.

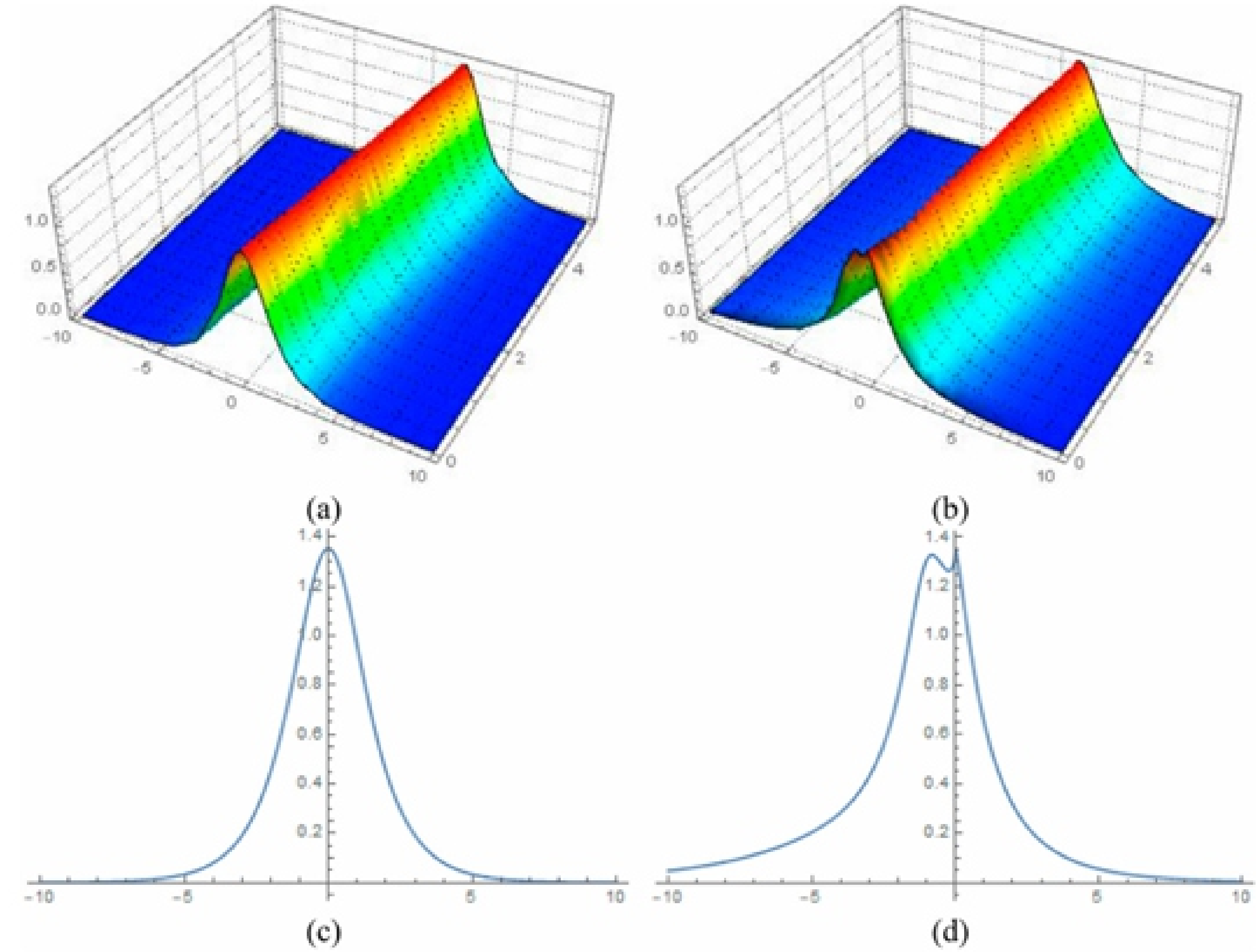


Figure 3. The bright chirp soliton solution for (1) at: $a_1 = 1, a_2 = 1, a_3 = 4, b_1 = 0.01, b_2 = 0.04, \lambda = 0.0001$, and $v = 0.4$, on $x \in [-10, 10]$ and $t \in [0, 5]$ where (a) 3D plot of $|\varphi_1(x, t)|$ at $\alpha = 1$, (b) 3D plot of $|\varphi_1(x, t)|$ at $\alpha = 0.65$, (c) 2D plot of $|\varphi_1(x, 0)|$ at $\alpha = 1$, (d) 2D plot of $|\varphi_1(x, 0)|$ at $\alpha = 0.65$.

For more illustrations,the effect of the fractional derivative on the evolution of the bright chirp soliton solution $\phi 1(x,t)$ is introduced in Figure 4 at various fractional derivative orders. Moreover, the profile of chirping, $\delta\omega(x,t)$ in (24) at $\mu-$ and 1 ,hasbeendepicted as a function of the coordinate $\xi$ in Figure 5 at different values of the frequency and the speed of the soliton. It is obvious from the presented figures. The fractional derivative directlyaffectsthevolumeof theobtainedbrightsolitons.Notethat theselectedvalues for the parameters in Figures 3–5 satisfy the constraints (23), which make the amplitude function $(\xi)$and the phase modification parameter $\varphi(\xi)$be real-valued functions.

### 4.2. Singularchirpsoliton

To get the singular chirp soliton solution for the governing equation, the solution of the integer-order ODE (13) can be considered in the form

$$\Psi(\xi) = \frac{P_3}{P_4 + \sinh(\mu\xi)}, \tag{27}$$

where the constants $P_3$ and $P_4$ are determine by inserting the hypothesis (27) into the integer-order ODE (13) and simplifying the obtained rational expression and grouping

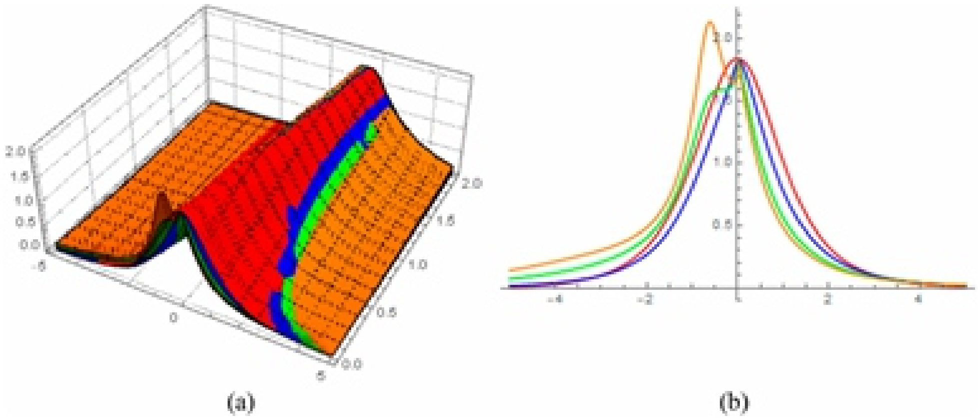


**Figure 4.** Effect the fractional derivative on bright chirp soliton behavior at: $a_1 = 1, a_2 = 1, a_3 = 4, b_1 = 0.01, b_2 = 0.04, \lambda = 0.0001$, and $v = 0.8$, on $x \in [-5, 5]$ and $t \in [0, 2]$ such that: red; $\alpha = 1$, blue; $\alpha = 0.8$, green; $\alpha = 0.65$, and orange; $\alpha = 0.6$, where (a) 3D plot of $|\varphi_1(x, t)|$ and (b) 2D plot of $|\varphi_1(x, 0)|$.

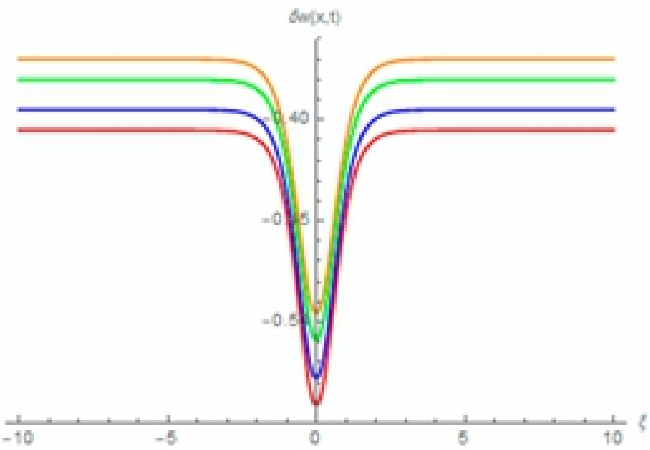

**Figure 5.** The profile of chirping (22) at: $a_1 = 1, a_2 = 1, a_3 = 4, b_1 = 0.01$, and $b_2 = 0.04$, where red; $\lambda = 0.0001$ and $v = 0.8$, blue; $\lambda = 0.0002$ and $v = 0.78$, green; $\lambda = 0.0003$ and $v = 0.75$, orange; $\lambda = 0.0004$ and $v = 0.73$.

the coefficients of the independent terms in the numerator, which are listed as

$$\begin{aligned}
\text{fixed}: &\frac{3}{8}P_3R_1 - 3P_3P_4^2R_1 + P_3P_4^4R_1 - \frac{1}{2}P_3^3R_2 + P_3^3P_4^2R_2 + P_3^5R_3 \\
&- \frac{5}{8}P_3\mu^2 + \frac{5}{2}P_3P_4^2\mu^2, \\
\sinh(\mu\xi): &-3P_3P_4R_1 + 4P_3P_4^3R_1 + 2P_3^3P_4R_2 + \frac{13}{4}P_3P_4\mu^2 - P_3P_4^3\mu^2, \\
\sinh^2(\mu\xi): &-\frac{1}{2}P_3R_1 + 3P_3P_4^2R_1 + \frac{1}{2}P_3^3R_2 + \frac{1}{2}P_3\mu^2 - \frac{1}{2}P_3P_4^2\mu^2,
\end{aligned}$$

$$\begin{aligned}
\cosh^2(\mu\xi) &: -\frac{1}{2}P_3R_1 + 3P_3P_4^2R_1 + \frac{1}{2}P_3^3R_2 + \frac{1}{2}P_3\mu^2 - \frac{1}{2}P_3P_4^2\mu^2,\\
\sinh^3(\mu\xi) &: P_3P_4R_1 + \frac{1}{4}P_3P_4\mu^2,\\
\sinh^4(\mu\xi) &: \frac{1}{8}P_3R_1 + \frac{1}{8}P_3\mu^2,\\
\cosh^4(\mu\xi) &: \frac{1}{8}P_3R_1 + \frac{1}{8}P_3\mu^2,\\
\cosh^2(\mu\xi)\sinh(\mu\xi) &: 3P_3P_4R_1 + \frac{3}{4}P_3P_4\mu^2,\\
\cosh^2(\mu\xi)\sinh^2(\mu\xi) &: \frac{3}{4}P_3R_1 + \frac{3}{4}P_3\mu^2.
\end{aligned} \tag{28}$$

By solving the nonlinear algebraic system that is obtained by setting the coefficients in (28) to be zero we have

$$\begin{aligned}
\mu^{\pm} &= \pm\sqrt{-\frac{4a_1\lambda + (v+b_1)(v-2a_3+b_1)}{4a_1^2}},\\
P_3^{\pm} &= \pm\sqrt{\frac{-2(4a_1\lambda + (v+b_1)(v-2a_3+b_1))}{-4a_1a_2 + a_3^2 - 2(v+b_1)b_2 + a_3(2c+3b_2)}}, P_4 = 0.
\end{aligned} \tag{29}$$

These obtained values correspond with the following essential constraints

$$\begin{aligned}
c &= \frac{1}{2}(b_2 - a_3),\ \lambda < \frac{(v+b_1)(-v+2a_3-b_1)}{4a_1},\\
a_2 &< \frac{a_3^2 - 2(v+b_1)b_2 + a_3(2c+3b_2)}{4a_1},\ a_1 \neq 0.
\end{aligned} \tag{30}$$

Upon these obtained values of the parameters, we construct the associated chirp by inserting the constants (29) and (27) in (11) that are found as

$$\begin{aligned}
\delta\omega(x,t) = &-\left(\frac{a_3+3b_2+2c}{4a_1}\right)\\
&\left(\frac{\pm\sqrt{\frac{-2(4a_1\lambda+(v+b_1)(v-2a_3+b_1))}{-4a_1a_2+a_3^2-2(v+b_1)b_2+a_3(2c+3b_2)}}}{\sinh\left(\pm\sqrt{-\frac{4a_1\lambda+(v+b_1)(v-2a_3+b_1)}{4a_1^2}}\left(\frac{x^\alpha}{\alpha} - v\frac{t^\alpha}{\alpha}\right)\right)}\right)^2 - \left(\frac{v+b_1}{2a_1}\right).
\end{aligned} \tag{31}$$

Accordingly, the chirp factor established by using (29) and (27) in (9) and integrating the result with respect to $\xi$ which is given as

$$\phi_{1,2}(x,t) = \left(\frac{\nu+b_1}{2a_1}\right)\left(\frac{x^\alpha}{\alpha} - \nu\frac{t^\alpha}{\alpha}\right) - \frac{\left(\frac{a_3+3b_2+2c}{4a_1}\right)\left(\frac{-2(4a_1\lambda+(\nu+b_1)(\nu-2a_3+b_1))}{-4a_1a_2+a_3^2-2(\nu+b_1)b_2+a_3(2c+3b_2)}\right)\coth\left(\pm\sqrt{-\frac{4a_1\lambda+(\nu+b_1)(\nu-2a_3+b_1)}{4a_1^2}}\left(\frac{x^\alpha}{\alpha}-\nu\frac{t^\alpha}{\alpha}\right)\right)}{\pm\sqrt{-\frac{4a_1\lambda+(\nu+b_1)(\nu-2a_3+b_1)}{4a_1^2}}}. \tag{32}$$

Using the chirp factor (32) and the values (29) in the formal solution (27) along with the transformation (4), we obtain the following singular chirp soliton solutions for the space–time pFGI Equation (1)

$$\varphi_{1,2,3,4}(x,t) = \frac{\pm\sqrt{\frac{-2(4a_1\lambda+(\nu+b_1)(\nu-2a_3+b_1))}{-4a_1a_2+a_3^2-2(\nu+b_1)b_2+a_3(2c+3b_2)}}}{\sinh\left(\pm\sqrt{-\frac{4a_1\lambda+(\nu+b_1)(\nu-2a_3+b_1)}{4a_1^2}}\left(\frac{x^\alpha}{\alpha}-\nu\frac{t^\alpha}{\alpha}\right)\right)} \times \mathrm{Exp}\left[i\left(\phi_{1,2}(x,t) - \lambda\frac{t^\alpha}{\alpha}\right)\right]. \tag{33}$$

To illustrate the physical nature of the explored solution (33), we introduce the profile of the singular chirp soliton by depicting the modulus of ϕ1 (x,t), where it considers in case μ−andP+ 3 in 3 D and 2 D plots at selected parameters with in teger and fractional deriva tive orders. See Figure6 .Figure7 (a) presents the behaviour of the singular chirpsoliton atdifferent fractional orders for further demonstration.The associate chirps δ ω (x,t) in Equation (31) are plotted as a function of the coordinate ξ at various selected values for the soliton frequency and soliton speed, which are shown in Figure7 (b). Theselected parameters in the presented igures cross with the constraints (30).

### 4.3. Darkchirpsoliton

The following assumption of the solution for the integer- order ODE (13) possess dark chirp soliton solution for the governing Equation (1).

$$\Psi(\xi) = P_5 \tanh^{n}(\mu\xi), \tag{34}$$

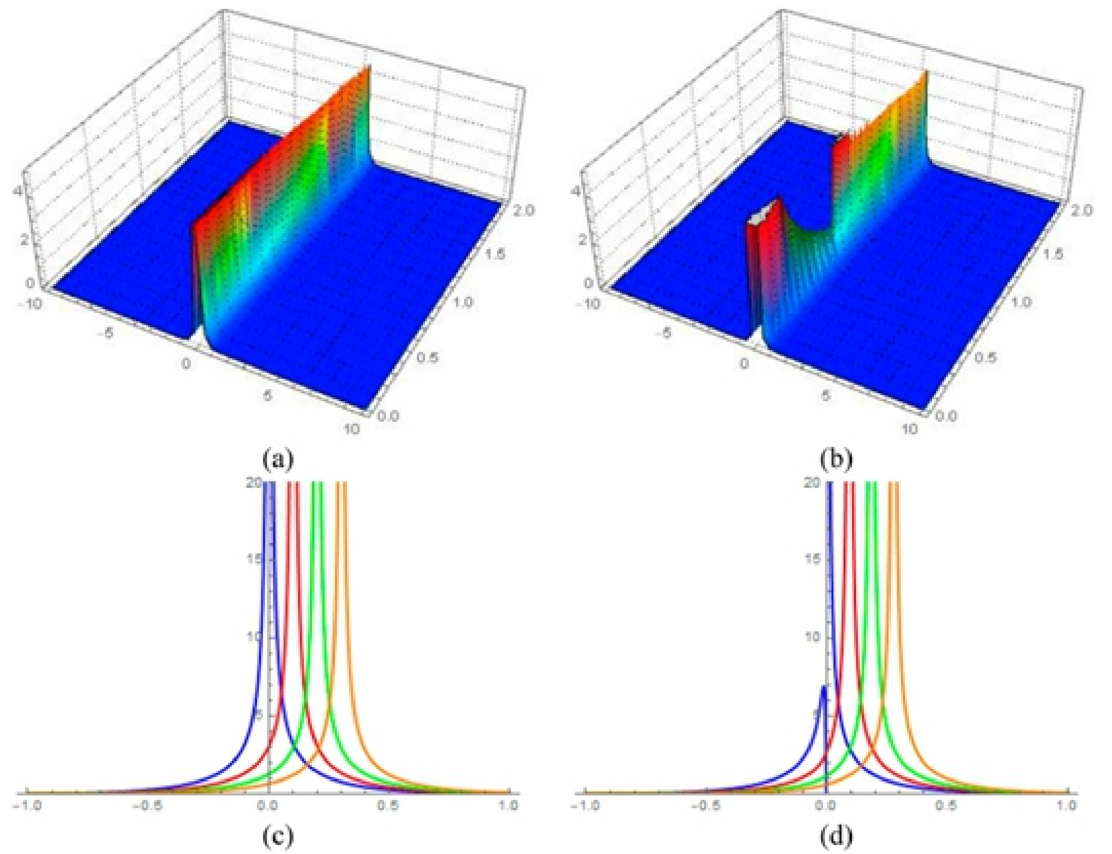


**Figure 6.** The singular chirp soliton solution for (1) at: $a_1 = 0.1, a_2 = 0.1, a_3 = 2, b_1 = 0.1, b_2 = 0.1, \lambda = 0.1$, and $v = 0.2$, where (a) 3D plot of $|\varphi_1(x,t)|$ at $\alpha = 1$, (b) 3D plot of $|\varphi_1(x,t)|$ at $\alpha = 0.95$, (c) 2D plot of $|\varphi_1(x,t)|$ at $\alpha = 1$, (d) 2D plot of $|\varphi_1(x,t)|$ at $\alpha = 0.95$; blue; $t = 0$, red; $t = 0.5$, green; $t = 1$, orange; $t = 1.5$.

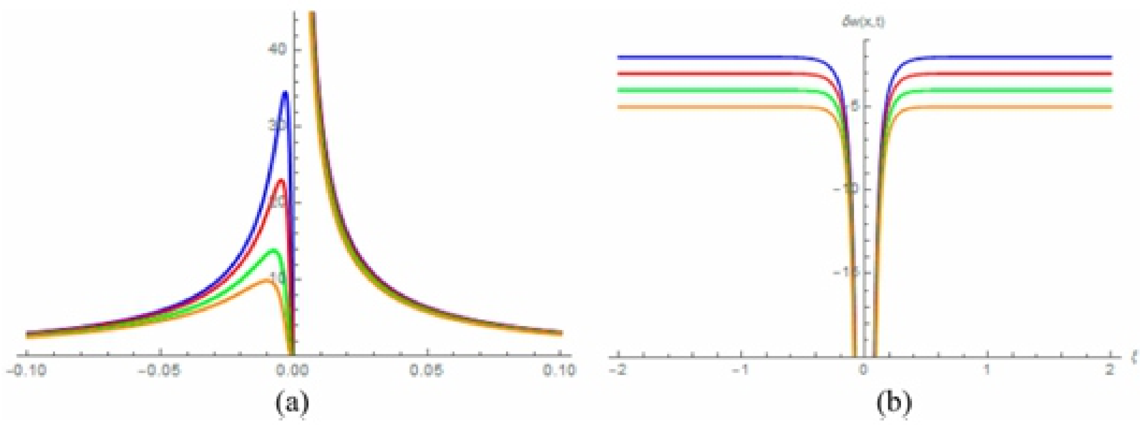


**Figure 7.** (a) Effect of the fractional derivative on the singular chirp soliton: 2D plot of $|\varphi_1(x,0)|$ where blue; $\alpha = 0.99$, red; $\alpha = 0.985$, green; $\alpha = 0.975$, orange; $\alpha = 0.965$, (b) The profile of associate chirp $\delta\omega(x,t)$ in (31): blue; $\lambda = 0.1$ and $v = 0.3$, red; $\lambda = 0.2$ and $v = 0.5$, green; $\lambda = 0.3$ and $v = 0.7$, orange; $\lambda = 0.4$ and $v = 0.9$. Both figures plotted at: $a_1 = 0.1, a_2 = 0.1, a_3 = 2, b_1 = 0.1$, and $b_2 = 0.1$.

where $n, \mu$ and $P_5$ are constants to be determined. Substituting formula (34) into the integer-order ODE (13) and simplifying the result leads to the following equation

$$\begin{aligned}
&\frac{1}{8}P_5R_1\tanh(\mu\xi)^{-2+n} + \frac{3}{4}P_5R_1\tanh(\mu\xi)^n - nP_5\mu^2\mathrm{csch}(\mu\xi)^2\tanh(\mu\xi)^n \\
&- nP_5\mu^2\mathrm{sech}(\mu\xi)^2\tanh(\mu\xi)^n - \frac{1}{8}P_5R_1\mathrm{csch}(\mu\xi)^2\mathrm{sech}(\mu\xi)^2\tanh(\mu\xi)^n \\
&+ n^2P_5\mu^2\mathrm{csch}(\mu\xi)^2\mathrm{sech}(\mu\xi)^2\tanh(\mu\xi)^n + \frac{3}{4}P_5^3R_2\tanh(\mu\xi)^{3n} \\
&- \frac{1}{8}P_5^3R_2\mathrm{csch}(\mu\xi)^2\mathrm{sech}(\mu\xi)^2\tanh(\mu\xi)^{3n} + \frac{3}{4}P_5^5R_3\tanh(\mu\xi)^{5n} \\
&- \frac{1}{8}P_5^5R_3\mathrm{csch}(\mu\xi)^2\mathrm{sech}(\mu\xi)^2\tanh(\mu\xi)^{5n} + \frac{1}{8}P_5R_1\tanh(\mu\xi)^{2+n} \\
&+ \frac{1}{8}P_5^3R_2\tanh(\mu\xi)^{-2+3n} + \frac{1}{8}P_5^3R_2\tanh(\mu\xi)^{2+3n} + \frac{1}{8}P_5^5R_3\tanh(\mu\xi)^{-2+5n} \\
&+ \frac{1}{8}P_5^5R_3\tanh(\mu\xi)^{2+5n} = 0.
\end{aligned} \tag{35}$$

Thus, apply the balancing principle to get the exponent $n = 1$. Insert $n = 1$ in (35) then group the coefficients of the independent terms to obtain.

$$\begin{aligned}
&\tanh(\mu\xi): && \frac{5}{16}P_5R_1 + \frac{5}{16}P_5^3R_2 + \frac{5}{16}P_5^5R_3, \\
&\mathrm{sech}^2(\mu\xi)\tanh(\mu\xi): && \frac{9}{16}P_5R_1 - \frac{3}{16}P_5^3R_2 - \frac{15}{16}P_5^5R_3\mu^2, \\
&\mathrm{sech}^4(\mu\xi)\tanh(\mu\xi): && \frac{1}{8}P_5R_1 - \frac{1}{8}P_5^3R_2 + \frac{5}{8}P_5^5R_3 - \frac{1}{2}P_5\mu^2 \\
&\tanh^3(\mu\xi): && \frac{5}{8}P_5R_1 + \frac{5}{8}P_5^3R_2 + \frac{5}{8}P_5^5R_3, \\
&\mathrm{sech}^2(\mu\xi)\tanh^3(\mu\xi): && \frac{3}{16}P_5R_1 - \frac{1}{16}P_5^3R_2 - \frac{5}{16}P_5^5R_3\mu^2, \\
&\tanh^5(\mu\xi): && \frac{1}{16}P_5R_1 + \frac{1}{16}P_5^3R_2 + \frac{1}{16}P_5^5R_3.
\end{aligned} \tag{36}$$

Setting the coefficients in (36) to be zero and solving the obtained nonlinear algebraic system implies

$$\begin{aligned}
\mu^{\pm} &= \pm\sqrt{\frac{4a_1\lambda+(v+b_1)(v-2a_3+b_1)}{8a_1^2}}, \\
P_5^{\pm} &= \pm\sqrt{\frac{4a_1\lambda+(v+b_1)(v-2a_3+b_1)}{-4a_1a_2+a_3^2-2(v+b_1)b_2+a_3(2c+3b_2)}}.
\end{aligned} \tag{37}$$

Indeed, these inferred values are associated with the following constraints

$$c = \frac{1}{2}(b_2 - a_3), \lambda > \frac{(\nu + b_1)(-\nu + 2a_3 - b_1)}{4a_1},$$
$$a_2 < \frac{a_3^2 - 2(\nu + b_1)b_2 + a_3(2c + 3b_2)}{4a_1}. \tag{38}$$

For these obtained values, the corresponding chirp can be written a

$$\delta\omega(x,t) = -\left(\frac{\nu + b_1}{2a_1}\right) - \left(\frac{a_3 + 3b_2 + 2c}{4a_1}\right) \times \left(\pm\sqrt{\frac{4a_1\lambda + (\nu + b_1)(\nu - 2a_3 + b_1)}{-4a_1a_2 + a_3^2 - 2(\nu + b_1)b_2 + a_3(2c + 3b_2)}} \times \tanh\left(\pm\sqrt{-\frac{4a_1\lambda + (\nu + b_1)(\nu - 2a_3 + b_1)}{4a_1^2}}\left(\frac{x^\alpha}{\alpha} - \nu\frac{t^\alpha}{\alpha}\right)\right)\right)^2. \tag{39}$$

Consequently, the chirp factor is obtained as

$$\phi_{1,2}(x,t) = \left(\left(\frac{\nu + b_1}{2a_1}\right) + \frac{\left(\frac{a_3+3b_2+2c}{4a_1}\right)\left(\frac{4a_1\lambda+(\nu+b_1)(\nu-2a_3+b_1)}{-4a_1a_2+a_3^2-2(\nu+b_1)b_2+a_3(2c+3b_2)}\right)}{\pm\sqrt{-\frac{4a_1\lambda+(\nu+b_1)(\nu-2a_3+b_1)}{4a_1^2}}}\right) \times \left(\frac{x^\alpha}{\alpha} - \nu\frac{t^\alpha}{\alpha}\right) - \frac{\left(\frac{a_3+3b_2+2c}{4a_1}\right)\left(\frac{4a_1\lambda+(\nu+b_1)(\nu-2a_3+b_1)}{-4a_1a_2+a_3^2-2(\nu+b_1)b_2+a_3(2c+3b_2)}\right)}{\pm\sqrt{-\frac{4a_1\lambda+(\nu+b_1)(\nu-2a_3+b_1)}{4a_1^2}}} \times \tanh\left(\pm\sqrt{-\frac{4a_1\lambda + (\nu + b_1)(\nu - 2a_3 + b_1)}{4a_1^2}}\left(\frac{x^\alpha}{\alpha} - \nu\frac{t^\alpha}{\alpha}\right)\right). \tag{40}$$

Accordingly, the dark chirp soliton solution for the space–time pFGI equation can be represented as.

$$\varphi_{1,2,3,4}(x,t) = \pm\sqrt{\frac{4a_1\lambda + (\nu + b_1)(\nu - 2a_3 + b_1)}{-4a_1a_2 + a_3^2 - 2(\nu + b_1)b_2 + a_3(2c + 3b_2)}} \times \tanh\left(\pm\sqrt{-\frac{4a_1\lambda + (\nu + b_1)(\nu - 2a_3 + b_1)}{4a_1^2}}\left(\frac{x^\alpha}{\alpha} - \nu\frac{t^\alpha}{\alpha}\right)\right) \tag{41}$$

$$\times \text{Exp}\left[i\left(\phi_{1,2}(x,t) - \lambda\frac{t^{\alpha}}{\alpha}\right)\right].$$

The profile of modulus of ϕ1 (x,t) that considers the case μ+and P+ 5 is depicted in 3D and 2 D at chosen parameters where the derivative order sare considered in intege rand fractional orders inFigure8.Furthermore, theeffectof thefractionalderivativeonthe evolution of the explored dark chirp soliton has been investigated where Figure9 shows the 3 D and 2 D plot of the modulus of ϕ2(x,t) that considers the caseμ −andP− 5 at different fractional derivative orders .Moreover ,the profile of chirping, ϕ1,2(x,t) (40)has been depicted as a function of the coordinatein Figure10 at different values of the frequency and the speed of the soliton.

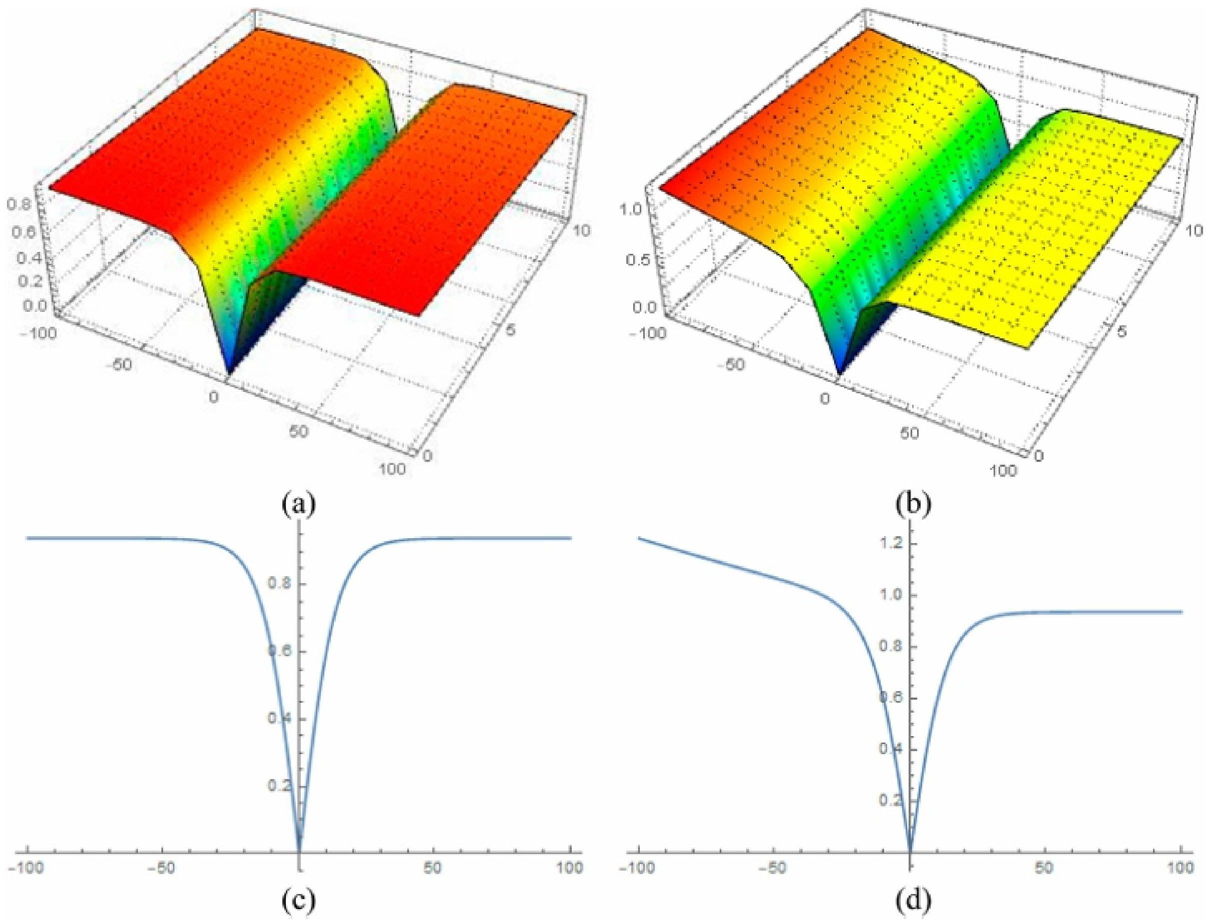

**Figure 8.** The dark chirp soliton solution for (1) at: $a_1 = 1.5, a_2 = 0.01, a_3 = -0.01, b_1 = 0.1, b_2 = -0.4, \lambda = 0.01$, and $v = 0.1$, on $x \in [-100, 100]$ and $t \in [0, 10]$ where (a) 3D plot of $|\varphi_1(x,t)|$ at $\alpha = 1$, (b) 3D plot of $|\varphi_1(x,t)|$ at $\alpha = 0.995$, (c) 2D plot of $|\varphi_1(x,0)|$ at $\alpha = 1$, (d) 2D plot of $|\varphi_1(x,0)|$ at $\alpha = 0.995$.

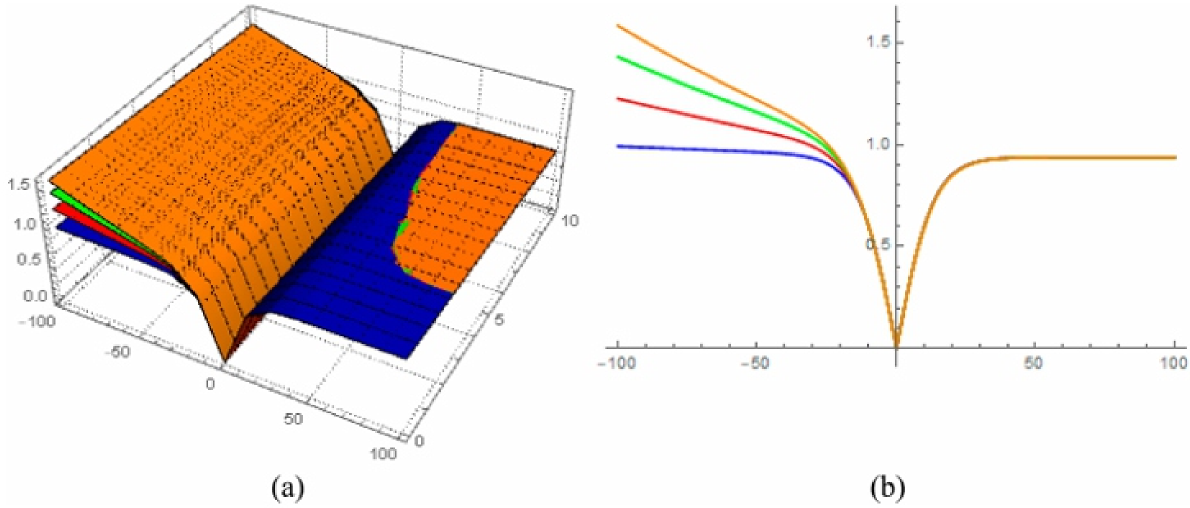


**Figure 9.** Effect of the fractional derivative on dark chirp soliton behaviour at: $a_1 = 1.5, a_2 = 0.01, a_3 = -0.01, b_1 = 0.1, b_2 = -0.4, \lambda = 0.01$, and $v = 0.1$, on $x \in [-100, 100]$ and $t \in [0, 10]$ such that: red; $\alpha = 0.999$, blue; $\alpha = 0.995$, green; $\alpha = 0.992$, and orange; $\alpha = 0.99$, where (a) 3D plot of $|\varphi_2(x,t)|$ and (b) 2D plot of $|\varphi_2(x,0)|$.

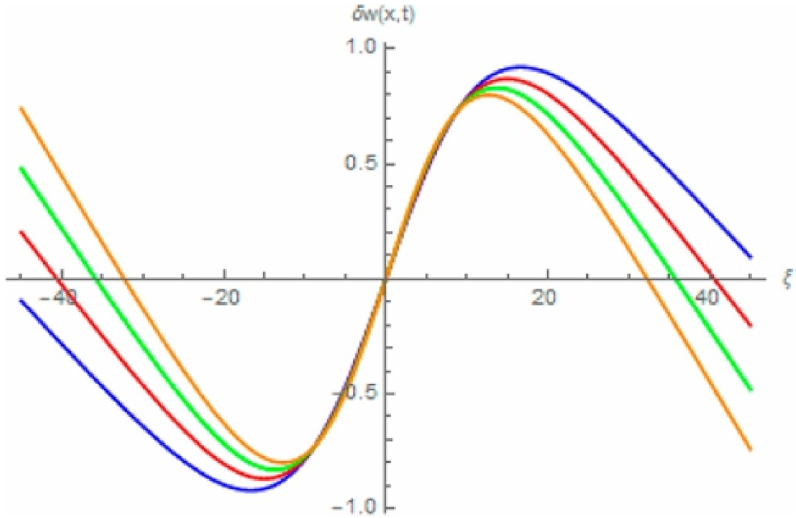


**Figure 10.** The profile of chirping (41) at: $a_1 = 1.5, a_2 = 0.01, a_3 = -0.01, b_1 = 0.1$ and $b_2 = -0.4$, where blue; $\lambda = 0.001$ and $v = 0.2$, red; $\lambda = 0.002$ and $v = 0.21$, green; $\lambda = 0.003$ and $v = 0.22$, orange; $\lambda = 0.004$ and $v = 0.23$.

## 5. Comparison and discussions

This study's chirp soliton solutions show promise for a range of real-world uses, especially in the field of optical communication systems, where their ability to form and maintain optical pulses promotes effective data transfer and signal integrity. Moreover, these solutions advance our knowledge of nonlinear wave dynamics, which has broad ramifications for a variety of physical systems, including Bose–Einstein condensates, fluid dynamics, and plasmaphysics. Thesesolitonsprovidenewpossibilitiesforthestudyofintricate, memorydependent events in a variety of scientific and technical domains thanks to the description of them using fractional calculus. Chirp solitons are extremely useful for preserving waveform stability in optical systems and laser applications, such as materials processing and medical lasers, because of their stability and robustness. Open questions and several obstacles still exist, though. For real-world applications and long-term stability, it is crucial to comprehendthestability and robustness of chirp solitons under a variety of circumstances and perturbations. Experimental validation is typically a barrier in the translation of theoretical results into practical applications, so in order to confirm thepresenceandbehaviour of chirp solitons, real-world tests are required. It will take interdisciplinary cooperation in the fields of mathematics, physics, engineering, and materials science to fully realize the promise of chirp solitons. It is difficult and still unexplored to analyse chirp solitons in a wider class of fractional nonlinear partial differential equations. Finding the best parameter values for certain applications and comprehending how they affect soliton behaviour are still crucial issues in the industry.

As mentioned earlier in this work, the study and exploration of chirp soliton solutions to the governing Equation (1) is presented for the first time in our work. Despite this, several works have been presented to study the governing Equation (1) in literature. The tanh methodandthetanh-cothmethodhavebeenappliedtoobtainnewsolitarywavesolutions for (1) in [44]. The fractional H-expansion method and fractional projective Riccati expansion approach are utilized to extract analytical solutions based on the Mittag-Leffler function for (1) in [45]. The authors in [46] investigated novel dark and other soliton solu tions and compared them with the existing results. In [47], new exact solitary solutions have been obtained with the aid of conformable derivative and the Kudryashov method.

## 6. Discussion and conclusion

We have made important discoveries on the intricate dynamics of the space–time pFGI equation under quintic nonlinearity and self-steepening. Numerous noteworthy conclusions have been drawn from thist horough examination.Bright,singular, and dark solitons are three different chirp soliton solutions that we have identified and thoroughly investigated. These solutions are important in nonlinear wave dynamics and have real-world applications in fluid dynamics, nonlinear physics, and optics. Furthermore, to provide a morecomprehensive knowledge of the behaviour of the system, we presented a novel fractional complex travelling wave transformation that reduces the equation to an easier-to manage integer-order ordinary differential equation. Our examination of the integer-order ODE's dynamical behaviour and equilibrium bifurcation provides important information about the stability and behaviour of solutions, illuminating the pFGI equation's underlying dynamics. To improve comprehension, we have included graphical depictions of every solution that we were able to get for clarifying the physical properties and actions of the solitons when certain parameter limits are satisfied.

To gain a better understanding of how fractional calculus shapes the behaviour of the pFGI equation, we also investigated the impactoffractional derivatives on the evolution profile of these solutions. Our results have practical ramifications beyond theory; the generated chirp soliton solutions are promising for various applications, especially in systems with quintic nonlinearity effects and selfsteepening. The design and functionality of nonlinear physical systems, such as optical communication systems, could be improved by these techniques.

Regarding future research directions, this paper provides several important avenues for investigation. Firstly, an expansion to higher-dimensional systems is necessary, which will shed light on the spatiotemporal evolution of the soliton behaviour in more intricate physical situations. Secondly, to comprehend the adaptability of chirp soliton solutions to various circumstances, a detailed examination of the impact of varied material qualities and nonlinear effects is necessary. It is also advised to perform a thorough stability analysis on chirp solitons to evaluate their resilience in real-world scenarios where waveform stability is essential. In addition, future research ought to concentrate on recognizing and creating practical applications, particularly in the fields of fluid dynamics, plasma physics, and optical communication.

## Author's contributions

MA a made significant contributions to the creation of the work. SAl and MAl con tributed to the design of the work and handled the analysis. SM conceptualized and doublechecked the Analysis part. DLS was involved in the manuscripts drafting or critical revision for important intellectual content. All authors read and approved the final version of manuscript.

## Disclosure statement

Nopotential conflict of interest was reported by the author(s).

## Data availability statement

No data were used to support this study.

## Funding

Thisstudydidnotreceiveanyfundinginanyform.

***References***

*[1] Adigüzel RS, Aksoy Ü, Karapinar E, et al. On the solution of a boundary value problem asso ciated with a fractional differential equation. Math Methods ppl Sci. 2020:1–12. doi:10.1002/ mma.6652*

*[2] MiaR,MiahMM,OsmanMS.Anewimplementationofanovelanalyticalmethodforfinding the analytical solutions of the (2+1)-dimensional KP-BBM equation. Heliyon.2023;9(5):1–10.*

*[3] Adiguzel RS, Aksoy Ü, Karapinar E, et al. Uniqueness of solution for higher-order nonlinear fractional differential equationswithmulti-pointandintegralboundaryconditions.RACSAM. 2021;115:155. doi:10.1007/s13398-021-01095-3*

*[4] Al-Smadi M, Abu Arqub O, Hadid S. Approximate solutions of nonlinear fractional KunduEckhaus and coupled fractional massive thirring equations emerging in quantum field theory using conformable residual power series method. Phys Scr. 2020;95(10):105205. doi:10.1088/1402-4896/abb420*

*[5] Al-SmadiM,AbuArqubO,MomaniS.Numericalcomputationsofcoupledfractionalresonant Schrödinger equations arising in quantum mechanics under conformable fractional derivative sense. Phys Scr. 2020;95(7):075218. doi:10.1088/1402-4896/ab96e0*

*[6] Hasan S, Al-Smadi M, Freihet A, et al. Two computational approaches for solving a fractional obstacle systeminHilbertspace.AdvDifferEqu.2019;2019:55.doi:10.1186/s13662-0191996-5*

*[7] Al-Smadi M, Freihat A, Arqub OA, et al. A novel multistep generalized differential transform method for solving fractional-order Lü Chaotic and hyperchaotic systems. J Comput Anal Appl. 2015;19(4):713–724.*

*[8] Altawallbeh Z, Al-Smadi M, Komashynska I, et al. Numerical solutions of fractional systems of two-point BVPs by using the iterative reproducing kernel algorithm. Ukr Math J. 2018;70(5):687–701. doi:10.1007/s11253-018-1526-8*

*[9] Al-Smadi M, Arqub OA, Zeidan D. Fuzzy fractional differential equations under the MittagLeffler kernel differential operator of the ABC approach: theorems and applications. Chaos, Solitons Fractals. 2021;146:110891. doi:10.1016/j.chaos.2021.110891*

*[10] Wang M, Li X, Zhang J. The (G/G)–expansion method and travelling wave solutions of nonlinear evolution equations in mathematical physics. Phys Lett A. 2008;372(4):417–423.*

*[11] Alabedalhadi M, Al-Smadi M, Al-Omari S, et al. Structure of optical soliton solution for nonliear resonant space-time Schrödinger equation in conformable sense with full nonlinearity term. Phys Scr. 2020;95(10):105215. doi:10.1088/1402-4896/abb739*

*[12] Alabedalhadi M. Exact travelling wave solutions for nonlinear system of spatiotemporal fractional quantum mechanics equations. Alexandria Eng J. 2022;61(2):1033–1044. doi:10.1016/j.aej.2021.07.019*

*[13] Tariq KU, Rezazadeh H, Zubair M, et al. New exact and solitary wave solutions of non linear*

*Schamel–KdV equation. Int J Appl Comput Math. 2022;8(3):114. doi:10.1007/s40819-022 01315-3*

*[14] Osman MS, Rezazadeh H, Eslami M, et al. Analytical study of solitons to Benjamin-Bona Mahony-peregrine equation with power law nonlinearity by using three methods. UPB Sci Bull, Ser A. 2018;80(4):267–278.*

*[15] Tariq KU, Rezazadeh H, Zubair M, et al. New exact and solitary wave solutions of non linear Schamel–KdV equation. Int J Appl Comput Math. 2022;8(3):114. doi:10.1007/s40819-022 01315-3*

*[16]HouweA,Abbagari S,NisarKS, et al. Influenceof fractional timeorder onW-shaped and modulation instability gain in fractional nonlinear Schrödinger equation. Results Phys. 2021;28:104556. doi:10.1016/j.rinp.2021.104556*

*[17] Siddique I, Jaradat MM, Zafar A, et al. Exact traveling wave solutions for two prolific conformable M-fractional differential equations via three diverse approaches. Results Phys. 2021;28:104557. doi:10.1016/j.rinp.2021.104557*

*[18] Akbar MA, Wazwaz AM, Mahmud F, et al. Dynamical behavior of solitons of the per turbednonlinearSchrödingerequationandmicrotubulesthroughthegeneralizedKudryashov scheme. Results Phys. 2022;43:106079. doi:10.1016/j.rinp.2022.106079*

*[19] Mirzazadeh M, Sharif A, Hashemi MS, et al. Optical solitons with an extended (3+1) dimensional nonlinear conformable Schrödinger equation including cubic–quintic nonlinear ity. Results Phys. 2023;49:106521. doi:10.1016/j.rinp.2023.106521*

*[20] Malik S, Almusawa H,KumarS,etal. A(2+1)-dimensional Kadomtsev–Petviashvili equation with competing dispersion effect: Painlevé analysis, dynamical behavior and invariant solu tions. Results Phys. 2021;23:104043. doi:10.1016/j.rinp.2021.104043*

*[21] Djennadi S, Shawagfeh N, Osman MS, et al. The Tikhonov regularization method for the inverse source problem of time fractional heat equation in the view of ABC-fractional tech nique. Phys Scr. 2021;96(9):094006. doi:10.1088/1402-4896/ac0867*

*[22] Al-Smadi M, Abu Arqub O, Gaith M. Numerical simulation of telegraph and Cattaneo fractional-type models using adaptive reproducing kernelframework.MathMethodsApplSci. 2021;44(10):8472–8489. doi:10.1002/mma.6998*

*[23] Adiguzel RS, Aksoy U, Karapinar E, et al. On the solutions of fractional differential equations via Geraghty type hybrid contractions. Appl Math Comput 2021;20(2):313–333.*

*[24] Lazreg JE, Abbas S, Benchohra B, et al. Impulsive Caputo-Fabrizio fractional problems via Hilfer fractional derivative on b-metric spaces. Adv Differ Equ 2020;2020:616.*

*[25] Ardjouni A. Asymptotic stability in Caputo-Hadamard fractional dynamic equations. Results Nonlinear Anal. 2021;4(2):77–86. doi:10.53006/rna.865900*

*[26] BenchohraaM,SlimaneM.Fractionaldifferentialinclusions withNoninstantaneous impulses in banach spaces. Results Nonlinear Anal. 2019;2(1):36–47.*

*[27] Foroutan M, Kumar D, Manafian J, et al. New explicit soliton and other solutions for the con formable fractional Biswas–Milovic equation with Kerr and parabolic nonlinearity through an integration scheme. Optik (Stuttg). 2018;170:190–202. doi:10.1016/j.ijleo.2018.05.129*

*[28] Yépez-Martínez H, Gómez-Aguilar JF. M-derivative applied to the soliton solutions for the Lakshmanan–Porsezian–Daniel equation with dual-dispersion for optical fibers. Opt Quantum Electron. 2019;51(1):31. doi:10.1007/s11082-018-1740-5*

*[29] Rezazadeh H, Mirhosseini-Alizamini SM, Eslami M, et al. New optical solitons of nonlinear conformable fractional Schrödinger-Hirota equation. Optik (Stuttg). 2018;172:545–553. doi:10.1016/j.ijleo.2018.06.111*

*[30] Gerdjikov VS, Ivanov I. A quadratic pencil of general type and nonlinear evolution equations. II. Hierarchies of Hamiltonian Structures. J Phys Bulgar. 1983;10:130–143.*

*[31] Kaur L, Wazwaz AM. Optical solitons for perturbed Gerdjikov–Ivanov equation. Optik (Stuttg). 2018;174:447–451. doi:10.1016/j.ijleo.2018.08.072*

*[32] Arshed S. Two reliable techniques for the soliton solutions of perturbed Gerdjikov–Ivanov equation. Optik (Stuttg). 2018;164:93–99. doi:10.1016/j.ijleo.2018.02.119*

*[33] Yaşar E, Yıldırım Y, Yaşar E. New optical solitons of space-time conformable fractional perturbed Gerdjikov-Ivanov equation by sine-Gordon equation method. Results Phys. 2018;9:1666–1672. doi:10.1016/j.rinp.2018.04.058*

*[34] Hosseini K, Mirzazadeh M, Ilie M, et al. Dynamics of optical solitons in the perturbed Gerdjikov–Ivanov equation. Optik (Stuttg). 2020;206:164350. doi:10.1016/j.ijleo.2020.164350*

*[35] Abdel-Gawad HI. Approximate-analytic optical soliton solutions of a modified-Gerdjikov– Ivanov equation: modulation instability. Opt Quantum Electron. 2023;55(4):298. doi:10.1007/ s11082-023-04566-6*

*[36] Osman MS, Zafar A, Ali KK, et al. Novel optical solitons to the perturbed Gerdjikov–Ivanov equation with truncated M-fractional conformable derivative. Optik (Stuttg). 2020;222:165418. doi:10.1016/j.ijleo.2020.165418*

*[37] Kilbas AA, Srivastava HM, Trujillo JJ. Theory and applications of fractional differential equations, Vol. 204, 2006.*

*[38] Podlubny I. Fractional differential equations: an introduction to fractional derivatives, fractional differential equations, to methods of their solution and some of their applications. Elsevier; 1998.*

*[39] Caputo M, Fabrizio M. A new definition of fractional derivative without singular kernel. Progr Fract Differ Appl. 2015;1(2):1–13.*

*[40] Atangana A, Baleanu D. New fractional derivatives with nonlocal and non-singular kernel: theory and application to heat transfer model. Thermal Sci. 2016;20(2):763–769. doi:10.2298/TSCI160111018A*

*[41] Salim A, Benchohra B, Karapinar E, et al. Existence and Ulam stability for impulsive generalized Hilfer-type fractional differential equations. Adv Differ Equ 2020;601:1–18.*

*[42] Khalil R, Al Horani M, Yousef A, et al. A new definition of fractional derivative. J Comput Appl Math. 2014;264:65–70. doi:10.1016/j.cam.2014.01.002*

*[43] Abdeljawad T. On conformable fractional calculus. J Comput Appl Math. 2015;279:57–66. doi:10.1016/j.cam.2014.10.016*

*[44] Zulfiqar A, Ahmad J. New optical solutions of conformable fractional perturbed GerdjikovIvanov equation in mathematical nonlinear optics. Results Phys. 2021;21:103825. doi:10.1016/ j.rinp.2021.103825*

*[45] Li C, Li G, Chen L. Fractional optical solitons of the space-time perturbed fractional Gerdjikov Ivanov equation. Optik (Stuttg). 2020;224:165638. doi:10.1016/j.ijleo.2020.165638*

*[46] Zafar A, Ali KK, Raheel M, et al. Abundant M-fractional optical solitons to the pertubed Gerd jikov–Ivanov equation treating the mathematical nonlinear optics. Opt Quantum Electron. 2022;54(1):25. doi:10.1007/s11082-021-03394-w*

*[47] Agh A, Sharif A. Exact solitary wave solutions to the fractional Gerdjikov-Ivanov equation with conformable derivative, 2023*

ISSN 2986 - 0776

# Solution of local fractional generalized coupled Korteweg–de Vries (cKdV) equation using local fractional homotopy analysis method and Adomian decomposition method

**Awatif Muflih Alqahtania and Jyoti Geetesh Prasadb,c**
a Department of Mathematics, Shaqra University, Riyadh, Saudi Arabia;
b Department of Mathematics, AMITY School of Applied Sciences, AMITY University Rajasthan, Jaipur, India;
c MKSSS's Cummins College ofEngineering for Women, Pune, India

## A B S T R A C T

*In this study, time-fractional coupled Korteweg–de Vries (cKdV) equations are solved using an efficient and reliable numerical technique. The classical cKdV system has been generalized into thetime-fractional cKdV system. We employ the local fractional homotopy analysis method (LFHAM) and the Adomian decompositionmethod (ADM) to propose an approximate solution for fractionalcKdV equations. Both approaches determinedfindings are comparedtogether. The findings clearly demonstrate that the suggested methods are appropriate and efficient for handling both linear and non linear issues in engineering and sciences. To demonstrate the suggested approaches' competencies, examples are provided. Convergent series form has been used to make the solutions. The relevanceof the techniques is illustrated through graphic representations ofthe solution*

***ARTICLE HISTORY*** *Received 29 November 2022 Accepted 14 December 2023*

***KEYWORDS*** *Local fractional derivative; coupled Korteweg–de Vriesequation; homotopy analysis method; Adomian decomposition method*

***2010 MATHEMATICS SUBJECT CLASSIFICATIONS*** *34A34; 65M06; 26A33*

## 1. Introduction

Real-life problem of engineering and sciences gives rise to nonlinear ordinary differential equations ( ODEs) and partial differential equations ( PDEs). Non-linear system has varied range of engineering applications. Most of the real-life problems are convertible intononlinear mathematical models. Therefore, resolving such a system has its significance anddemands in-depth research. Researchers are motivated to develop and investigated effective methods and techniques to solve such dynamical systems, which exhibit nonlinearities.Yang et al. have shown nonlinear dynamics for local fractional Burger equation arisingin fractal flow [1], similarly, Yang, Gao and Srivastava have worked for non-differentiableexact solutions for the nonlinear ODEs defined on fractal sets [2] and Dubey and Goswamihave solved the nonlinear diffusion equation [3]. In this regard, time-dependent nonlinear

coupled Korteweg–de Vries (cKdV) equations attracted a lot of study interest. A part from the nonlinear system, we see frequent presence of ODEs, PDEs of fractional orde
in many fields like fluid dynamics, biology and physics. Numerous disciplines, including mechanics, electrical, chemistry, biology and economics, particularly control theory, signalimage processing and groundwater issues, have benefited greatly from the use of fractionalcalculus. Many phenomena occurred in engineering, physical and medical science problems can be described by fractional order ODEs, PDEs effectively. Khan et al. have workedfor the numerical solution of advection–diffusion equations involving Atangana–Baleanutime fractional derivative [4], Baleanu et al. have worked on the mathematical modelling ofhuman liver with Caputo–Fabrizio fractional derivative [5], Defterli et al. have solved problems related to accelerated mass-spring system by fractal treatment [6]. Many researchershave been working to find analytical approximate solution of local fractional PDEs [7–11].
Local fractional calculus operator is first introduced by Kolwankar and Gangal[12] which is established on the fractional derivative of Riemann–Lioville sense. Nondifferentiate functions can be easily handled by above-mentioned operators. A lot ofscholars have also worked on the development of the fractal fractional derivative; in addition to this, He et al. have given new promises and future challenges of fractal calculus fromtwo scale thermodynamics to fractal variational principle [13].
Numerous numerical and analytical techniques have been used by researchers during the past 20 years to get analytical or approximate solutions of local fractional PDEs, such as the local fractional Laplace transform, local fractional variational iteration, localfractional homotopy perturbation, local fractional Laplace homotopy perturbation, localfractional reduced differential transform methods, Laplace variational iteration methodsand so on. Dubey et al. have solved Klein–Gordon equations by using homotopy perturbation Mohand transform method [14], Yang et al. have used local fractional series expansionmethod to solve Klein–Gordon equations on Cantor sets [15], Wang et al. have appliedlocal fractional function decomposition method for solving inhomogeneous wave equations with local fractional derivative [16]. Similarly many research works have been donein this context [17–21].
This study's main goal is to find a local fractional derivative solution to the generalized fractional cKdV equation.
In the exploration of nonlinear physical processes, the investigation of travelling wave solutions for the nonlinear system of equations is a vital step. The fluid flow beneath apressure surface is visible along lakeshores and beaches as shallow water waves. For thepast three decades, researchers have been working on a mathematical model of this phenomenon in a variety of science and engineering fields, including oceanography. For example, the long-wave short-wave interaction equation [22–26], the Kadomtsev–Petviashviliequation [24], the Gear–Grimshaw model [25] and the Schrödinger–Boussinesq equation[26] are some of the mathematical models that are presented in this context. To define a wide range of physical occurrences utilized to simulate the interaction and evolution

of non-linear waves, the study of the KdV equation is important [27]. Waves on shallow water surfaces are quantitatively represented by the KdV equation. Boussinesq first presented theKdV equation in 1877, and Diederik Korteweg and Gustav de Vries later rediscovered it (1895) [28].

Now, we write fractional-order KdV equation:

$$D_t^{\alpha} v + v^n D_x^{\alpha} v + D_x^{3\alpha} v = 0, t > 0, \alpha < 1. \qquad (1)$$

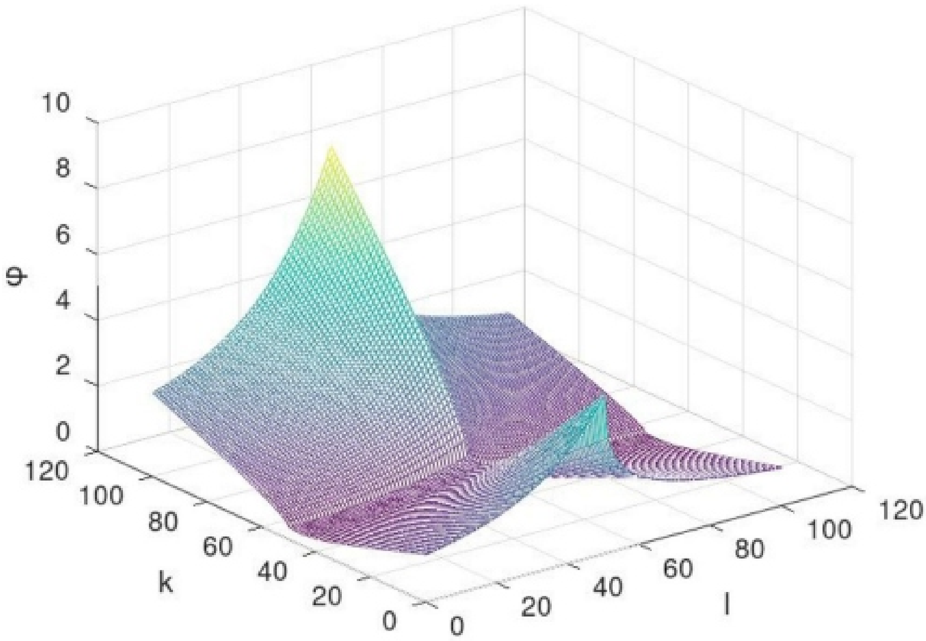


**Figure 1.** Graphical representation of solution of Equation (19) for $\nu = 0.5$.

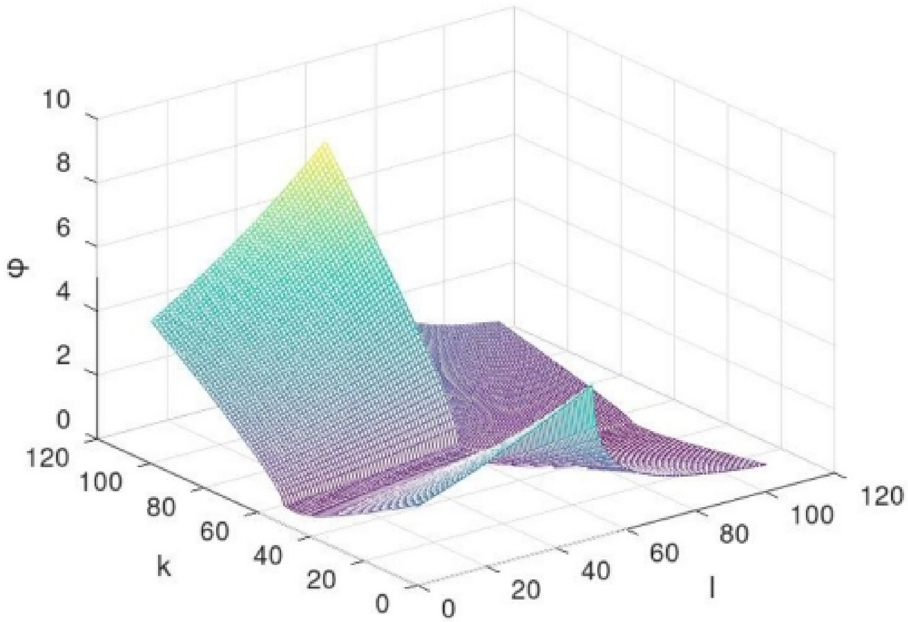


**Figure 2.** Graphical representation of solution of Equation (19) for $\nu = 0.8$.

This research work is a good discussion on the solution of nonlinear fractional cKdV equation. Hirota and Satsums introduced the cKdV equation in 1981. They discussed theinteraction of two long waves with different dispersion relations [29].

The function of trigonometric transform approach, the F-expansion approach, the homotopy perturbation as well as its transformation approach, and the Adomian decomposition method (ADM) are the primary methods that have been used by various author

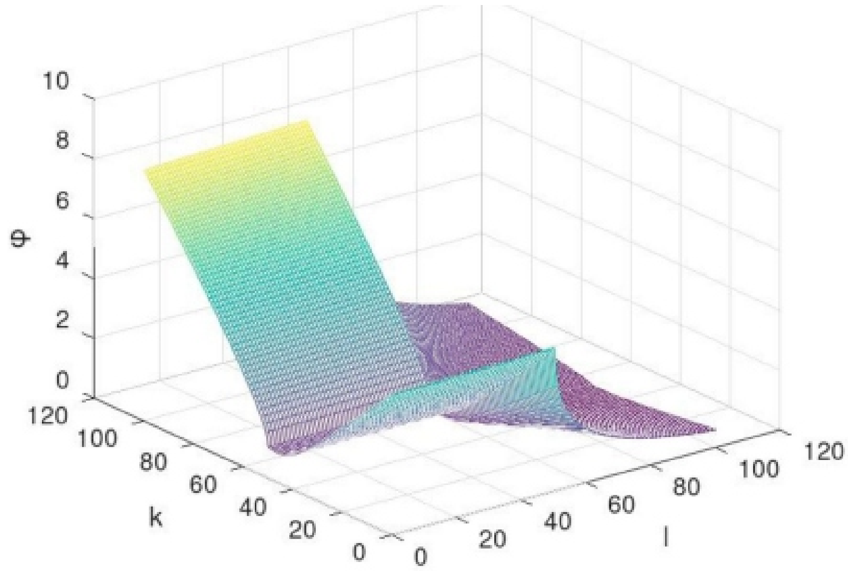


**Figure 3.** Graphical representation of solution of Equation (19) for $\nu = 0.99$.

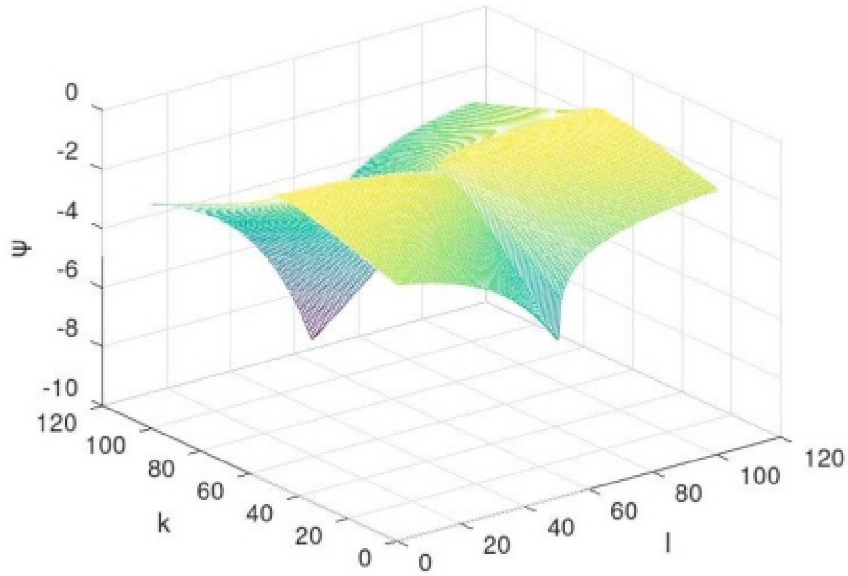


**Figure 4.** Graphical representation of solution of Equation (20) for $\nu = 0.5$.

to solve coupled equations [30, 31]. Furthermore, the local fractional reduced differential transform and local fractional Laplace variational iteration methods were also used by Jafari et al. [32, 33] to find approximations of solutions for cKdV equations.

They have solved the following system of fractional cKdV equations:

$$\frac{\partial^{\upsilon}\phi}{\partial k^{\upsilon}} + \frac{\partial^{3\upsilon}\phi}{\partial l^{3\upsilon}} + 2\phi\frac{\partial^{\upsilon}\phi}{\partial l^{\upsilon}} + 2\psi\frac{\partial^{\upsilon}\phi}{\partial l^{\upsilon}} = 0, \tag{2}$$

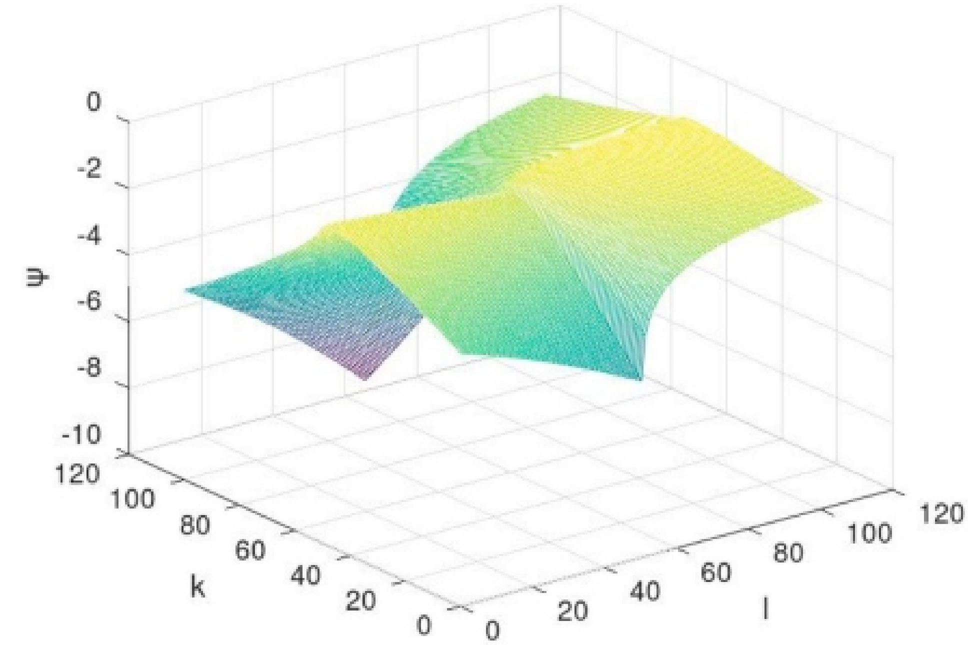


**Figure 5.** Graphical representation of solution of Equation (20) for $\nu = 0.8$.

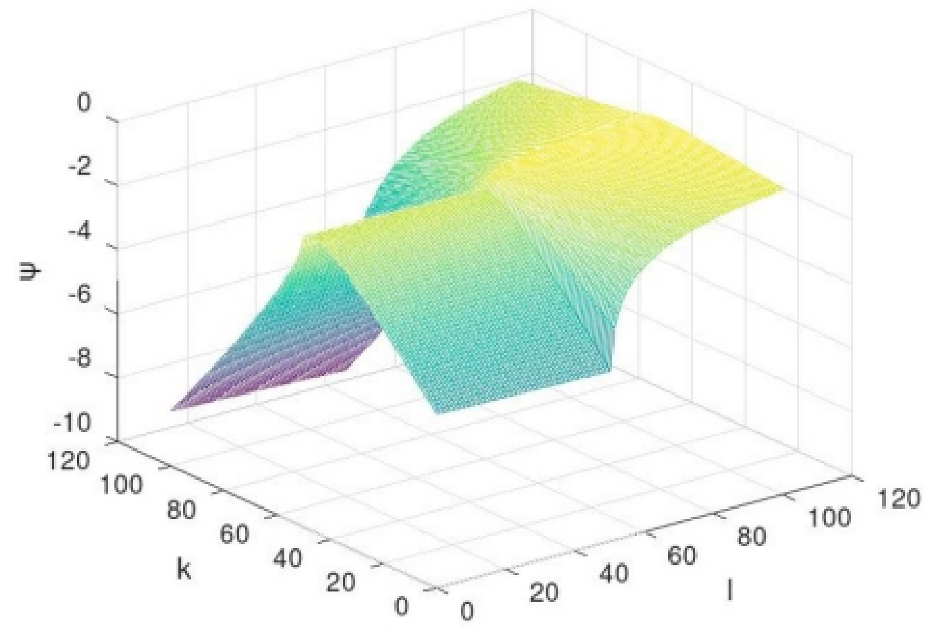


**Figure 6.** Graphical representation of Equation (20) for $\nu = 0.99$.

$$\frac{\partial^{\upsilon}\psi}{\partial k^{\upsilon}}+\frac{\partial^{3\upsilon}\psi}{\partial l^{3\upsilon}}+2\psi\frac{\partial^{\upsilon}\psi}{\partial l^{\upsilon}}+2\phi\frac{\partial^{\upsilon}\psi}{\partial l^{\upsilon}}=0. \quad (3)$$

Due to its frequent occurrence in numerous real-world problems, nonlinear cKdV equations have been the subject of many research studies; therefore, understanding its generalized form is significant. In this research, authors investigate the most general kind ofcoupled nonlinear fractional KdV equation.

Consider the following the n-generalized fractional cKdV equation:

$$\frac{\partial^{\upsilon}\phi}{\partial k^{\upsilon}}+\frac{\partial^{3\upsilon}\phi}{\partial l^{3\upsilon}}+2\phi^{n}\frac{\partial^{\upsilon}\phi}{\partial l^{\upsilon}}+2\psi^{m}\frac{\partial^{\upsilon}\phi}{\partial l^{\upsilon}}=0, \quad (4)$$

$$\frac{\partial^{\upsilon}\psi}{\partial k^{\upsilon}}+\frac{\partial^{3\upsilon}\psi}{\partial l^{3\upsilon}}+2\psi^{n}\frac{\partial^{\upsilon}\psi}{\partial l^{\upsilon}}+2\phi^{m}\frac{\partial^{\upsilon}\psi}{\partial l^{\upsilon}}=0, \quad (5)$$

with initial conditions $\phi(l,0)=\phi_0(l)$, $\psi(l,0)=\psi_0(l)$.

In the present paper, authors suggest two approaches to produce analytical approximate solution for generalized fractional cKdV equations, with initial conditions

$$\phi(l,0)=E_{\upsilon}(-l^{\upsilon}),\quad \psi(l,0)=-E_{\upsilon}(-l^{\upsilon}).$$

The focus of this study is on the fractional cKdV equations and the use of the ADM and local fractional homotopy analysis method (LFHAM). Numerous problems in the realworld, including those involving magma movement, surface waves, Rossby waves, internalwaves in a fluid with stratified density, and plasma waves, depend on the KdV equation.Maitama and Zhao introduced the local homotopy analysis method initially [34], LFHAMis a very helpful tool for solving the differential equations. By carefully choosing the parameters h and H, this approach LFHAM is particularly effective in regulating and controlling the convergence of the solution [35].

A numerical technique based on Adomian's invention [36] of the ADM is presented in this study as an approximate method for solving fractional cKdV equations. The ADM isa potent method that offers effective algorithms for approximate analytical answers andnumerical simulations for practical applications in applied sciences and engineering [37,38].

Both approaches are excellent techniques for solving generalized nonlinear fractional differential equations, even though the outcome is expressed in terms of an infinite The method's drawback is that numerous terms from the infinite series must be taken intoaccount to obtain high accuracy. To develop an analytical approximate solution for local fractional PDEs, numerous scholars have been working

In this section, some basic expert duties are covered. For a moment, suppose that Herrmann and Hilfer's fractional partial differential conditions, like time-fractional NS conditions, are not completely predetermined by applications in a variety of scientific a planning fields. Recently, El-Shahed and Salem conducted a sporadic presentation of NS circumstances in 2005. For summing out-of-date NS conditions, makers employed Laplacechange, constrained Hankel change, and finite Fourier Sine change. By combining HPMand LTA, Kumar et al. deductively addressed a nonlinear partial model of the NS condition. By using the homotopy evaluation technique, Ganji et al., in addition to Ragab et al.,has resolved non-straight time fragmented Navier–Stokes system. ADM was developed byOdibat, Momani, and Birajdar to provide numerical estimates of the time-fractional NScondition. While Chaurasia and Kumar had inclined to a comparative condition by combining limited Hankel change and Laplace change, Kumar et al. obtained a canny plan of thetime-partial NS condition utilizing a combination of ADM and Laplace change. To handle nonlinear and instantaneous ODEs and PDEs, M. Rawashdeh and S. Maitama introducedNDM in 2014. The partial order Whitham–Broer–Kaup conditions, fractional order heatand wave conditions, fractional actual models, fractional order PDEs with relative deferment, and the fractional order dissemination conditions are just a few of the real-worldissues that were concentrated using NDM.

The sensible strategy of fractional soliciting NS circumstances is emphasized on the ongoing creation. Since a long time ago, examiners have been interested in the arrangement of typical NS conditions. Actually, the main area of agreement between researchersand mathematicians is the intelligent designs of the fragmented request NS condition. Thiswas the active endeavour to develop or promote the ongoing systems for the strategiesof NS soliciting that was not complete. A noteworthy portion of them have developedinnovative methods to deal with Navier–Stokes of fragmentary order. In this way, streamresearch efforts make a sensible addition to the Navier–Stokes partial order conditions'logical framework.

In more recent works, Chu et al. used the variation iteration transform approach along with Caputo derivative and Laplace transform to solve the problem. Singh and Kumarused the fractional reduced differential transform technique to get the approximate solution of the system, whereas Kavvas and Ercan used a completely different strategy to findthe solution of the Navier–Stokes system. They made use of the momentum equationsystem.

In this paper, we performed logical operations, particularly the Laplace transformation approach, but we also assessed them and presented an argument in favour of the application of the recommended calculations. In this work, we first apply existence and onenesstheorem to show the existence and oneness of result. Using the Laplace transform, wewill continue to solve the problem iteratively. In order to find an approximate solutionof Navier–Stokes system, this work employs a unique technique and strategy. Our focus isin fact primarily on the stream, the effects and adjustments brought about by the

In this section, some basic expert duties are covered. For a moment, suppose that Herrmann and Hilfer's fractional partial differential conditions, like time-fractional NS conditions, are not completely predetermined by applications in a variety of scientific a planning fields. Recently, El-Shahed and Salem conducted a sporadic presentation of NS circumstances in 2005. For summing out-of-date NS conditions, makers employed Laplacechange, constrained Hankel change, and finite Fourier Sine change. By combining HPMand LTA, Kumar et al. deductively addressed a nonlinear partial model of the NS condition. By using the homotopy evaluation technique, Ganji et al., in addition to Ragab et al.,has resolved non-straight time fragmented Navier–Stokes system. ADM was developed byOdibat, Momani, and Birajdar to provide numerical estimates of the time-fractional NScondition. While Chaurasia and Kumar had inclined to a comparative condition by combining limited Hankel change and Laplace change, Kumar et al. obtained a canny plan of thetime-partial NS condition utilizing a combination of ADM and Laplace change. To handle nonlinear and instantaneous ODEs and PDEs, M. Rawashdeh and S. Maitama introducedNDM in 2014. The partial order Whitham–Broer–Kaup conditions, fractional order heatand wave conditions, fractional actual models, fractional order PDEs with relative deferment, and the fractional order dissemination conditions are just a few of the real-worldissues that were concentrated using NDM.

The sensible strategy of fractional soliciting NS circumstances is emphasized on the ongoing creation. Since a long time ago, examiners have been interested in the arrangement of typical NS conditions. Actually, the main area of agreement between researchersand mathematicians is the intelligent designs of the fragmented request NS condition. Thiswas the active endeavour to develop or promote the ongoing systems for the strategiesof NS soliciting that was not complete. A noteworthy portion of them have developedinnovative methods to deal with Navier–Stokes of fragmentary order. In this way, streamresearch efforts make a sensible addition to the Navier–Stokes partial order conditions'logical framework.

In more recent works, Chu et al. used the variation iteration transform approach along with Caputo derivative and Laplace transform to solve the problem. Singh and Kumarused the fractional reduced differential transform technique to get the approximate solution of the system, whereas Kavvas and Ercan used a completely different strategy to findthe solution of the Navier–Stokes system. They made use of the momentum equationsystem.

In this paper, we performed logical operations, particularly the Laplace transformation approach, but we also assessed them and presented an argument in favour of the application of the recommended calculations. In this work, we first apply existence and onenesstheorem to show the existence and oneness of result. Using the Laplace transform, wewill continue to solve the problem iteratively. In order to find an approximate solutionof Navier–Stokes system, this work employs a unique technique and strategy. Our focus isin fact primarily on the stream, the effects and adjustments brought about by the

[39–42].

**Definition 1.1:** The local fractal derivative for a real-valued function, L at g = g0 is defined as [43, 44]

$$D^{\beta}L(g_0) = \frac{d^{\beta}}{dg^{\beta}}L(g)|_{g_0}$$
$$= \lim_{g \to g_0} \frac{\Delta^{\beta}(L(g) - L(g_0))}{(g - g_0)^{\beta}},$$

such that

$$|L(g) - L_0(g)| < \in^{\beta},$$

where

$$\Delta^{\beta}(L(g) - L(g_0)) \cong [L(g) - L(g_0)]\,\Gamma(1+\beta).$$

**Section 1: Introduction**

**Section 2: Existence and Oneness of the Solution**

**Section 3: Analysis of the methods and applications**

**Section 4: Conclusion**

## 2. Existence and oneness of the solution

$N$-generalized fractional cKdV equations are given as follows:

$$\begin{cases} \frac{\partial^{\upsilon}\phi}{\partial\lambda^{\upsilon}} + \frac{\partial^{3\upsilon}\phi}{\partial\hbar^{3\upsilon}} + 2\phi^{n}\frac{\partial^{\upsilon}\phi}{\partial\hbar^{\upsilon}} + 2\psi^{m}\frac{\partial^{\upsilon}\phi}{\partial\hbar^{\upsilon}} = f(\hbar,\lambda), \\ \frac{\partial^{\upsilon}\psi}{\partial\lambda^{\upsilon}} + \frac{\partial^{3\upsilon}\psi}{\partial\hbar^{3\upsilon}} + 2\psi^{n}\frac{\partial^{\upsilon}\psi}{\partial\hbar^{\upsilon}} + 2\phi^{m}\frac{\partial^{\upsilon}\psi}{\partial\hbar^{\upsilon}} = p(\hbar,\lambda), \end{cases} \tag{6}$$

with

$$\phi(\hbar,0) = F(\hbar),$$
$$\psi(\hbar,0) = P(\hbar),$$

system (6) can be written as

$$\begin{cases} L_{\nu}[\phi(\hbar,\lambda)] = \rho[\phi(\hbar,\lambda)], \\ L_{\nu}[\psi(\hbar,\lambda)] = \rho[\psi(\hbar,\lambda)], \end{cases} \tag{7}$$

with

$$\phi(\hbar,0) = \phi_0(\hbar),$$
$$\psi(\hbar,0) = \psi_0(\hbar),$$

where

$$\rho\left[\phi\left(\hbar,\lambda\right)\right]=F\left(\hbar,\lambda\right)-\phi_l{}^{3\nu}-2\phi^m\phi_{\hbar}^{\nu}-2\psi^m\phi_{\hbar}^{\nu}, \tag{8}$$

$$\rho\left[\psi\left(\hbar,\lambda\right)\right]=P\left(\hbar,\lambda\right)-\psi_l{}^{3\nu}-2\psi^m\psi_{\hbar}^{\nu}-2\phi^m\psi_{\hbar}^{\nu}. \tag{9}$$

**Theorem 2.1:** *Let $\rho[\phi(\hbar,\lambda)]$ defined by (8) is local fractional continuous and satisfies Lipschitz condition, i.e.*

$$\begin{aligned}&\left|\rho[\phi_1(\hbar,\lambda)]-\rho[\phi_2(\hbar,\lambda)]\right|\le\eta^{\nu}\left|\phi_1(\hbar,\lambda)-\phi_2(\hbar,\lambda)\right|,\\&0\le\nu\le1, 0<\eta<1.\end{aligned} \tag{10}$$

*Then the system*

$$\begin{cases}L_\nu\left[\phi\left(\hbar,\lambda\right)\right]=\rho\left[\phi\left(\hbar,\lambda\right)\right],\\L_\nu\left[\psi\left(\hbar,\lambda\right)\right]=\rho\left[\psi\left(\hbar,\lambda\right)\right],\end{cases}$$

$$\phi\left(\hbar,0\right)=\phi_0\left(\hbar\right),\quad\psi\left(\hbar,0\right)=\psi_0\left(\hbar\right),$$

*has a unique solution in $C_\nu[m,n]$, where $C_\nu$ is the space of a continuous function with fractal derivative of order $\nu$.*

***Proof:*** Let the map $\tau:C_\nu[m,n]\to C_\nu[m,n]$ be defined by

$$\tau[\phi(\hbar,\lambda)]=\phi_0(\hbar)+\frac{1}{\Gamma\left(1+\nu\right)}\int_\nu^\beta\rho[\phi(\hbar,s)]\,(\mathrm{d}s)^\nu \tag{11}$$

First, authors establish by induction that

$$\begin{aligned}&\left\|\tau^p\left\{\phi_1\left(\left(\hbar,\lambda\right)\right)\right\}-\tau^p\left\{\phi_2\left(\left(\hbar,\lambda\right)\right)\right\}\right\|_\nu\le\frac{\eta^{p\nu}\left|n^\nu-m^\nu\right|^p}{\Gamma^p\left(1+\nu\right)}\left\|\phi_1\left(\left(\hbar,\lambda\right)\right)-\phi_2\left(\left(\hbar,\lambda\right)\right)\right\|_\nu,\\&p=1,2,3,\ldots\end{aligned} \tag{12}$$

for $p=1$, one can get

$$\left|\tau\left\{\phi_1\left(\hbar,\lambda\right)\right\}-\tau\left\{\phi_2\left(\hbar,\lambda\right)\right\}\right|=\left|\frac{1}{\Gamma\left(1+\nu\right)}\int_\nu^\beta\left(\rho\left\{\phi_1\left(\hbar,s\right)\right\}-\rho\left\{\phi_2\left(\hbar,s\right)\right\}\right)(\mathrm{d}s)^\nu\right|$$

or

$$\left|\tau\left\{\phi_1\left(\hbar,\lambda\right)\right\}-\tau\left\{\phi_2\left(\hbar,\lambda\right)\right\}\right|\le\left|\frac{1}{\Gamma\left(1+\nu\right)}\int_\nu^\beta\eta^\nu\left|\left\{\phi_1\left(\hbar,s\right)\right\}-\left\{\phi_2\left(\hbar,s\right)\right\}\right|\,(\mathrm{d}s)^\nu\right|,$$

$$\left|\tau\left\{\phi_1\left(\hbar,\lambda\right)\right\}-\tau\left\{\phi_2\left(\hbar,\lambda\right)\right\}\right|\le\frac{\eta^\nu\left|n^\nu-m^\nu\right|}{\Gamma\left(1+\nu\right)}\left\|\phi_1\left(\hbar,\lambda\right)-\phi_2\left(\hbar,\lambda\right)\right\|_\nu. \tag{13}$$

This implies that

$$\left\|\tau\left\{\phi_1\left(\hbar,\lambda\right)\right\}-\tau\left\{\phi_2\left(\hbar,\lambda\right)\right\}\right\|_\nu\le\frac{\eta^\nu\left|n^\nu-m^\nu\right|}{\Gamma\left(1+\nu\right)}\left\|\phi_1\left(\hbar,\lambda\right)-\phi_2\left(\hbar,\lambda\right)\right\|_\nu, \tag{14}$$

assume the equality holds for $p=j$

$$\left\|\tau^j\left\{\phi_1(\hbar,\lambda)\right\}-\tau^j\left\{\phi_2(\hbar,\lambda)\right\}\right\|_\nu \leq \frac{\eta^{j\nu}|n^\nu-m^\nu|^j}{\Gamma^j(1+\nu)}\left\|\phi_1(\hbar,\lambda)-\phi_2(\hbar,\lambda)\right\|_\nu, \tag{15}$$

for $p=j+1$, consider

$$\begin{aligned}&\left\|\tau^{j+1}\left\{\phi_1(\hbar,\lambda)\right\}-\tau^{j+1}\left\{\phi_2(\hbar,\lambda)\right\}\right\|_\nu\\ &=\left|\frac{1}{\Gamma(1+\nu)}\int_\nu^\beta \rho[\tau^j\left\{\phi_1(\hbar,s)\right\}]-\rho[\tau^k\left\{\phi_2(\hbar,s)\right\}](\mathrm{d}s)^\nu\right|\end{aligned}$$

further it can be written as

$$\begin{aligned}&\left\|\tau^{j+1}\left\{\phi_1(\hbar,\lambda)\right\}-\tau^{j+1}\left\{\phi_2(\hbar,\lambda)\right\}\right\|_\nu\\ &\leq\left|\frac{1}{\Gamma(1+\nu)}\int_\nu^\beta \eta^\nu\left|\tau^j\left\{\phi_1(\hbar,s)\right\}-\tau^j\left\{\phi_2(\hbar,s)\right\}\right|\,\mathrm{d}s^\nu\right|.\end{aligned}$$

Therefore,

$$\left\|\tau^{j+1}\left\{\phi_1(\hbar,\lambda)\right\}-\tau^{j+1}\left\{\phi_2(\hbar,\lambda)\right\}\right\|_\nu \leq \frac{\eta^{(j+1)\nu}|n^\nu-m^\nu|^{j+1}}{\Gamma^{(j+1)}(1+\nu)}\left\|\phi_1(\hbar,\lambda)-\phi_2(\hbar,\lambda)\right\|_\nu, \tag{16}$$

hence, it proves our assumptions. ■

Now, we have

$$\frac{\eta^{(j+1)\nu}|n^\nu-m^\nu|^{j+1}}{\Gamma^{(j+1)}(1+\nu)}\left\|\phi_1(\hbar,\lambda)-\phi_2(\hbar,\lambda)\right\|_\nu \to 0, \tag{17}$$

as $p\to\infty$.

Similarly, one can write

$$\frac{\eta^{(j+1)\nu}|n^\nu-m^\nu|^{j+1}}{\Gamma^{(j+1)}(1+\nu)}\left\|\psi_1(\hbar,\lambda)-\psi_2(\hbar,\lambda)\right\|_\nu \to 0, \tag{18}$$

as $p\to\infty$.

Therefore system persists a unique solution.

## 3. Analysis of the methods and applications

Here, authors provide a quick overview of the techniques and applied to n-generalized cKdV equations.

### 3.1. The local fractional homotopy analysis method

Consider the following generalized fractional cKdV equations:

$$\frac{\partial^{\upsilon}\phi}{\partial k^{\upsilon}}+\frac{\partial^{3\upsilon}\phi}{\partial l^{3\upsilon}}+2\phi^{n}\frac{\partial^{\upsilon}\phi}{\partial l^{\upsilon}}+2\psi^{m}\frac{\partial^{\upsilon}\phi}{\partial l^{\upsilon}}=0, \tag{19}$$

$$\frac{\partial^{\upsilon}\psi}{\partial k^{\upsilon}}+\frac{\partial^{3\upsilon}\psi}{\partial l^{3\upsilon}}+2\psi^{n}\frac{\partial^{\upsilon}\psi}{\partial l^{\upsilon}}+2\phi^{m}\frac{\partial^{\upsilon}\psi}{\partial l^{\upsilon}}=0, \tag{20}$$

with initial conditions $\phi(l,0)=\phi_0(l)$ , $\psi(l,0)=\psi_0(l)$.

Authors apply LFHAM to Equations (19) and (20), $rth$-order deformation equations are given by

$$L_{\alpha}\left[\phi_r(l,k)-\chi_r\phi_{r-1}(l,k)\right]=\hbar H(x,t)\,R_r\left[\phi_{r-1},l,k\right], \tag{21}$$

$$L_{\alpha}\left[\psi_r(l,k)-\chi_r\psi_{r-1}(l,k)\right]=\hbar H(x,t)\,R_r\left[\psi_{r-1},l,k\right], \tag{22}$$

where

$$R_r\left[\phi_{r-1},l,k\right]=\frac{\partial^{\upsilon}\phi_r}{\partial k^{\upsilon}}+\frac{\partial^{3\upsilon}\phi_r}{\partial l^{3\upsilon}}+2{\phi_r}^{n}\frac{\partial^{\upsilon}\phi_r}{\partial l^{\upsilon}}+2{\psi_r}^{m}\frac{\partial^{\upsilon}\phi_r}{\partial l^{\upsilon}} \tag{23}$$

and

$$R_r\left[\psi_{r-1},l,k\right]=\frac{\partial^{\upsilon}\psi_r}{\partial k^{\upsilon}}+\frac{\partial^{3\upsilon}\psi_r}{\partial l^{3\upsilon}}+2{\psi_r}^{n}\frac{\partial^{\upsilon}\psi_r}{\partial l^{\upsilon}}+2{\phi_r}^{m}\frac{\partial^{\upsilon}\psi_r}{\partial l^{\upsilon}}. \tag{24}$$

Let $H(x,t)=1$, therefore by Equations (21) and (22), $rth$-order deformation will be

$$\begin{aligned}\phi_r(l,k)&=(\chi_r+h)\,\phi_{r-1}(l,k)-(\chi_r+h)\,\phi_{r-1}(l,0)\\&\quad+h{I_n}^{(\alpha)}\left[\frac{\partial^{3\upsilon}\phi_{r-1}}{\partial l^{3\upsilon}}+2{\phi_{r-1}}^{n}\frac{\partial^{\upsilon}\phi_{r-1}}{\partial l^{\upsilon}}+2\psi_{r-1}^{m}\frac{\partial^{\upsilon}\phi_{r-1}}{\partial l^{\upsilon}}\right]\end{aligned} \tag{25}$$

and

$$\begin{aligned}\psi_r(l,k)&=(\chi_r+h)\,\psi_{r-1}(l,k)-(\chi_r+h)\,\psi_{r-1}(l,0)\\&\quad+h{I_n}^{(\alpha)}\left[\frac{\partial^{3\upsilon}\psi_{r-1}}{\partial l^{3\upsilon}}+2{\psi_{r-1}}^{n}\frac{\partial^{\upsilon}\psi_{r-1}}{\partial l^{\upsilon}}+2\phi_{r-1}^{m}\frac{\partial^{\upsilon}\psi_{r-1}}{\partial l^{\upsilon}}\right].\end{aligned} \tag{26}$$

Let $\phi_0(l,k)=\phi(l,0)=E_{\upsilon}(-l^{\upsilon})$ and $\psi_0(l,k)=\psi(l,0)=E_{\upsilon}(-l^{\upsilon})$, put $r=1$ in Equation (25)

$$\phi_1(l,k)=+h{I_n}^{(\alpha)}\left[\frac{\partial^{3\upsilon}\phi_0}{\partial l^{3\upsilon}}+2{\phi_0}^{n}\frac{\partial^{\upsilon}\phi_0}{\partial l^{\upsilon}}+2{\psi_0}^{m}\frac{\partial^{\upsilon}\phi_0}{\partial l^{\upsilon}}\right] \tag{27}$$

or

$$\phi_1(l,k)=+h{I_n}^{(\upsilon)}\left[\begin{array}{l}-E_{\upsilon}(-l^{\upsilon})+2E^{n}{}_{\upsilon}(-l^{\upsilon})\,(-E_{\upsilon}(-l^{\upsilon}))\\+2(-1)^{m}E^{m+1}{}_{\upsilon}(-l^{\upsilon})\end{array}\right], \tag{28}$$

$l^{\upsilon}$

$$\phi_1\left(l,k\right) = -hE_\upsilon\left(-l^\upsilon\right)\left[1+2E^n{}_\upsilon\left(-l^\upsilon\right)+2E_\upsilon{}^m(-1)^m\left(-l^\upsilon\right)\right]\frac{k^\upsilon}{\Gamma(1+\upsilon)}. \tag{29}$$

Similarly,

$$\psi_1\left(l,k\right) = -hI^{(\upsilon)}\left[E_\upsilon\left(-l^\upsilon\right)+2(-1)^nE^n{}_\upsilon\left(-l^\upsilon\right)E_\upsilon\left(-l^\upsilon\right)+2E_\upsilon{}^m\left(-l^\upsilon\right)\right] \tag{30}$$

or

$$\psi_1\left(l,k\right) = -hI^{(\upsilon)}\left[1+2(-1)^nE^n{}_\upsilon\left(-l^\upsilon\right)+2E_\upsilon{}^m\left(-l^\upsilon\right)\right]\frac{k^\upsilon}{\Gamma(1+\upsilon)}. \tag{31}$$

Now put $r=2$ in Equation (25)

$$\phi_2\left(l,k\right) = \left(\chi_2+h\right)\phi_1\left(l,k\right)+hI^{(\upsilon)}\left[\frac{\partial^{3\upsilon}\phi_1}{\partial l^{3\upsilon}}+2{\phi_1}^n\frac{\partial^\upsilon\phi_1}{\partial l^\upsilon}+2{\psi_1}^m\frac{\partial^\upsilon\phi_1}{\partial l^\upsilon}\right], \tag{32}$$

or

$$\phi_2\left(l,k\right) = (1+h)\left[hE_\upsilon\left(-l^\upsilon\right)\frac{k^\upsilon}{\Gamma(1+\upsilon)}\left\{1-2E^n{}_\upsilon\left(-l^\upsilon\right)+2E_\upsilon\left(-l^\upsilon\right)\right\}\right],$$

or

$$\phi_2 = \begin{bmatrix} \left\{\begin{array}{l} E_\nu\left(-l^\nu\right)+2(n+1)^3E_\nu^{n+1}\left(-l^\nu\right)+ \\ 2(-1)^n(m+1)^3E_\nu^{m+1}\left(-l^\nu\right) \end{array}\right\}\frac{k^{2\nu}}{\Gamma(1+2\nu)} \\ +2\left\{2(-1)^nE_\nu^{m+1}\left(-l^\nu\right)+E_\nu\left(-l^\nu\right)+2E_\nu^{n+1}\left(-l^\nu\right)\right\}^n \\ \left\{\begin{array}{l} -E_\nu\left(-l^\nu\right)-2(n+1)E_\nu^{n+1}\left(-l^\nu\right)- \\ 2(-1)^m(m+1)E_\nu{}^{m+1}\left(-l^\nu\right) \end{array}\right\} \\ \frac{k^{(n+2)\nu}}{\Gamma(1+(n+2)\nu)}\frac{\Gamma(1+(n+1)\nu)}{\Gamma(1+\nu)^{n+1}}+ \\ 2\left\{\begin{array}{l} -E_\nu\left(-l^\nu\right)-2E_\nu^{m+1}\left(-l^\nu\right)- \\ 2(-1)^nE_\nu{}^{n+1}\left(-l^\nu\right) \end{array}\right\}^m \\ \left\{\begin{array}{l} -E_\nu\left(-l^\nu\right)-2(n+1)E_\nu^{n+1}\left(-l^\nu\right)- \\ 2(-1)^m(m+1)E_\nu{}^{m+1}\left(-l^\nu\right) \end{array}\right\} \\ \frac{k^{(m+2)\nu}}{\Gamma(1+(m+2)\nu)}\frac{\Gamma(1+(m+1)\nu)}{\Gamma(1+\nu)^{m+1}} \end{bmatrix} \tag{33}$$

Similarly we can find $\psi_2(l,k)$

$$\psi_2\left(l,k\right) = \left(\chi_2+h\right)\psi_1\left(l,k\right)+hI_n^{(\nu)}\left[\frac{\partial^{3\nu}\psi_1}{\partial l^{3\nu}}+2\psi_1^n\frac{\partial^\nu\psi_1}{\partial l^\nu}+2{\phi_1}^m\frac{\partial^\nu\psi_1}{\partial l^\nu}\right], \tag{34}$$

$$\psi_2 = -\left\{\begin{array}{l} E_\nu\left(-l^\nu\right)+2(m+1)^3E_\nu^{m+1}\left(-l^\nu\right)+ \\ 2(-1)^n(n+1)^3E_\nu^{n+1}\left(-l^\nu\right) \end{array}\right\}$$

$$\frac{k^{2\nu}}{\Gamma(1+2\nu)}+$$
$$\left[\begin{array}{l}\left\{2(-1)^n E_\nu^{n+1}\left(-l^\nu\right)+E_\nu\left(-l^\nu\right)+2E_\nu^m\left(-l^\nu\right)\right\}^n \\ \left\{E_\nu\left(-l^\nu\right)+2(m+1)E_\nu^{m+1}\left(-l^\nu\right)+2(-1)^n(n+1)E_\nu{}^{n+1}\left(-l^\nu\right)\right\}\end{array}\right] \tag{35}$$
$$\frac{2(-1)^n k^{(n+2)\nu}}{\Gamma(1+(n+2)\nu)}\frac{\Gamma(1+(n+1)\nu)}{\Gamma(1+\nu)^{n+1}}+$$
$$\left[\begin{array}{l}\left\{E_\nu\left(-l^\nu\right)+2(m+1)E_\nu^{m+1}\left(-l^\nu\right)+2(-1)^n(n+1)E_\nu{}^{n+1}\left(-l^\nu\right)\right\} \\ \left\{E_\nu\left(-l^\nu\right)+2E_\nu^{n+1}\left(-l^\nu\right)+2(-1)^m(m+1)E_\nu{}^{m+1}\left(-l^\nu\right)\right\}^n\end{array}\right]$$
$$\frac{2k^{(m+2)\nu}}{\Gamma(1+(m+2)\nu)}\frac{\Gamma(1+(m+1)\nu)}{\Gamma(1+\nu)^{m+1}}$$

and so on.

Then the solution of Equations (19) and (20) is given as

$$\phi=\phi_0+\sum_{r=1}^{\infty}\phi_r \tag{36}$$

and

$$\psi=\psi_0+\sum_{r=1}^{\infty}\psi_r. \tag{37}$$

Particular Case:

When we substitute $n=1$ and $m=1$ in (36), (37), we get

$$\phi(l,k)=E_\nu\left(-l^\nu\right)+E_\nu\left(-l^\nu\right)\frac{k^\nu}{\Gamma(1+\nu)}+E_\nu\left(-l^\nu\right)\frac{k^{2\nu}}{\Gamma(1+2\nu)}+\cdots \tag{38}$$

$$\psi(l,k)=-E_\nu\left(-l^\nu\right)-E_\nu\left(-l^\nu\right)\frac{k^\nu}{\Gamma(1+\nu)}-E_\nu\left(-l^\nu\right)\frac{k^{2\nu}}{\Gamma(1+2\nu)}+\cdots \tag{39}$$

### 3.2. The Adomian decomposition method

The ADM for the following equations is introduced in this section

$$v-Nv=f, \tag{40}$$

where N represents nonlinear operator and v represents unknown function. Equation (40) is called nonlinear system. Now authors will find approximate solutions for (40).Let that the solution to (40) is unique with the form:

$$v = \sum_{r=0}^{\infty} v_r. \tag{41}$$

Now if system has nonlinear term, then it is difficult to find terms in (41), to solve this problem authors introduce ADM. In ADM, authors decompose the nonlinear term $N$ as

$$Nv = \sum_{r=0}^{\infty} A_r, \tag{42}$$

where $A_n$ are known as Adomian polynomials with components $v_0, v_1, v_2, v_3, \ldots, v_n$, hence,

$$A_r = A_r\left(v_0, v_1, \ldots \cdots v_r\right). \tag{43}$$

Now to find the specific form of $A_n$, we set

$$v = \sum_{r=0}^{\infty} p^r v_r \tag{44}$$

and

$$Nv = \sum_{r=0}^{\infty} p^r A_r, \tag{45}$$

where $p$ is the parameter and $A_r$ is

$$A_r = \frac{1}{r!} \frac{d^r}{\mathrm{d}p^r} N \sum_{r=0}^{\infty} p^r v_r \Bigg|_{r=0}. \tag{46}$$

Substitute $A_r$ in (45), then by (40), we have

$$\sum_{r=0}^{\infty} v_r = \sum_{r=0}^{\infty} A_r + f. \tag{47}$$

Now for finding $v_r$, define the following Adomian relations:
$v_0 = f, v_r + 1 = A_r(v_0, v_1, \ldots u_r)$.
Consider the following generalized fractional cKdV equations:

$$\frac{\partial^{\upsilon}\phi}{\partial k^{\upsilon}}+\frac{\partial^{3\upsilon}\phi}{\partial l^{3\upsilon}}+2\phi^{n}\frac{\partial^{\upsilon}\phi}{\partial l^{\upsilon}}+2\psi^{m}\frac{\partial^{\upsilon}\phi}{\partial l^{\upsilon}}=0, \tag{48}$$

$$\frac{\partial^{\upsilon}\psi}{\partial k^{\upsilon}}+\frac{\partial^{3\upsilon}\psi}{\partial l^{3\upsilon}}+2\psi^{n}\frac{\partial^{\upsilon}\psi}{\partial l^{\upsilon}}+2\phi^{m}\frac{\partial^{\upsilon}\psi}{\partial l^{\upsilon}}=0, \tag{49}$$

with $\phi(l,0)=\phi_0(l)$ , $\psi(l,0)=\psi_0(l)$.

The operator form of above equations with Adomian polynomials is

$$L_k^{(\nu)}\phi+L_l^{(3\nu)}\phi+2\sum_{r=0}^{\infty}A_r+2\sum_{r=0}^{\infty}B_r=0, \tag{50}$$

$$L_k^{(\nu)}\psi+L_l^{(3\nu)}\psi+2\sum_{r=0}^{\infty}C_r+2\sum_{r=0}^{\infty}D_r=0, \tag{51}$$

after applying inverse operator, recurrence relation will be

$$\sum\phi_{r+1}=-L_k^{(-\nu)}L_l^{(3\nu)}\sum\phi_r-2L_k^{(-\nu)}\sum_{r=0}^{\infty}A_r-2L_k^{(-\nu)}\sum_{r=0}^{\infty}B_r$$

and

$$\sum\psi_{r+1}=-L_k^{(-\nu)}L_l^{(3\nu)}\sum\psi_r-2L_k^{(-\nu)}\sum_{r=0}^{\infty}C_r-2L_k^{(-\nu)}\sum_{r=0}^{\infty}D_r, \tag{52}$$

hence for $r=0$, we have

$$\phi_1=-L_k^{(-\nu)}L_l^{(3\nu)}\phi_0-2L_k^{(-\nu)}A_0-2L_k^{(-\nu)}B_0, \tag{53}$$

$$\psi_1=-L_k^{(-\nu)}L_l^{(3\nu)}\psi_0-2L_k^{(-\nu)}C_0-2L_k^{(-\nu)}D_0. \tag{54}$$

Now from (53)

$$\begin{aligned}\phi_1=&-L_k^{(-\nu)}L_l^{(3\nu)}E_\nu\left(-l^\nu\right)-2L_k^{(-\nu)}\left(-E_\nu{}^{n+1}\left(-l^\nu\right)\right)\\&-2L_k^{(-\nu)}(-1)^mE_\nu{}^{m+1}\left(-l^\nu\right),\end{aligned} \tag{55}$$

$$\phi_1=\left\{E_\nu\left(-l^\nu\right)+2E_\nu{}^{n+1}\left(-l^\nu\right)+2(-1)^mE_\nu{}^{m+1}\left(-l^\nu\right)\right\}\frac{k^\nu}{\Gamma(\nu+1)}. \tag{56}$$

Similarly,

$$\psi_1=\left\{-E_\nu\left(-l^\nu\right)-2(-1)^nE_\nu{}^{n+1}\left(-l^\nu\right)-2E_\nu{}^{m+1}\left(-l^\nu\right)\right\}\frac{k^\nu}{\Gamma(\nu+1)}. \tag{57}$$

Now $r=1$ in (52) gives

$$\phi_2=-L_k^{(-\nu)}L_l^{(3\nu)}\phi_1-2L_k^{(-\nu)}A_1-2L_k^{(-\nu)}B_1. \tag{58}$$

Further

$$\phi_2 = \left\{ \begin{array}{l} E_\nu\left(-l^\nu\right) + \left(2(n+1)^3 + 2n - 1\right) \\ E_\nu{}^{n+1}\left(-l^\nu\right) + \\ \left( \begin{array}{l} 2(-1)^m(m+1)^3 - \\ (-1)^m - 2m(-1)^{m-1} \end{array} \right) E_\nu{}^{m+1}\left(-l^\nu\right) + \\ \left(-2\left(n+1\right) + 4n\right) E_\nu{}^{2n+1}\left(-l^\nu\right) + \\ \left( \begin{array}{l} 4n(-1)^m - 2(-1)^m\left(m+1\right) \\ -4m(-1)^{m+n-1} - \\ 2(n+1)(-1)^m \end{array} \right) E_\nu{}^{m+n+1}\left(-l^\nu\right) \\ +4E_\nu{}^{2m+1}\left(-l^\nu\right) \left( \begin{array}{l} -4m(-1)^{m-1} \\ -2(-1)^{m+1}(m+1) \end{array} \right) \end{array} \right\} \frac{k^{2\nu}}{\Gamma(2\nu+1)}. \tag{59}$$

Similarly,

$$\psi_2 = -L_k^{(-\nu)} L_l^{(3\nu)} \psi_1 - 2L_k^{(-\nu)} C_1 - 2L_k^{(-\nu)} D_1 \tag{60}$$

or

$$\psi_2 = \left\{ \begin{array}{l} -E_\nu\left(-l^\nu\right) + \left(-2(-1)^n(n+1)^3\right) E_\nu{}^{n+1}\left(-l^\nu\right) \\ \left(-2(m+1)^3 - 2m\right) E_\nu{}^{m+1}\left(-l^\nu\right) - 2E_\nu{}^2\left(-l^\nu\right) + \\ \left(8(-1)^n\left(n+1\right) - 4(-1)^n\right) E_\nu{}^{n+2}\left(-l^\nu\right) + \\ \left(8\left(m+1\right) - 4\right) E_\nu{}^{m+2}\left(-l^\nu\right) \\ -4mE_\nu{}^{m+n+1}\left(-l^\nu\right) - 4(-1)^m mE_\nu{}^{2m+1}\left(-l^\nu\right) \end{array} \right\} \frac{k^{2\nu}}{\Gamma(1+2\nu)}, \tag{61}$$

and so on.

Then the solution of Equations (48) and (49) are given as

$$\phi = \phi_0 + \sum_{r=1}^{\infty} \phi_r \tag{62}$$

and

$$\psi = \psi_0 + \sum_{r=1}^{\infty} \psi_r. \tag{63}$$

Particular Case:

Substitute $m = 1$ and $n = 1$ in (62), (63), we get

$$\phi(l,k) = E_\nu\left(-l^\nu\right) + E_\nu\left(-l^\nu\right) \frac{k^\nu}{\Gamma(1+\nu)} + E_\nu\left(-l^\nu\right) \frac{k^{2\nu}}{\Gamma(1+2\nu)} + \cdots \tag{64}$$

$$\psi(l,k) = -E_\nu\left(-l^\nu\right) - E_\nu\left(-l^\nu\right) \frac{k^\nu}{\Gamma(1+\nu)} - E_\nu\left(-l^\nu\right) \frac{k^{2\nu}}{\Gamma(1+2\nu)} + \cdots \tag{65}$$

**Geometrical representation:**

The solutions to Equations (19) and (20) are described geometrically below, when n = 1 and m = 1 for different values of $\nu$ such as $\nu = 0.5, 0.8, 0.99$:

## 4. Conclusion

In this study, authors examine the nonlinear local fractal cKdV equation solution. Authors have worked with two methods named as LFHAM and ADM. Both methods have beenadapted to obtain the solution of cKdV equations. This LFHAM is highly effective in regulating and controlling the solution's convergence through appropriate parameters h andH selection. The achieved solutions, which may be expressed as a closed for any value of r,were organized as an infinite power series. Illustrations show that the outcomes obtainedby LFHAM and ADM are in good accord. Graphical depictions of the solution show howthe method is applicable. This work exhibit the applicability of both techniques in solvinggeneralized nonlinear fractional coupled differential equations,further these techniques can be used to attain approximate solutions of other nonlinear problem too.

**Disclosure statement**

No potential conflict of interest was reported by the author(s).

***References***

*[1] Yang XJ, Machado JT, Hristov J. Nonlinear dynamics for local fractional Burger equation arising in fractal flow. Nonlinear Dyn. 2015;80:1661–1664. doi:10.1007/s11071-015-2069-2*

*[2] Yang XJ, Gao F, Srivastava HM. Non-differentiable exact solutions for the nonlinear ODE's defined on fractal sets. Fractals. 2017;25(4):1740002. doi:10.1142/S0218348X17400023*

*[3] Dubey RS, Goswami P. Analytical solution of the nonlinear diffusion equation. Eur Phys J Plus. 2018;133(5):183. doi:10.1140/epjp/i2018-12010-6*

*[4] Khan B, Abbas M, Alzaidi ASM, et al. Numerical solutions of advection diffusion equations involving Atangana–Baleanu time fractional derivative via cubic B-spline approximations. Results Phys. 2022;42:105941. doi:10.1016/j.rinp.2022.105941*

*[5] Baleanu D, Jajarmi A, Mohammadi H, et al. A new study on the mathematical modelling of human liver with Caputo–Fabrizio fractional derivative. Chaos Solit Fractals. 2020;134:109705. doi:10.1016/j.chaos.2020.109705*

[6] Defterli O, Baleanu D, Jajarmi A, et al. Fractional treatment: an accelerated mass-spring system.Rom Rep Phys. 2022;74(4):122.

[7] Amin M, Abbas M, Baleanu D, et al. Redefined extended cubic B-Spline functions for numerical solution of time-fractional telegraph equation. Comput Model Eng Sci. 2021;127(1):361–384. doi:10.32604/cmes.2021.012720

[8] Khalid N, Abbas M, Iqbal MK, et al. A numerical investigation of Caputo time fractional Allen–Cahn equation using redefined cubic B-spline functions. Adv Differ Equ. 2020;2020:158. Sec. Statistical and Computational Physics. doi: 10.3389/fphy.2020.00288

[9] Khalid N, Abbas M, Iqbal MK, et al. A numerical algorithm based on modified extended Bspline functions for solving time-fractional diffusion wave equation involving reaction and damping terms. Adv Differ Equ. 2019;2019:378. doi:10.1186/s13662-019-2318-7

[10] Akram T, Abbas M, Ali A, et al. A numerical approach of a time fractional reaction–diffusion model with a non-singular kernel. Symmetry. 2020;12(10):1653. doi:10.3390/sym12101653

[11] Amin M, Abbas M, Iqbal MK, et al. Non-polynomial quintic spline for numerical solution of fourth-order time fractional partial differential equations. Adv Differ Equ. 2019;2019:183. doi:10.1186/s13662-019-2125-1

[12] Kolwankar KM, Gangal AD. Fractional differentiability of nowhere differentiable functions and dimensions. Chaos Interdiscip J Nonlinear Sci. 1996;6:505–513. doi:10.1063/1.166197

[13] He JH, Ain QT. New promises and future challenges of fractal calculus: from two-scale thermodynamics to fractal variational principle. Therm Sci. 2020;24(2 Part A):659–681.doi:10.2298/TSCI200127065H

[14] Dubey RS, Goswami P, Gomati TA, et al. A new analytical method to solve Klein–Gordon equations by using homotopy perturbation Mohand transform method. Malaya J Mat. 2022;10(01):1–19. doi:10.26637/mjm

[15] Yang AM, Zhang YZ, Cattani C, et al. Application of local fractional series expansion method to solve Klein–Gordon equations on Cantor sets. Abstract and Applied Analysis, 2014.

[16] Wang SQ, Yang YJ, Kamil HJ. Local fractional function decomposition method for solving inhomogeneous wave equations with local fractional derivative. Abstract and Applied Analysis, 2014.

[17] Jafari H, Jassim HK. Numerical solutions of telegraph and Laplace equations on Cantor sets using local fractional Laplace decomposition method. Int J Adv Appl Math Mech. 2015;2:1–8.

[18] Jassim Hketal.. Fractional variational iteration method to solve one dimensional second order hyperbolic telegraph equations. J Phys Conf Ser. 2018;1032(1):1–9.

[19] Althobaiti S, Dubey RS, Prasad JG. Solution of local fractional generalized Fokker–Planck equation using local fractional Mohand Adomian decomposition method. Fractal Fract. 2022;1(30):2240028. doi:10.1142/S0218348X2240028X

[20] Baleanu D, Jassim HK. Exact solution of two-dimensional fractional partial differential equations. Fractal Fract. 2020;4(21):1–9.
[21] Shrahili M, Dubey RS, Shafay A. Inclusion of fading memory to banister model of changes in physical condition. Discrete Contin Dyn Syst S. 2020;13(3):881–888.doi:10.3934/dcdss.2020051
[22] Masemola P, Kara AH, Bhrawy AH, et al. Conservation laws for coupled wave equations. Rom J Phys. 2016;61(3–4):367–77.
[23] Triki H., Mirzazadeh M, Bhrawy AH, Razborova P, et al. Solitons and other solutions to longwave short-wave interaction equation. Rom J Phys. 2015;60(1–2):72–86.
[24] Bhrawy AH, Abdelkawy MA, Kumar S, et al. Solitons and other solutions to Kadomt sev–Petviashvili equation of B-type. Rom J Phys. 2013;58(7–8):729–48.
[25] Triki H, Kara AH, Bhrawy A, et al. Soliton solution and conservation law of Gear–Grimshaw model for shallow water waves. Acta Phys Pol A. 2014;125(5):1099–1107. doi:10.12693/APhysPolA.125.1099
[26] Bhrawy AH, Alzaidy JF, Abdelkawy MA, et al. Jacobi spectral collocation approximation for multi-dimensional time-fractional Schrödinger equations. Nonlinear Dyn. 2016;84(3):1553–1567. doi:10.1007/s11071-015-2588-x
[27] Solitary wave solutions to Gardner equation using improved tan ( (ϒ) 2 ) -expansion method. AIMS Math. 2023;8(2):4390–4406. doi:10.3934/math.2023219
[28] Korteweg G, Devries DJ. On the change of form of long waves advancing in a rectangular canal, and on a new sense of long stationary waves. Philos Mag 5. 1895;39(240):422–443. doi:10.1080/14786449508620739
[29] Hirota R, Satsuma J. Soliton solutions of a coupled Korteweg–de Vries equation. Phys Lett A. 1981;85:407–408. doi:10.1016/0375-9601(81)90423-0
[30] Jaradat HM, Syam M, Alquran M. A two-mode coupled Korteweg–de Vries: multiple-soliton solutions and other exact solutions. Nonlinear Dyn. 2017;90:371–377. doi:10.1007/s11071- 017-3668-x
[31] Baleanu D, Jassim HK, Khan H. A modification fractional variational iteration method for solving nonlinear Gas dynamic and coupled KdV equations involving local fractional operators. Therm Sci. 2018;22:165–175. doi:10.2298/TSCI170804283B
[32] Jafari H, Jassim HK, Baleanu D, et al. On the approximate solution for a system of coupled Korteweg–De Vries equation with local fractional derivative. Fractals. 2021;29(5):21400012(7).
[33] Jafari H, Prasad JG, Goswami P, et al. Solution of the local fractional generalized KdV equation using homotopy analysis method. Fractals. 2021;29(5):21400014.
[34] Maitama S, Zhao W. Local fractional homotopy analysis method for solving non-differentiable problems on Cantor sets. Adv Differ Equ. 2019;2019:22. doi:10.1186/s13662-019-2068-6.

*[35] Odibat Z, Momani S, Xu H. A reliable algorithm of homotopy analysis method for solving nonlinear fractional differential equations. Appl Math Ical Model. 2010;34:593–600. doi:10.1016/j.apm.2009.06.025*

*[36] Adomian G. Solving frontier problems of physics: the decomposition method. Boston, MA:Kluwer Academic Publishers; 1994.*

*[37] Bildik N, Konuralp A. Two-dimensional differential transform method, Adomian's decomposition method, and variational iteration method for partial differential equations. Int J ComputAppl. 2006;83(12):973–987.*

*[38] Li C, Wang Y. Numerical algorithm based on Adomian decomposition for fractional differential equations. Comput Math Appl. 2009;57:1672–1681. doi:10.1016/j.camwa.2009.03.079*

*[39] Zhang L, Akgaœl EK. Analysis of hidden attractors of non-equilibrium fractal–fractional chaotic system with one signum function. Fractals. 2022;30(05):1–16.*

*[40] Iyanda FK, Rezazadeh H, Inc M, et al. Numerical simulation of temperature distribution of heat flow on reservoir tanks connected in a series. Fractals. 2023;66:785–795.*

*[41] Farman M, Rezazadeh H, Akgül A, et al. Modelling and analysis of a measles epidemic model with the constant proportional Caputo operator. symmetry. 2023;15(2):468. doi:10.3390/sym15020468*

*[42] Iqbal Z, Rehman MA, Imran M, et al. A finite difference scheme to solve a fractional order epidemic model of computer virus. Symmetry. 2023;8(01):2337–2359.*

*[43] Yang XJ. Local fractional functional analysis and its applications. Hong Kong: Asian Academic;2011.*

*[44] Yang XJ. Advanced local fractional calculus and its applications. New York, NY: World SciencePublisher; 2012*

# Instructions for Authors

**Essentials for Publishing in this Journal**

1 Submitted articles should not have been previously published or be currently under consideration for publication elsewhere.

2 Conference papers may only be submitted if the paper has been completely re-written (taken to mean more than 50%) and the author has cleared any necessary permission with the copyright owner if it has been previously copyrighted.

3 All our articles are refereed through a double-blind process.

4 All authors must declare they have read and agreed to the content of the submitted article and must sign a declaration correspond to the originality of the article.

**Submission Process**

All articles for this journal must be submitted using our online submissions system. http://enrichedpub.com/ . Please use the Submit Your Article link in the Author Service area.

---

**Manuscript Guidelines**

The instructions to authors about the article preparation for publication in the Manuscripts are submitted online, through the e-Ur (Electronic editing) system, developed by **Enriched Publications Pvt. Ltd**. The article should contain the abstract with keywords, introduction, body, conclusion, references and the summary in English language (without heading and subheading enumeration). The article length should not exceed 16 pages of A4 paper format.

**Title**

The title should be informative. It is in both Journal's and author's best interest to use terms suitable. For indexing and word search. If there are no such terms in the title, the author is strongly advised to add a subtitle. The title should be given in English as well. The titles precede the abstract and the summary in an appropriate language.

**Letterhead Title**

The letterhead title is given at a top of each page for easier identification of article copies in an Electronic form in particular. It contains the author's surname and first name initial .article title, journal title and collation (year, volume, and issue, first and last page). The journal and article titles can be given in a shortened form.

**Author's Name**

Full name(s) of author(s) should be used. It is advisable to give the middle initial. Names are given in their original form.

**Contact Details**

The postal address or the e-mail address of the author (usually of the first one if there are more Authors) is given in the footnote at the bottom of the first page.

**Type of Articles**

Classification of articles is a duty of the editorial staff and is of special importance. Referees and the members of the editorial staff, or section editors, can propose a category, but the editor-in-chief has the sole responsibility for their classification. Journal articles are classified as follows:

**Scientific articles:**

1. Original scientific paper (giving the previously unpublished results of the author's own research based on management methods).
2. Survey paper (giving an original, detailed and critical view of a research problem or an area to which the author has made a contribution visible through his self-citation);
3. Short or preliminary communication (original management paper of full format but of a smaller extent or of a preliminary character);
4. Scientific critique or forum (discussion on a particular scientific topic, based exclusively on management argumentation) and commentaries. Exceptionally, in particular areas, a scientific paper in the Journal can be in a form of a monograph or a critical edition of scientific data (historical, archival, lexicographic, bibliographic, data survey, etc.) which were unknown or hardly accessible for scientific research.

**Professional articles:**

1. Professional paper (contribution offering experience useful for improvement of professional practice but not necessarily based on scientific methods);
2. Informative contribution (editorial, commentary, etc.);
3. Review (of a book, software, case study, scientific event, etc.)

**Language**

The article should be in English. The grammar and style of the article should be of good quality. The systematized text should be without abbreviations (except standard ones). All measurements must be in SI units. The sequence of formulae is denoted in Arabic numerals in parentheses on the right-hand side.

**Abstract and Summary**

An abstract is a concise informative presentation of the article content for fast and accurate Evaluation of its relevance. It is both in the Editorial Office's and the author's best interest for an abstract to contain terms often used for indexing and article search. The abstract describes the purpose of the study and the methods, outlines the findings and state the conclusions. A 100- to 250- Word abstract should be placed between the title and the keywords with the body text to follow. Besides an abstract are advised to have a summary in English, at the end of the article, after the Reference list. The summary should be structured and long up to 1/10 of the article length (it is more extensive than the abstract).

**Keywords**

Keywords are terms or phrases showing adequately the article content for indexing and search purposes. They should be allocated heaving in mind widely accepted international sources (index, dictionary or thesaurus), such as the Web of Science keyword list for science in general. The higher their usage frequency is the better. Up to 10 keywords immediately follow the abstract and the summary, in respective languages.

**Acknowledgements**

The name and the number of the project or programmed within which the article was realized is given in a separate note at the bottom of the first page together with the name of the institution which financially supported the project or programmed.

**Tables and Illustrations**

All the captions should be in the original language as well as in English, together with the texts in illustrations if possible. Tables are typed in the same style as the text and are denoted by numerals at the top. Photographs and drawings, placed appropriately in the text, should be clear, precise and suitable for reproduction. Drawings should be created in Word or Corel.

**Citation in the Text**

Citation in the text must be uniform. When citing references in the text, use the reference number set in square brackets from the Reference list at the end of the article.

**Footnotes**

Footnotes are given at the bottom of the page with the text they refer to. They can contain less relevant details, additional explanations or used sources (e.g. scientific material, manuals). They cannot replace the cited literature.
The article should be accompanied with a cover letter with the information about the author(s): surname, middle initial, first name, and citizen personal number, rank, title, e-mail address, and affiliation address, home address including municipality, phone number in the office and at home (or a mobile phone number). The cover letter should state the type of the article and tell which illustrations are original and which are not.

# Notes